

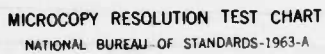
AD-A139 129 AIR WEATHER SERVICE MODEL OUTPUT STATISTICS SYSTEMS(U)
AIR FORCE GLOBAL WEATHER CENTRAL OFFUTT AFB NE
D L BEST ET AL. OCT 83 AFGWC/PR-83/001 SBI-AD-E850 549

AIR WEATHER SERVICE MODEL OUTPUT STATISTICS SYSTEMS(U)
AIR FORCE GLOBAL WEATHER CENTRAL OFFUTT AFB NE
D L BEST ET AL. OCT 83 AFGWC/PR-83/001 SBI-AD-E850 549

NL

F/G 4/2





AD E 850 549

①

AFGWC/PR-83/001



AIR WEATHER SERVICE
MODEL OUTPUT STATISTICS SYSTEM
PROJECT REPORT

By

LT COL DONALD L. BEST
MAJ STEPHEN P. PRYOR

AD A 139129



APPROVED FOR PUBLIC RELEASE, DISTRIBUTION UNLIMITED

OCTOBER 1983

UNITED STATES AIR FORCE
AIR WEATHER SERVICE (MAC)
AIR FORCE GLOBAL WEATHER CENTRAL
OFFUTT AFB NE 68113

DTIC FILE COPY

DTIC
ELECTE
FEB 24 1984
S B D

84 02 24 042

REVIEW AND APPROVAL STATEMENT

This publication approved for public release. There is no objection to unlimited distribution of this document to the public at large, or by the Defense Technical Information Center (DTIC) or the the National Technical Information Service (NTIS).

This technical publication has been reviewed and is approved for publication.

Charles W. Cook

CHARLES W. COOK, GM-13
Reviewing Official

FOR THE COMMANDER

Peter J. Havanac

PETER J. HAVANAC, Lt Col, USAF
Chief, Technical Services Division

DTIC
ELECTE
FEB 14 1984
2
B

DTIC LIFE COPY

UNCLASSIFIED

SECURITY CLASSIFICATION OF THIS PAGE (When Data Entered)

REPORT DOCUMENTATION PAGE		READ INSTRUCTIONS BEFORE COMPLETING FORM
1. REPORT NUMBER AFGWC/PR-83/001	2. GOVT ACCESSION NO. ADA139129	3. RECIPIENT'S CATALOG NUMBER
4. TITLE (and Subtitle) Air Weather Service Model Output Statistics System		5. TYPE OF REPORT & PERIOD COVERED
		6. PERFORMING ORG. REPORT NUMBER
7. AUTHOR(s) Donald L. Best Stephen P. Pryor		8. CONTRACT OR GRANT NUMBER(s)
9. PERFORMING ORGANIZATION NAME AND ADDRESS HQ Air Force Global Weather Central (MAC) Offutt AFB, Nebraska 68113		10. PROGRAM ELEMENT, PROJECT, TASK AREA & WORK UNIT NUMBERS
11. CONTROLLING OFFICE NAME AND ADDRESS HQ Air Force Global Weather Central (MAC) Offutt AFB, Nebraska 68113		12. REPORT DATE October 1983
		13. NUMBER OF PAGES 85 + iv
14. MONITORING AGENCY NAME & ADDRESS (if different from Controlling Office)		15. SECURITY CLASS. (of this report) UNCLASSIFIED
		15a. DECLASSIFICATION DOWNGRADING SCHEDULE
16. DISTRIBUTION STATEMENT (of this Report) Approved for public release; distribution unlimited.		
17. DISTRIBUTION STATEMENT (of the abstract entered in Block 20, if different from Report) N/A		
18. SUPPLEMENTARY NOTES		
19. KEY WORDS (Continue on reverse side if necessary and identify by block number) Model Output Statistics Predictability Statistical Forecasting Predictand Probability Forecasting Regression Scalar Forecasting Coefficients Probability Thesholding		
20. ABSTRACT (Continue on reverse side if necessary and identify by block number) The development and operation of the Air Weather Service Model Output Statistics (MOS) System is described. A short history of the migration of MOS technology and software from the National Weather Service Technique Development Laboratory (TDL) to the Air Force Global Weather Central is provided.		

DD FORM 1 JAN 73 1473

EDITION OF 1 NOV 65 IS OBSOLETE

UNCLASSIFIED

SECURITY CLASSIFICATION OF THIS PAGE (When Data Entered)

PREFACE

This Project Report (PR) describes the Air Weather Service (AWS) Model Output Statistics (MOS) System developed at the Air Force Global Weather Central (AFGWC), Offutt AFB, Nebraska. Emphasis is placed on the AWS MOS system's integration into the AFGWC production scheme, its capabilities, limitations, and the options available.

The AWS MOS system was tested operationally for 18 months. The verification results from the test showed very limited skill. Because of this HQ AWS terminated the production of operational AWS MOS forecasts. Further development of AWS MOS equations has been postponed until sufficient spectral model data has been archived.

The authors wish to thank those who were most responsible for the production of this PR:

Lt Col Frank Globokar for his pioneer work with TDL in developing MOS software and for his management efforts that established an AWS MOS capability at AFGWC; SMS John Martin for his tireless and masterful programming of the original AWS MOS system with all its highly automated features; SSgt Kenneth Nelmes and SrA Gregory Gaddis for their similarly significant contributions in the evolving MOS software; Maj Bryan Lilius for pulling this Project Report together in its late editorial phase; Rhonda Fischer and Mary Ann Kosmicki in the word processing center, without whose support the publication date would certainly have been another year away; Col Kenneth German (Chief, Technical Services Division, AFGWC), Major Kenneth Peterson and Capt Jeanette Baker (TDL Liaison Officers), Mr Jon Whiteside (USAFETAC/OL-A), and Lt Col Peter Havanac (USAFETAC/DN) who contributed significant comment to the final publication. Finally, We give special thanks to Dr Harry Glahn (Director, TDL) whose original brilliance and insight brought the world Model Output Statistics.

Accession For	
NTIS GRA&I	<input checked="checked" type="checkbox"/>
DTIC TAB	<input type="checkbox"/>
Unannounced	<input type="checkbox"/>
Justification	
By	
Distribution/	
Availability Codes	
Dist	Avail and/or Special
A-1	



TABLE OF CONTENTS

	PAGE
LIST OF FIGURES.....	iv
LIST OF TABLES.....	iv
SECTION 1 INTRODUCTION.....	1
SECTION 2 HISTORY.....	2
2.1 Basic Methodologies.....	2
2.1.1 Classical Statistics.....	2
2.1.2 Perfect Prog.....	2
2.1.3 MOS.....	2
2.2 Background.....	3
SECTION 3 MOS EQUATIONS.....	4
SECTION 4 AWS MOS SYSTEM.....	6
4.1 Data Archive System.....	6
4.1.1 AWSPE Data Collection.....	6
4.1.2 Five Layer Data Collection.....	9
4.1.3 3DNEPH Data Collection.....	9
4.1.4 Surface Observation Data Save.....	10
4.1.5 Climatology.....	13
4.2 Development Subsystem.....	13
4.2.1 Data Flow.....	15
4.2.2 Regional Equation Development.....	15
4.3 Operational Subsystem.....	16
4.4 Verification Subsystem (MOSVER).....	24
SECTION 5 MOS FORECASTING.....	26
5.1 Operational Production.....	26
5.2 Capabilities and Limitations.....	29
5.3 Probability Versus Scalar Forecasting.....	30
5.3.1 Probability Forecasting.....	30
5.3.2 Scalar Forecasting.....	31
5.4 Classification.....	32
5.4.1 Probability Thresholding.....	32
5.4.2 Inflation of Scalar Forecasts.....	32
SECTION 6 MOS FORECASTING HINTS ON USAGE.....	34
6.1 Interpreting Probabilities.....	34
6.2 Limits of Predictability.....	34
6.3 Adjusting MOS to Local Conditions.....	35
6.3.1 Golden Rules of MOS Support.....	35
6.3.2 Tracking Biases.....	36
6.3.3 Regional Verification.....	37

TABLE OF CONTENTS (Continued)

	PAGE
REFERENCES.....	39
APPENDIX A--Miller-Best II Threshold Model.....	40
APPENDIX B--List of Overseas Development and Operational Stations.....	45
APPENDIX C--List of CONUS and Alaska Operational Stations (SOFTRIX Support).....	74
GLOSSARY OF TERMS.....	83
ACRONYMS.....	84

LIST OF FIGURES

FIGURE	PAGE
1. Data Archive and Development Subsystems.....	7
2. Present Data Archive Areas for the AWS MOS System.....	8
3. European MOS Window Showing Regions Used in Equation Development.....	18
4. Asian MOS Window Showing Regions Used in Equation Development.....	19
5. South China Sea MOS Window Showing Regions Used in Equation Development.....	20
6. Middle East and African MOS Windows Showing Regions Used in Equation Development.....	21
7. Operational Subsystem.....	22
8. Depiction of Data Flow Through the Operational Subsystem.....	23
9. Verification Subsystem.....	25

LIST OF TABLES

TABLE	
1. Variables Archived from AWSPE.....	6
2. Variables Archived from AFGWC 5LYR Cloud Forecast Model.....	9
3. Variables Archived from the 3DNEPH Cloud Analysis Model.....	10
4. Archived Surface Weather Elements.....	10
5. MOS Surface Weather Elements.....	14
6. MOS Windows and Regions.....	16
7. SOFTRIX Data Elements.....	26
8. Forecast Projections Available in SOFTRIX Data Base.....	28
9. MOS Verification Contingency Table.....	38
10. MOS Probability Verification Table.....	38

1. INTRODUCTION

Model Output Statistics (MOS) is a statistical procedure that allows one to use mathematics and dynamic model outputs to forecast or diagnose some unknown quantity. The traditional application of MOS has been to forecast the sensible weather elements; that is, the weather elements a surface-based observer would report. MOS as a procedure can generate forecast equations that yield either scalar or probability responses.

MOS support is currently available from two sources. The National Weather Service (NWS) produces MOS forecasts at the National Meteorological Center (NMC) in Suitland, Maryland, and develops and maintains the system at their Techniques Development Laboratory (TDL) in Silver Spring, Maryland. The Air Weather Service (AWS) developed, produced, and maintained its system at the AFGWC, Offutt AFB, Nebraska. The NWS MOS system supports civilian and DOD locations throughout the contiguous United States (CONUS) and Alaska. The AWS MOS system supported the DOD in providing forecast guidance for locations in the Western Pacific/SE Asia, Europe, Middle East, and NE Africa. The procedure for DOD support using NWS MOS was to first acquire the raw MOS forecasts twice daily for some 362 CONUS and 39 Alaska locations, and secondly to apply software within the AFGWC computer systems to format the MOS bulletins and MOS maps that AWS forecasters use.

AWS has long had weather support customers who required probability information on expected mission-limiting weather events. Historically, the solutions to this support were manual production with tailored support-specific mathematical solutions. The burden of increasing demands for this type of support and the attendant high cost led AWS to investigate alternative means to systemize the probability forecasting business; hence the interest in TDL's development of the MOS technique. MOS was a clever means to solve a large number of probability forecast support problems with one objective, computer-based system. For economic reasons alone, this was a desirable methodology to seek for AWS applications. In the best spirit of joint cooperation, the AWS and NWS now share the TDL MOS development subsystem to support both military and civilian locations in the CONUS and Alaska. However, only an AWS MOS system could best serve DOD support needs in terms of its global support mission and the need to tailor many forecasts to unique military requirements. The AWS MOS capability was spawned from TDL's inventiveness and experience, but in many respects has surpassed its forebearer in capability. The AWS MOS system is more flexible to change and more expandable. It has a more comprehensive climatology support subsystem, and has an impressive level of automation in the development of the forecast equations. For example, a complete set of equations--all elements, all time periods, primary and backup sets, 00 and 12Z cycles, and all regions support--could be solved, if the computer were not interrupted, in only one job submission! This configuration gives AWS the low-cost, expansive, easily maintainable, and responsive probability forecast production system it needed.

2. HISTORY

2.1 Basic Methodologies. Probability forecasting is not a new idea, nor is MOS the first practical solution to come along. There are three basic methodologies that were evolutionary in time and in accuracy that encompass nearly all techniques: classical statistics, perfect prog, and MOS.

2.1.1 Classical Statistics. Wide use of means, data stratification, and simple statistical models were the early ways to solve some forecast assistance problems. Applications include climatology tables, local studies based on relationships inferred between observed data (e.g., surface observations and upper air soundings) and observed weather later in the day, map typing (e.g., how many times does it snow with such-and-such synoptic pattern to the west of the station), rules of thumb, and simple regression models or discriminant functions. See Panofsky and Brier (1965) for more insight and examples.

2.1.2 Perfect Prog. This method (Klein, 1971) establishes diagnostic relationships among same-time observed upper air parameters and observed sensible weather elements. Multivariate regression is used to establish the degree to which parameters are important in this relationship and in the assessment of relative weights thereof. Once a satisfactory diagnostic relationship (normally in the form of a statistical equation) is established, the equations are overlayed onto the dynamic model forecast fields (or prognoses) and solved as though these fields were future analyses. This procedure works well under the assumption that the prognoses are perfect. Although this technique works very well and is an improvement over more simplistic classical statistical solutions, the fact remains that the progs are not perfect, and will grow in error as time advances. Therefore, use of the diagnostic perfect prog equations will reflect the dynamic model's biases in predicting associated future weather elements.

2.1.3 MOS. Glahn and Lowry (1972) did the obvious (on hindsight)--if the dynamic model's biases introduce bias to the predicted weather, why not use the dynamic model's output as the source of predictability? This approach would permit the statistics of the situation to account for model biases and to provide for an unbiased solution. Now, the statistical equations that were solved through this association were only limited in their ability to accurately forecast future weather by the limited ability of the dynamic model to do its part. Improve the dynamics and MOS will improve the terminal forecast. The obvious limit in dynamic model performance would return us to the perfect prog solution, but even with an absolutely perfect prog, the statistical equations cannot perfectly diagnose the weather as seen from the ground. There are many real reasons for this of course, but improvements can still be made in (1) closing the accuracy gap by identifying new predictors that account for the non-linearities in the atmosphere, (2) introducing and using statistical procedures that will improve the equations themselves, and (3) modifying centralized MOS forecasts by the local forecaster to account for local effects that are not always easily captured in a grand centralized sense.

2.2 Background. In the early 1970's AWS became interested in this emerging MOS technology and established its first, one-man, liaison office at TDL. This first office assisted TDL scientists in the development of the first MOS system--a goal to overcome a growing fragmentation problem as more MOS forecast elements began to enter production. This office also contributed in the development of new MOS products (5-category ceiling and visibility and 3-category flying weather) for CONUS civilian locations. In the mid 1970's the second TDL liaison office arranged for over 100 NWS MOS bulletins for DOD locations to be transmitted to AFGWC where they were decoded for internal support of the AFGWC forecasters. The current 6-category ceiling and visibility and 4-category cloud cover MOS forecast equations were developed. In the late 1970's, AWS got more serious about the MOS issue: three AWS scientists were sent to the liaison office at TDL and AFGWC was tasked to develop an AWS MOS system for DOD support. This three-man liaison office changed the amount and form of MOS data transfer to AFGWC sending 10 times the original information flow at the same communications costs, expanded the TDL MOS system to include 54 and 60-hour forecasts, added DOD wind, temperature, and altimeter forecasts, added a new element to the TDL system--obstructions to vision, and kicked off the Alaskan MOS effort in cooperation with other TDL scientists so that both civilians and military users could get Alaskan MOS support. In the early 1980's the AWS MOS system at AFGWC went on line with overseas support. The fourth TDL liaison office got the job of maintaining and improving the NWS MOS link to AFGWC. The mid 1980's will witness a significant change in the AWS MOS system with the introduction of the spectral global dynamic model which will replace the hemispheric-limited dry PE models currently in use at AFGWC. The spectral model is demonstrated to be more accurate and will allow AFGWC to likewise produce more accurate AWS MOS guidance. Not only will AWS attain a more accurate set of MOS products, but will also have the ability to expand to a truly global scope--one that is strained by today's dynamic models. Beyond the mid 1980's support of DOD missions worldwide through the MOS system could enter a high level of sophistication. The automated interfaces of tomorrow's command and control and weather support systems beg for this conceptual capability: to be able to sit down at a computer terminal and request a terminal forecast for any point in the world. With a global dynamic model, computer access by the users (WWMCCS, AWDS, etc.), talent to operate and maintain the AWS MOS system, and visionary managers and planners, this is not an unthinkable goal or reality.

3. MOS EQUATIONS

The MOS equations (Klein and Glahn, 1974) are the heart of the MOS capability. They are, collectively, the model that converts "known" values into future expectations. They can yield probability or scalar estimations. They are typically a linear, least-squares regression model of the form:

$$Y = a_0 + a_1 X_1 + a_2 X_2 + \dots + a_k X_k + e$$

Here, the X-terms are the "known" values, or the independent variables. The Y-term is the predicted event, or the dependent variable. The a-terms are coefficients which are the optimum weights assigned to each independent variable (also known as predictors) through a statistical procedure called least-squares regression analysis. The number of terms (k) is determined either by the analyst's choice or by an error convergence check built into the computer program that performs the regression analysis. The e-term is the error left when fitting this model to real data. There are many least-squares regression procedures to use, but the procedure used by both the MWS and AWS MOS development subsystems is called forward step-wise selection. This procedure picks the predictor (of the many offered) that has the highest correlation with the dependent variable (also known as the predictand) as the first predictor. If we stop at this point, we have a single-predictor equation:

$$Y' = a_0 + a_1 X_1$$

Here, the a-terms are minimum variance, unbiased estimators, and Y' is the modeled estimate of the predictand. This should be recognized as an equation of a straight line, where a_0 is the y-intercept and a_1 is the slope of the line. The use of this equation to reproduce the predictand events can be measured through the correlation coefficient (R) between the equation-produced values (Y') and the observed values (Y). The range of the R-value is between zero and one, where $R=0$ means no relationship and $R=1$ means perfect relationship (i.e., where $e=0$). Of course, in the real world of MOS equations development, the R-value falls somewhere in between. The R-value can be used as a means to select more predictors, one-by-one. The second predictor is the one which when put into regression with the established single-predictor equation will yield the largest updated R-value. This would give a 2-term linear model:

$$Y' = a_0 + a_1 X_1 + a_2 X_2$$

The reader should understand that all of the coefficients change as more predictors enter regression. Before being satisfied that this 2-term equation is preferred over the 1-term equation, the R-values of each are examined. If, for example, the increase in R exceeds .01, then the 2-term equation is accepted and a third term is sought. Eventually, a term is found that will not improve the updated R-value by more than .01. At this point the computer program halts and prints out the equation that does not include the latest, unacceptable term; hence the final result:

$$Y' = a_0 + a_1 X_1 + a_2 X_2 + \dots + a_k X_k$$

This multivariate (many predictors or dimensions) linear regression model can be made to create probability or scalar estimates by a simple alteration of the predictand event. An equation to forecast probabilities, for example, is created by defining the predictand as a binary (0 or 1). Using a binary predictand in the regression computations forces the coefficients to weigh the predictors in such a way as to best fit a 0 or a 1. Depending on the mathematical regression model used, forecasts (Y') may at time fall outside the (0,1) range. To generate a MOS equation that will forecast scalar values, the predictand data is kept in its scalar (or some scaled) form.

4. AWS MOS SYSTEM

The AWS MOS software is divided into four subsystems. These are the (1) data archive subsystem, (2) the development subsystem, (3) the operational subsystem, and (4) the verification subsystem. This chapter describes the flow and processing of data through the subsystems.

4.1 Data Archive Subsystem. This subsystem begins with the flow of upper air and surface observations, satellite reports, and other miscellaneous reports into the AFGWC data base (figure 1). This data base provides the initialization for the AFGWC numerical models. The model outputs used by MOS come from the AWS Primitive Equation (AWSPE) model, the AFGWC 5-Layer cloud forecast model (5LYR), and the 3-dimensional cloud nephanalysis model (3DNEPH). In-house data procedures have been established to capture the AWSPE and 5LYR models. These data are saved on 6250 bpi 9-track computer tapes. The 3DNEPH output is archived at USAFETAC/OL-A and must be retrieved along with the surface observations. Figure 2 shows currently archived areas for the AWSPE and 5LYR models as well as current 3DNEPH windows that are on hand at HQ AFGWC. All 3DNEPH data are archived at USAFETAC/OL-A, but requests are for only those areas needed to meet current requirements for equation development.

4.1.1 AWSPE Data Collection. Forecast fields from the AWSPE model are archived over the Northern Hemisphere octagon 47 by 51 whole-mesh grid. Grids for all AFGWC models are described in great detail by Hoke *et.al.* (1981). Forecast fields saved are given in Table 1. The AWSPE model is described by Tarbell *et.al.*, (1982).

Table 1. Variables Archived from AWSPE. All variables are archived at 06, 12, 18, 24, 30, 36, 48, 60, and 72 hour projections.

<u>Variable</u>	<u>Levels (mb)</u>	<u>Units</u>
U and V wind components	1000, 850, 700, 500, 300, 200	msec ⁻¹ x 10
Temperature	Surface, 1000, 850, 700, 500, 300, 200	deg K
D-value	1000, 850, 700, 500, 300, 200	m x 10
Vertical Velocity	1000, 850, 500, 300	mbsec ⁻¹ x 10 ⁴
Absolute Vorticity	500	sec ⁻¹ x 10 ⁶

A DATA ARCHIVE SUBSYSTEM

DEVELOPMENT SUBSYSTEM

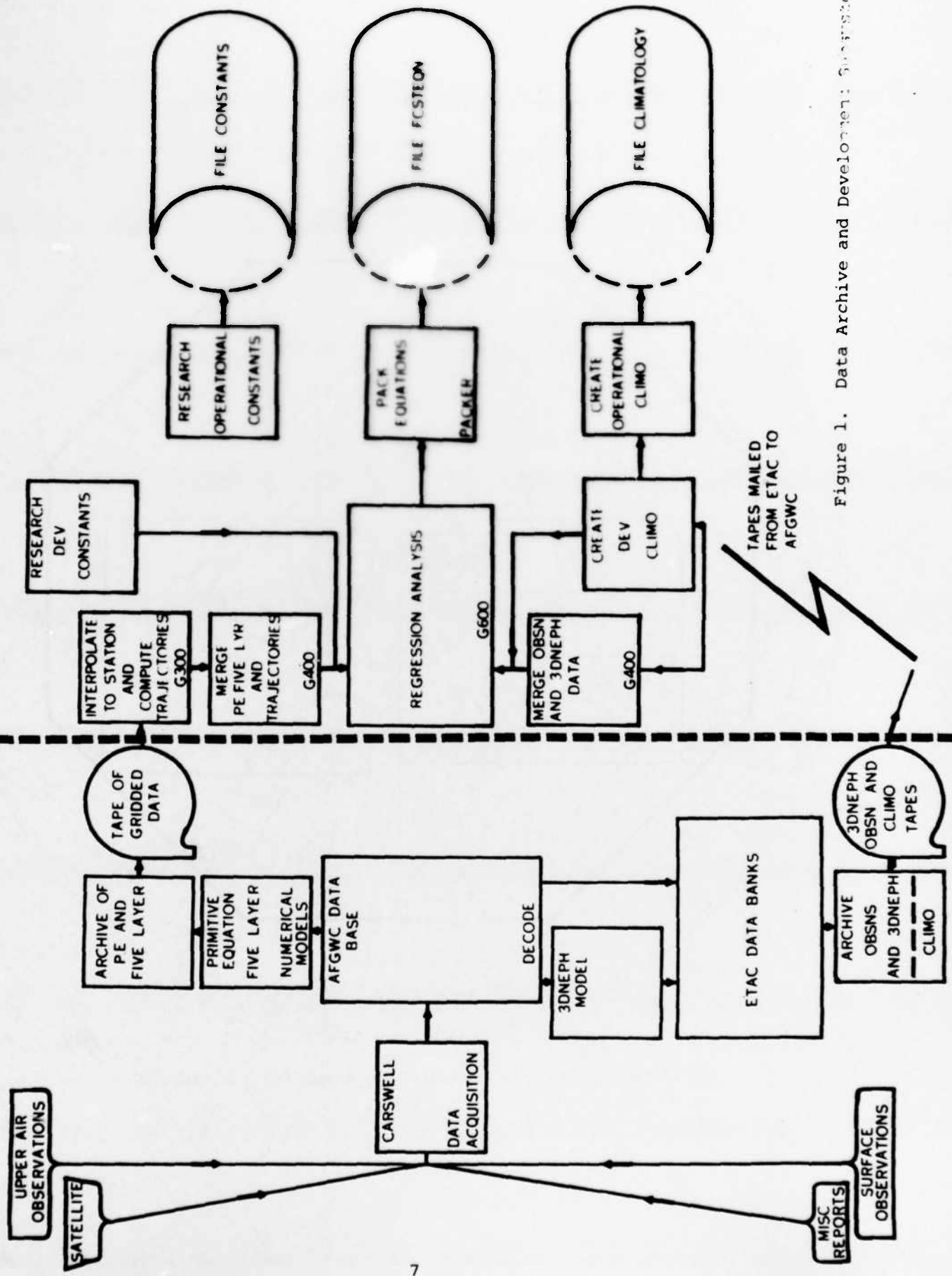


Figure 1. Data Archive and Development Subsystems

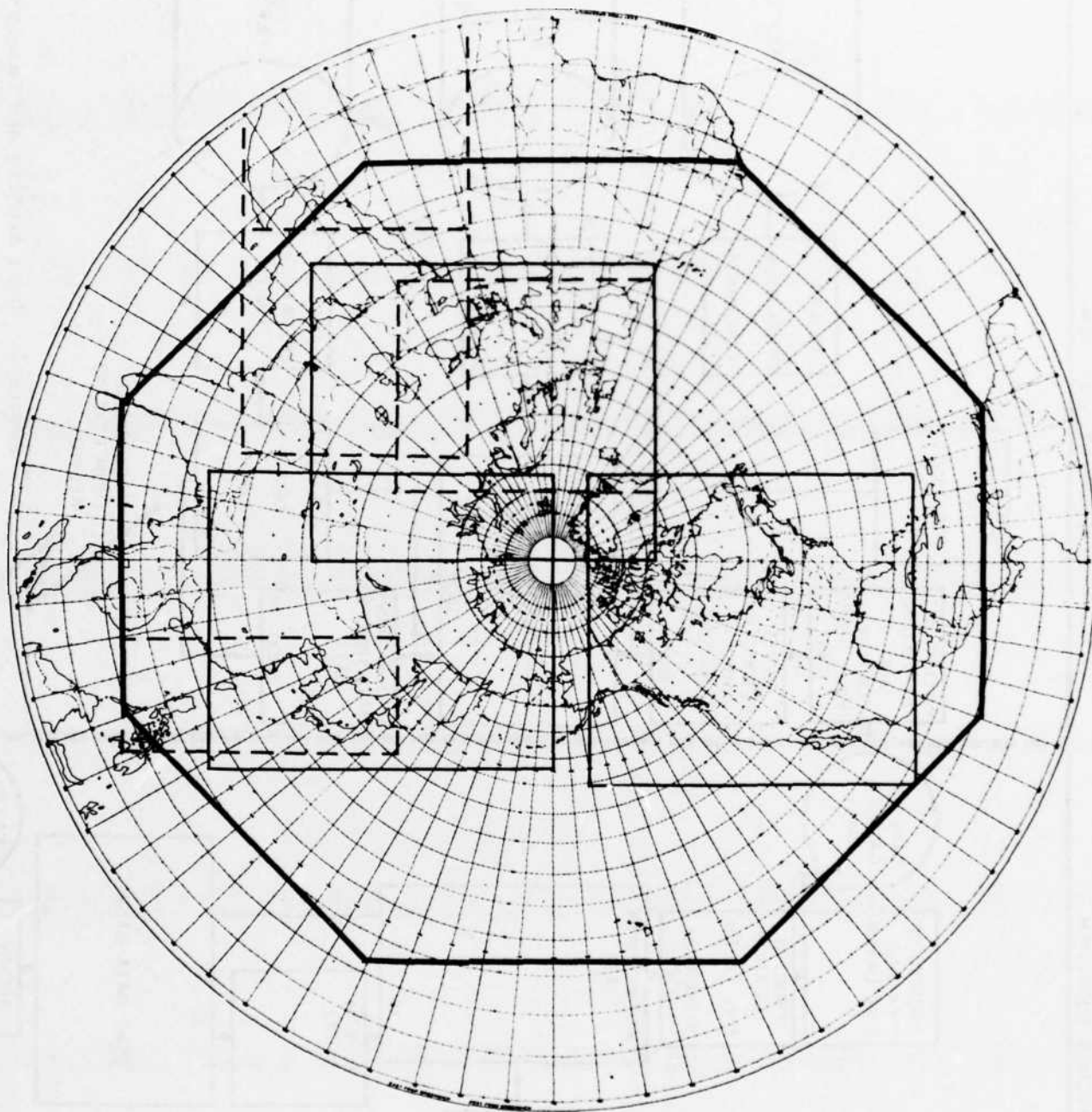


Figure 2. Present Data Archive Areas for the AWS MOS System

4.1.2 Five Layer Data Collection. Forecast fields from the 5LYR model are archived over the grids shown in Figure 2 (US, European, and Asian half-mesh grids). The three grids contain 37x39, 35x41, and 35x41 grids points, respectively. The fields that are saved are given in Table 2. Further details on the 5LYR model are given by Mitchell (1982).

Table 2. Variables Archived from AFGWC 5LYR Cloud Forecast Model

<u>Variable</u>	<u>Level (mb)</u>	<u>Units</u>	<u>Projection</u>
Condensation Pressure Spread (CPS)	Gradient 850,700	mbx10	6,12
Total Cloud Cover	-	Percent	6, 12, 18, 24, 30, 36, 42, 48
Layered Cloud	Gradient, 850, 700, 500, 300	Percent	6, 12, 18, 24, 30, 36, 42, 48
Temperature	Gradient, 850, 700, 500, 300	deg Kx10	6, 12, 18, 24, 30, 36, 42, 48
Dew Point	Gradient, 850, 700, 500, 300	deg Kx10	6, 12, 18, 24, 30, 36, 42, 48
QPF	-	Inchesx100	12, 24, 48
3 hr X-Displacement	850, 700, 500, 300	$\frac{\text{Grid Units} \times 10}{2}$	6, 12, 18, 24, 30, 36, 42, 48
3 hr Y-Displacement	850, 700, 500, 300	$\frac{\text{Grid Units} \times 10}{2}$	6, 12, 18, 24, 30, 36, 42, 48
3hr Vertical Displacement	850, 700, 500, 300	mb x 10	6, 12, 18, 24, 30, 36, 42, 48

4.1.3 3DNEPH Data Collection. Cloud analysis fields generated by the 3DNEPH model are produced at AFGWC and shipped to USAFETAC/OL-A for archive. For use in MOS development, the fields are retrieved for specific areas. Those areas for which AFGWC/TSMS currently retains data are shown in Figure 2. The 3DNEPH model is described in detail by Fye (1978). Table 3 lists variables archived from the 3DNEPH.

Table 3. Variables Archived from the 3DNEPH Cloud Analysis Model.
Data is saved for every 3-hourly cycle (00-21).

<u>Variable</u>	<u>Unit</u>	<u>Layers</u>
Cloud Type	1-15	Low, Mid, High
Present Weather	0-9 (WMO CODE 4677)	-
Maximum Tops	0-99 (WMO Code 1677)	-
Minimum bases	0-99 (WMO Code 1677)	-
Total Cloud Cover	Percent	-
Layered Cloud Cover	Percent	1-15

4.1.4 Surface Observations Data Save. When a requirement exists to produce MOS forecasts in an area, AFGWC/TSMS requests surface observations for the area from USAFETAC/OL-A. OL-A screens surface observation records from the area identifying those stations which have the best data. This station list is then furnished to TSMS to be used in data interpolation and to USAFETAC/DN for use in developing modeled climatology. Surface observation data for the required season are then processed into the MOS format at OL-A. Table 4 lists those surface weather elements that are archived for MOS.

Table 4. Archived Surface Weather Elements

<u>Element</u>	<u>Unit</u>
Sea level pressure	mb x 10
Obstruction to Visibility	Coded 0 = None of the following 1 = Smoke (K) 2 = Haze (H) and smoke and haze (HK) 3 = Blowing obstruction (BD, BN, BS, BY) 4 = Fog (F) 5 = Ice Fog (IF) 6 = Ground Fog (GF)
Ceiling	ft/100 (Unlimited = 888)

Table 4. Archived Surface Weather Elements (Continued)

Total Sky Cover	<p>Coded</p> <p>0 = clear</p> <p>1 = partial obscuration</p> <p>2 = thin scattered</p> <p>3 = thin broken</p> <p>4 = thin overcast</p> <p>5 = scattered</p> <p>6 = broken</p> <p>7 = overcast</p> <p>8 = obscured</p>
Visibility	meters
Present Weather	<p>Coded</p> <p>0 = None of the following</p> <p>1 = L-, L--</p> <p>2 = L</p> <p>3 = L+</p> <p>4 = R-, R--</p> <p>5 = R</p> <p>6 = R+</p> <p>7 = RW-, RW--</p> <p>8 = RW</p> <p>9 = RW+</p> <p>10 = ZL-, ZL--</p> <p>11 = ZL</p> <p>12 = ZL+</p> <p>13 = ZR-, ZR--</p> <p>14 = ZR</p> <p>15 = ZR+</p> <p>16 = any combination of frozen precipitation</p> <p>17 = IP-, IP--, IPW-, IPW--</p> <p>18 = IP, IPW</p> <p>19 = IP+, IPW+</p> <p>20 = S-, S--, SP-, SP--,</p> <p>21 = S, SP, SG</p> <p>22 = S+, SP+, SG+</p> <p>23 = SW-, SW--</p> <p>24 = SW</p> <p>25 = SW+</p>
Dew Point	Degrees Kelvin
Wind Direction	Degrees of the compass (reported to nearest ten degrees)
Wind Speed	Knots
U - Component (Wind)	Knots

Table 4. Archived Surface Weather Elements (Continued)

V - Component (Wind)	Knots
Temperature	Degrees Kelvin
6 - Hour Precipitation Amount	Millimeters
Maximum and Minimum Temperature	Degrees Kelvin
Severe Weather	Coded
	0 = None of the following
	1 = Squall (Q)
	2 = Thunderstorm (T)
	3 = Severe Thunderstorm (TS)
	4 = Hail (A)
	5 = Tornado
Snow Depth	Coded
	0 = None
	1 = Trace
	2 = 1 inches
	3 = 2 inches
	4 = 3 inches
	5 = 4 inches
	6 = 5 inches
	7 = 6-10 inches
	8 = 11-20 inches
	9 = over 20 inches

4.1.5 Climatology. Modeled climatology for the MOS system is prepared by USAFETAC/DNO. As of this date climatology for ceiling, visibility and surface wind (u,v components and speed) have been made available to AFGWC for all areas for which equations have been developed. The system provides climatology at synoptic hours for every month of the year. Since the climatology is modeled, the probability distributions can be derived for any categorical breakpoints desired. For ceiling and visibility these categories correspond to the forecast categories. An attempt is made to obtain climatology for each station on the development station list identified by USAFETAC/OL-A. Since this is not always possible the data is "spread" (interpolated) to those stations without adequate climatology by an objective analysis technique developed by Barnes (1964). When data density is insufficient for this, the only option left is manual entry of best-guess climatology values. Only MOS prediction equations for ceiling and visibility were developed using modeled climatology. To obtain better accuracy and speed, climatology for ceiling, visibility, surface wind and surface temperature was later regenerated in a "binned" (discrete) format; none of this was ever used in equation development due to the HQ AWS decision to terminate the MOS effort until the Global Spectral Model (GSM) data base is available.

4.2 Development Subsystem. The MOS development subsystem is designed to use the archived grid-point data from the AWSPE, 5LYR, and 3DNEPH models, surface observations, climatology, and constants to select those elements that can best predict surface weather. This subsystem solves the multiple, forward screening regression necessary to build the MOS prediction equation. Table 5 gives the surface weather elements for which equations are routinely developed. Figure 1 describes the basic flow of data through the development subsystem.

Table 5. MOS Surface Weather Elements

<u>Code</u>	<u>Element</u>	<u>Type</u>	<u>Categories</u>
WND 991	Wind	Scalar	Speed, U-component, V-component
SLP 834	Sea Level Pressure	Scalar	
TMP 294	Temperature	Scalar	
COV 804	Sky Cover	Probability	Clear, Scattered, Broken, Overcast
FOG 854	Obstructions to Visibility	Probability	None, Haze and Smoke, Blowing Phenomena, Fog
TRW 364	Thunderstorms	Probability	Yes/No
POP 604	Precipitation	Probability	Yes/No
LFZ 404	Precipitation Type	Probability	Liquid, Freezing, Frozen
LPT 304	Liquid Precipitation Type	Probability	Drizzle, Rain, Showers
CLG 104	Ceiling	Probability	0 C1 200 (ft AGL) 200 C2 500 500 C3 1000 1000 C4 3000 3000 C5 10000 10000 C6
VIS 154	Visibility	Probability	Europe/SWANEA: 0 V1 700 (meters) 700 V2 1800 1800 V3 3700 3700 V4 6000 6000 V5 8000 8000 V6 Asia/Pacific: 0 V1 800 (meters) 800 V2 1600 1600 V3 3200 3200 V4 4800 4800 V5 8000 8000 V6

4.2.1 Data Flow. To begin development of forecast equations the gridded AWSPE and 5LYR data must be interpolated to the individual stations on the station list obtained from USAFETAC/OL-A. The G300 program performs a bi-quadratic interpolation where possible, bi-linear in the outside grid interval, and linear extrapolation outside the grid. The program can process more than one gridded field at a time and can calculate predictor fields that were not available directly from the model as well as combine predictors derived from more than one model. Backward trajectory fields are computed from the AWSPE archived data by the G360 program. The output from G300 and G360 are merged onto a single tape or disk file called XTAPE which contains most of the model output predictors used in equation development. The G300 program is used to interpolate the 3DNEPH gridded data to station locations. These data are merged with the surface observations onto a single tape or disk file called YTAPE. The climatology data are written onto a third file. The primary statistical program used to produce regression equations is G600. This software performs a forward stepwise linear regression to develop an equation for each surface weather event or category offered. Although the capability exists for equations of up to 20 terms, only ten terms are used in the present AWS MOS set of equations. Predictors are taken from the XTAPE, YTAPE, climatology file, and constants file. G600 has the capability of producing single-station or pooled-stations (regional) equations. When a particular set of equations are complete they are packed, tested, and loaded into a file for operational use.

4.2.2 Regional Equation Development. Due to the short period of archived data available, it is difficult to capture a sufficient sample of some events which we need to predict. To overcome this deficiency, the AWS MOS system employs the regional equation concept. The data are grouped according to climatological factors and a set of equations is developed that, theoretically, applies equally throughout the region. This allows forecast equations to be developed in relatively data sparse regions and gives the advantage of being able to develop equations with a relatively small (2 to 3 years) data set. The regional concept makes it possible, also, to produce a forecast for any point in the region whether or not an observation had ever been taken at that point. The windows for which the AWS MOS system currently develops equations are shown in Figures 3 through 6. Each window is divided into a number of regions. The development station list for each region is listed in appendix B. The criteria for defining each window are given in Table 6. Even with the regional concept of equation development a complete equation set includes approximately 39,600 forecast equations requiring over 600 hours of development time on a UNIVAC 1100-series computer. The regional development concept becomes an obvious necessity.

Table 6. MOS Windows and Regions

<u>Window</u>	<u>Description</u>	<u>Number of Regions</u>
EUR	Europe	18
ASN	Asia (Korea and Japan)	11
SCS	South China Sea (Tawian and Phillippines)	5
OILP5	Near East area which falls within the usable portion of the European 5LYR archive window	7
OILPT	Near East area outside the 5LYER window but within the AWSPE octagon	6
AFRNO	African area for which the 3DNEPH is the only available model	1
AFRPT	African area outside the 5LYR window but within the AWSPE octagon	2

4.3 Operational Subsystem. Once the equation set is developed the equations can be integrated into the operational subsystem. Figure 7 shows the flow of data through the operational subsystem. The file CONSTANTS contains constants that were used in the equation development as predictors. The file FCSTEQN contains the equations after they have been packed along with the list of operational stations. The CLIMATOLOGY file contains station climatology for the operational stations. The operational program produces a file of forecasts for 0000 or 1200 GMT. Explanations of program execution times and products are given in in Section 5. Figure 8 gives a detailed diagram of all executable modules in the G900 runstream and all mass storage files accessed. An arrow from a file to a particular module indicates that data is being read from the file. An arrow from the module to the file indicates data is being written to the file. The following modules make up the operational runstream.

- G980 - determines the cycle of the run (either 0000 GMT or 1200 GMT) and passes this information to the run condition word.
- G910 - builds files MOSEQNS00 and MOSEQNS12 which contain all equations and options required for a particular run.
- G970 - checks the status of AFGWC data base for the required model fields, RHGWCF (5LYR), RTGWCF (AWSPE), RNGRDA(3DNEPH), and RTSFC(surface observations). G970 aborts the run if a required model is missing.
- G960 - builds the file TRAJECTORIES. G960 can compute a trajectory forecast for any point within the AFGWC Northern Hemisphere whole-mesh grid.
- G920 - calculates and writes all the predictor fields required for the run to the file PREDICTORS.
- G900 - computes forecasts for stations specified on the operational station list. G900 writes the forecasts to MOSMAT00 and MOSMAT12.

The execution of G900 terminates the operational runstream. The files MOSMAT00 and MOSMAT12 constitute the MOS data base for the 0000 GMT and 1200 GMT cycles. At this point any display program can access the files. The following programs make up the MOSXMT runstream which transmits the forecasts over the Automated Weather Network (AWN).

DISPAF - reads the MOS forecasts from either MOSMAT00 or MOSMAT12 file, formats them as bulletins, and writes them to the file FILE.

MOSSND - transmits the MOS bulletins via the AWN.

The following programs function off-line as part of the operational subsystem:

- G905 - packs equations produced by the development subsystem into the file FCSTEQN associating the operational stations with the appropriate equations.
- G940 - builds directories for files MOSMAT00, MOSMAT12, and CONSTANTS.
- G945 - builds the directory for the file CLIMATOLOGY.
- G950 - builds the file CONSTANTS.
- G955 - builds the file CLIMATOLOGY.



Figure 3. European MOS Window Showing Regions Used in Equation Development

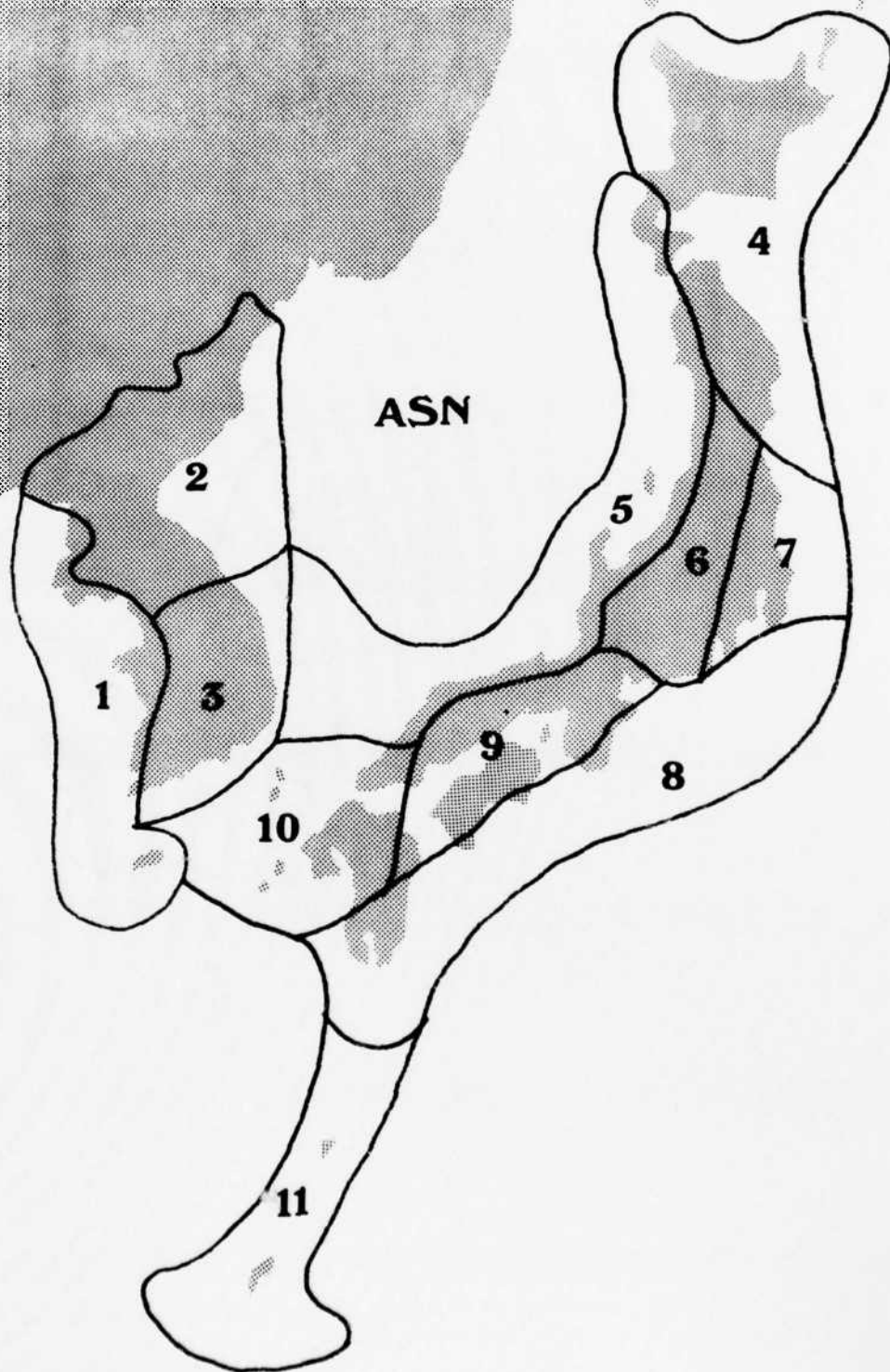


Figure 4. Asian MOS Window Showing Regions Used in Equation Development

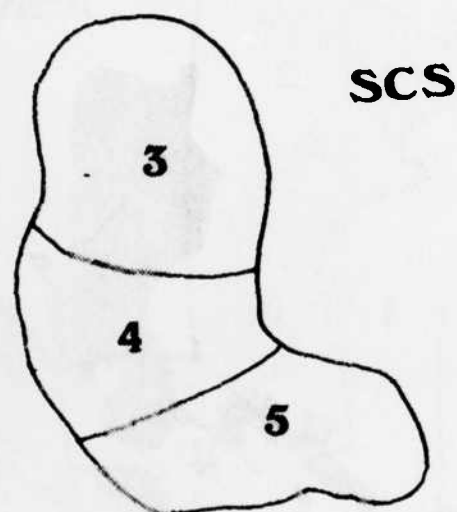
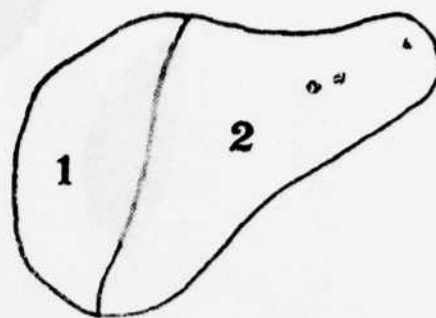


Figure 5. South China Sea MOS Window Showing Regions Used in Equation Development



Figure 6. Middle East and African MOS Window Showing Regions Used in Equation Development

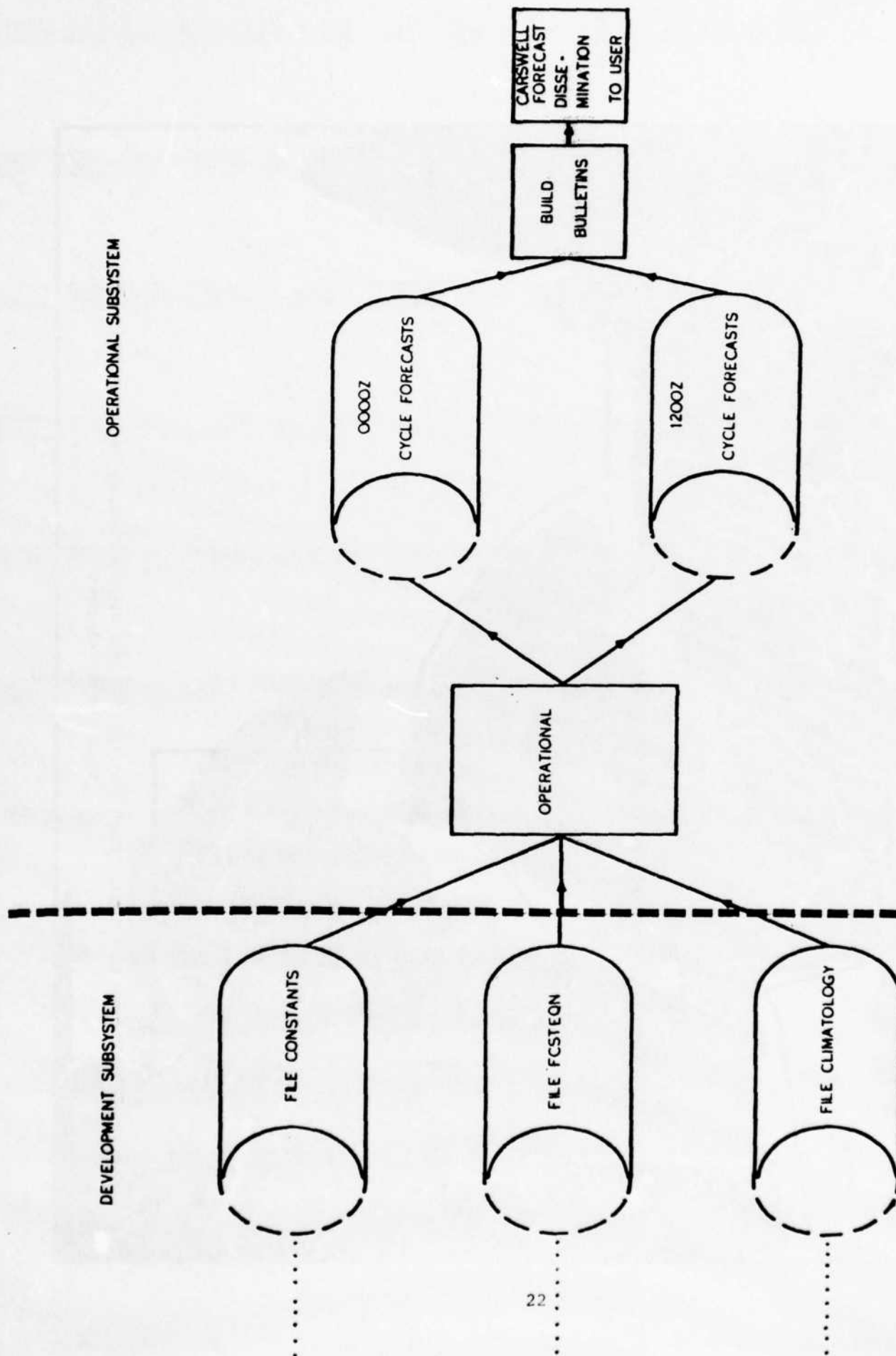
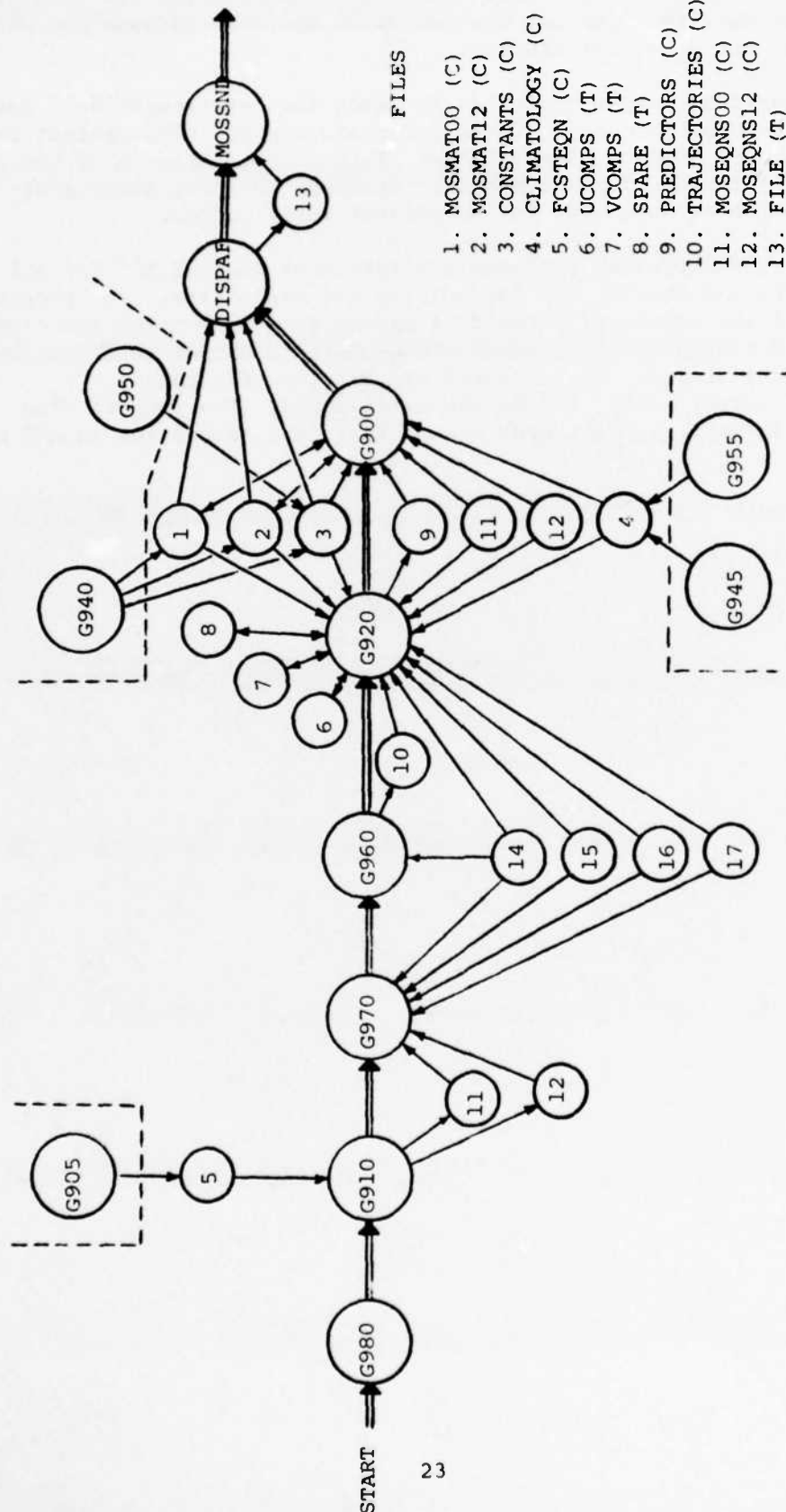


Figure 7. Operational Subsystem



C = Cataloged, T = Temporary

Figure 8. Depiction of Data Flow Through the Operational Subsystem

4.4 Verification Subsystem (MOSVER). Figure 9 shows the flow of data through the verification subsystem. Forecasts for the MOSMAT00 or MOSMAT12 files are saved daily following the execution of the operational run. Once a day the verifying surface observations are also saved. At the end of the month the verification is computed for the month and various statistics are displayed for analysis and quality control. The forecasts and observations are written to magnetic tape for permanent storage.

The forecast equations can be evaluated by using the development data base as input to generate MOS forecasts. These forecasts are verified against the development data set surface observations. This gives a measure of how well the forecasts fit the development sample. However, the most meaningful verification for operational use is independent verification.

Each month the MOSVER program produces statistics on the AWS MOS for all forecast elements and the NWS MOS for ceiling and visibility. The program calculates the Brier score, prepares contingency tables from the forecasts and verifying observations (see Section 6) and computes a number of scores based on the contingency tables. These scores are bias, prefigurance, post-agreement, threat score, and Heidke skill score. The program also produces a persistence forecast contingency table and calculates an AWS skill score.

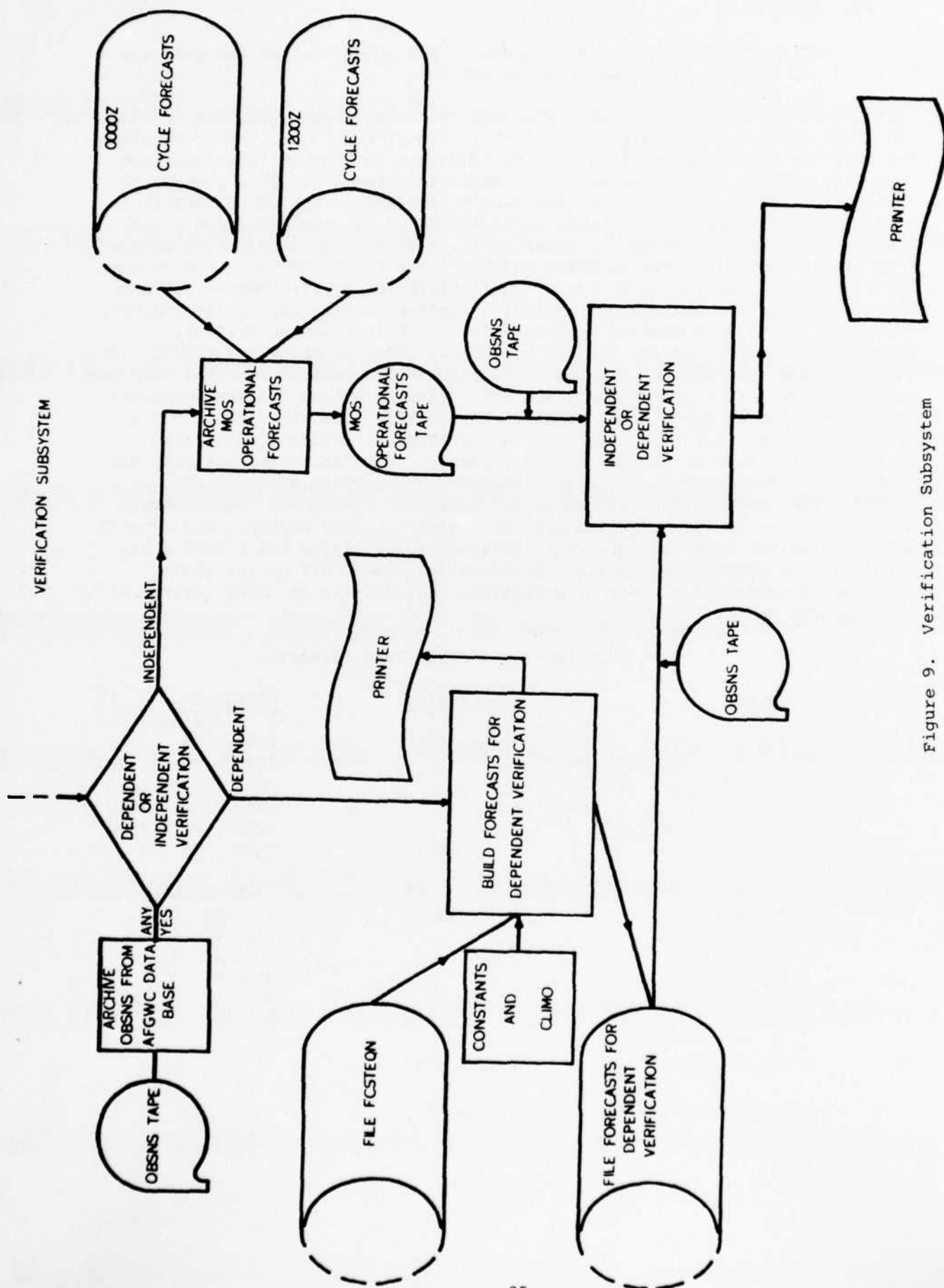


Figure 9. Verification Subsystem

5. MOS FORECASTING

5.1 Operational Production. AFGWC provides MOS guidance from two sources: NMC-produced NWS MOS and AFGWC-produced AWS MOS.

5.1.1 The NWS MOS forecasts are generated twice daily at approximately 0315Z and 1515Z following the completion of their LFM-II model run. AFGWC receives the complete MOS forecast files for 362 CONUS and 39 Alaskan locations (see Appendix 5) via a highly compacted communications package. This package is called the station-oriented forecast matrix (SOFTRIX). The CONUS SOFTRIX is received usually between the hours 0400Z and 0600Z for the 0000Z cycle and between 1630Z and 1830Z for the 1200Z cycle. The Alaska SOFTRIX is a separate transmission arriving between 0815Z and 0930Z for the 0000Z cycle and between 1930Z and 2100Z for the 1200Z cycle. Reliability of receipt varies for many reasons, but on the average, transmission receipt success rate is around 90%. After the SOFTRIX information is loaded into AFGWC's computer systems, AWS-owned software produces the MOS bulletins. MOS bulletins are produced for 149 CONUS and 13 Alaskan locations. These bulletins provide terminal forecast guidance from 6 to 48 hours past each cycle time in 6-hour snapshots (Alaska bulletins begin at the 12-hour point). The SOFTRIX data files contain most forecast elements out to 60 hours for all stations. Tables 7 and 8 give details on the content of the SOFTRIX elements. Details on the bulletin can be found in AFGWCP/105-1, Vol III. Other AWS MOS-derived products are extended forecasts (out to 60 hours) for CONUS TAC ranges and Space Shuttle missions, a 24- to 48-hour Eglin AFB, FL, range forecast message, and several map-oriented MOS displays (e.g. POP, ceiling probabilities below 3000 feet, etc.) for the Forecasting Services Division in AFGWC. All of the above describes an operational mode of operations that depends on joint government departmental cooperation.

Table 7. SOFTRIX Data Elements

<u>NCODE</u>	<u>Elements</u>	<u>Type (Unit)</u>	<u>Categories</u> (Ft AGL)
104	Ceiling	Probability	0 C1 200 200 C2 500 500 C3 1000 1000 C4 3000 3000 C5 7500 7500 C6
154	Visibility	Probability	(ST MILES) 0 V1 1/2 1/2 V2 1 1 V3 3 3 V4 5 5 V5 6 6 V6
204	Maximum Temperature	Scalar (°F)	
214	Minimum Temperature	Scalar (°F)	

Table 7. SOFTRIX Data Elements (Continued)

<u>NCODE</u>	<u>Elements</u>	<u>Type (Unit)</u>	<u>Categories</u>
294	Temperature	Scalar (°F)	
304	Liquid Precipitation Type	Probability	3-rain, drizzle, showers
364	Thunderstorms	Probability	1-percent chance
374	Severe Thunderstorms	Probability	1-percent chance of greater than 3/4 inch hail or wind greater the 50 knots in a thunderstorm
404	Precipitation Type	Probability	3-liquid, freezing, frozen
434	Probability of Snow Amount	Probability	1-Snow Accumulation greater than 4 inches in 12 hours
505	Wind Speed	Scalar (Knots)	
554	Wind Direction	Scalar (0-360°)	
604	6-hour Precipitation (POP)	Probability	1-precipitation accumulation greater than .01 inches in 6 hours
614	12-Hour Precipitation (POP)	Probability	1-precipitation accumulation greater than .01 inches in 12 hours
664	Dew Point temperature	Scalar (°F)	
704	6-Hour Precipitation Amount	Probability	3-6 hour accumulation exceeds or equals 1/4, 1/2, and 1 inch.
714	12-Hour Precipitation Amount	Probability	4-12 hour accumulation exceeds or equals 1/4, 1/2, 1, and 2 inches.
724	24-Hour Precipitation Amount	Probability	4-24 hour accumulation exceeds or equals 1/4, 1/2, 1, and 2 inches.
804	Sky Cover	Probability	4-clear, scattered, broken, overcast
834	Altimeter Setting	Scalar (inches)	
854	Obstruction to Visibility	Probability	4-none, haze or smoke, blowing phenomena, fog

Table 8. Forecast Projections Available in SOFTRIX Data Base
(C=Continental United States, A=Alaska, 00Z or 12Z=available
only with the 0000 or 1200 GMT cycle).

NCODE	PROJECTION									
	<u>6</u>	<u>12</u>	<u>18</u>	<u>24</u>	<u>30</u>	<u>36</u>	<u>42</u>	<u>48</u>	<u>54</u>	<u>60</u>
104	C	CA	CA	CA	CA	CA	CA	CA	C	C
154	C	CA	CA	CA	CA	CA	CA	CA	C	C
204				A-00Z		A-12Z		A-00Z		A-12Z
214				A-12Z		A-00Z		A-12Z		A-00Z
294	C	C	C	C	C	C	C	C	C	C
304		C	C	C	C	C	C		C	
364				C		C		C		
374				C		C		C		
404		CA	CA	CA	CA	CA	CA	CA		
434		C	C	C	C	C	C	C		
505	C	CA	CA	CA	CA	CA	CA	CA	CA	CA
554	C	CA	CA	CA	CA	CA	CA	CA	CA	CA
604		C	C	C	C	C	C	C	C-12Z	C-12Z
614				C		C		C		C
664	C	C	C	C	C	C	C	C	C	C
704		C	C	C	C	C	C			
714				C		C		C		
724						C		C		C
804	C	CA	CA	CA	CA	CA	CA	CA	C	C
834	CA	CA	CA	CA	CA	CA	CA	CA		
854	CA	CA	CA	CA	CA	CA	CA	CA		

Note: Alaskan NCODE=CONUS NCODE + 3

5.1.2 The AWS MOS forecasts are generated twice daily following the completed run of the 5LYR cloud prog model. Normally, MOS forecast files for 286 overseas locations (see Appendix 4) will be built by 0630Z and 1830Z immediately followed by the application programs. As of this date AWS MOS supports 194 European, 37 Middle-East, 21 NE Africa, and 34 West Pacific/SE Asian locations. The applications programs so far, only produce the MOS bulletin format with valid times 12 to 48-hours in 6-hour snapshots for 16 European, 37 Middle East, 20 NE African, and 34 W. Pac/SE Asian locations. No forecasts beyond a 48-hour projection are available from the AWS MOS system. However, saved data is available to set-up MOS equations to provide support out to 72 hours if needed.

5.2 Capabilities and limitation. The capabilities and limitations of both MOS systems as they impact potential DOD support are:

5.2.1 Add a station where MOS equations have coverage (i.e., NWS MOS covers the CONUS, but not Europe).

5.2.1.1 NWS: This can be done because the regionalization of most MOS equations permits an "anywhere" forecast capability--a surface observation is not mandatory for input. Requests to add CONUS and Alaskan stations are slow, however. The TDL liaison officer must be tasked to do the work who must arrange for changes in the NWS MOS system, allow for normal coordination through the mail system, and then wait for an implementation date. If the available file sizes and communications can handle the impact of an additional station, and the parties within NWS, NMC, and TDL agree, the new support can be established. Time to accomplish this task can run anywhere between 2 to 6 months.

5.2.1.2 AWS: AWS MOS's in a Contingency Response Capability (CRC) configuration. If the station is within the confines of an AWS MOS region and has been prepositioned in the climatology constants file, a new station can be on-the-air within 24 hours. If the prepositioned climatology file is unavailable, a new station requires 48 hours under optimum computer support, but may take up to 4 days.

5.2.2 Add a station where no MOS equation has been developed. The answer to this problem is valid for both NWS and AWS MOS support: build new MOS equations and implement. Both systems depend on an archive of forecast model fields which ultimately becomes the limiting factor.

5.2.2.1 NWS: The TDL archives the North American LFM-II and the North American area of the global spectral model outputs for equation development. Regions outside of these areas cannot use the MOS technology. Demands to establish new MOS regions outside of the established CONUS and Alaska areas would be more than the TDL liaison office could muster alone. Even if the manpower were available, such new areas (depending on how many elements are to be forecast) would take 1 to 2 years to complete if not longer.

5.2.2.2 AWS: AFGWC archives the entire NH AWSPE and three windows of the 5LYR cloud prog (North American, European, and Asia). The NH AWSPE is

considered usable with respect to its quality of forecast fields north of 22°N latitude. Below 22°N, the fields are either unreliable or non-existent. All regions, whether inside or outside these areas, require support from USAFETAC OL-A for associated 3DNEPH and surface observation data and from USAFETAC/DNO for climatology support. If a need to develop new MOS regions is identified, 6 to 12 months are needed depending on USAFETAC response (priority driven), in-house development computer time, and existing programmer expertise in TSMS.

5.2.3 Add a new forecast element. An example would be combined ceiling/visibility events such as IFR, MVFR, and VFR.

5.2.3.1 NWS: We would task our TDL liaison office which would develop the new product for existing supported locations. This would take between 6 to 12 months.

5.2.3.2 AWS: If the surface observation data base can support it, a MOS forecast equation can be made for any element in 1 to 2 months.

5.3 Probability Versus Scalar Forecasting. The MOS system (Klein, 1978) has the capability to produce forecasts in terms of a probability of an event occurrence or in terms of a scalar value. An example of an event which is ideally suited to probabilities is precipitation—it either occurs or it does not. This description of a binary event is fundamental to the understanding of how a MOS equation makes a probability forecasts. On the other hand, events which might be better suited to scalar form are temperature, wind speed, and altimeter. However, what is thought to be an ideal form for a given element may be controlled by several factors that should be examined.

5.3.1 Probability Forecasting. Virtually any meteorological event can be forecast using a probability scheme by partitioning the event into mutually exclusive and exhaustive categories. An example of this is the 4-category sky cover of clear (CLR), scattered (SCT), broken (BKN), and overcast (OVC). Each category is mutually exclusive; that is, if one were to convert the observed total sky cover from tenths (or eighths) into CLR, SCT, BKN, or OVC, one-and-only-one category would apply. For example, you cannot observe an event that will fall in two or more categories at the same time; hence a mutually exclusive categorization. Each category is also exhaustive in the sense that all contingencies are covered by these defined categories: CLR covers 0/10 (or 0/8), SCT covers 1/10 to 5/10 (or 1/8 to 4/8), BKN covers 6/10 to 9/10 (or 5/8 to 7/8), and OVC covers 10/10 (or 8/8) sky cover. Since we measure sky cover to the nearest tenth (or eighth), there is no observation that cannot be catalogued against one of these four categories. What about obscurations? Those cases are covered by defining which of the four categories they belong to. For example, partial obscurations can be placed in the CLR and total obscuration in the OVC categories. Now we're covered. Sky cover is not limited to four categories. It can just as easily be defined by categories that match every reportable value plus the two-condition obscuration for a total of 12 categories. The preferred way to decide on what categories to select is to match them against the categories that are required to be forecast. For example, if the requirement is to forecast ceiling vs no

ceiling, then a two-category yes/no categorization is all that is necessary. This is essentially a single probability value problem. This same procedure can be applied to temperatures (numerous categories, or perhaps below vs. above freezing), wind speeds, etc. Some elements are better categorized than kept in scalar form. Examples are visibility and ceiling. Both visibility and ceiling have open-ended values that causes a scalar approach to not perform as well as the categorization approach. The ceiling problem is that conditions above mid-level cloudiness are recorded by very crude terms such as "high", "250", and "300". How is "high" quantified as a scalar? Also, what if there is no ceiling, how is that quantified in a ceiling equation? This problem is avoided by grouping all "high" and no-ceiling events into a single category: above 8000 feet or no-ceiling. Visibility has the same problems. This event is highly localized in possible readings because of non-standardization in the placement of visibility markers (i.e., any building, TV tower, or mountain will do).

5.3.2 Scalar Forecasting. The clue to deciding whether a particular weather element would be an acceptable candidate for developing a scalar forecast equation instead of a probability forecast equation is judgement and common sense. If the element is considered fairly continuous in nature with no significant discontinuities, a scalar equation could be used. Here, reference is made mostly to analog-type events such as temperature, pressure, and wind where the changes from one response level to another are normally smooth. For example, when two successive observations show temperature readings of 82°F and 90°F, there is high confidence that all the temperatures in between did occur--they simply were not measured or recorded. The advantages of using scalar equations are that the output is directly useable (the system says 84°F, no more, no less) and needs only one equation versus many in a multi-category temperature equation set. The disadvantages are that there is no feel for how good that forecast is in either confidence limits or being able to convert into a probability environment (e.g. given a temperature forecast of 84°F, what is the probability that a temperature over 90°F will be observed?). Another subtle disadvantage is the distribution that scalar forecasts make as compared to the observed distribution of events. To illustrate this, consider using total sky cover in a scalar equation form. Instead of having four equations (one each for CLR, SCT, BKN, and OVC), one equation can be solved that will provide an answer in tenths (0 to 10). Now, let's take all the forecasts from such a scalar forecast equation and categorize them into the four CLR, SCT, BKN, OVC categories. Most of the forecast will fall in the SCT and BKN categories forming a bell-shaped distribution. If at the same time a frequency chart is made of the verifying observations, CLR and OVC conditions will be generally more frequent, thus forming a U-shaped distribution. If your objective is to create a sky-cover forecast with minimal absolute error or error variance, the scalar version will do; but if the objective was to replicate the observed U-shape distribution, it doesn't. There are at least two methods to obtain forecast distributions that match observed distributions: categorize for probability production or stretch-out the scalar forecasts in a specific way. The next paragraph describes both of these techniques.

5.4 Classification. Providing probability estimates of future events is perhaps the most realistic weather one can provide. After all, who can really tell the future in deterministic terms? The best anyone can do with their varying degrees of meteorological knowledge, skill, and experience is to predict in probabilities. Even when one "knows" that fog will occur, there always exists a chance that it won't. Whether this is called event-oriented forecasting or not, there exists either a level of confidence or probability of being correct (or incorrect). The underlying forecasting process is in fact probabilistic, not deterministic. It is only through some classification scheme that an event-oriented forecast can be made. In the fog example, that process is built within the forecaster's "mind." The MOS system's mind is a bit more simple than a human's and, therefore, needs an objective procedure to classify probability forecasts into event-oriented forecasts. One practical procedure used in both the NWS and AWS MOS systems is thresholding.

5.4.1 Probability Thresholding. Given a probability forecast, say p , what is the forecast choice? That is, will the event occur or not? If the choice is to predict occurrence at all times and the probability estimates are reliable, the number of correct forecasts will equal the number of occurrences (i.e. p times the number of forecasts you make). If the objective is to improve on this no-skill rate, some judgments will need to be made with respect to the value p itself. A first simple rule to use is the 50% rule. That is, if p exceeds .50, then forecast YES the event will occur, and if p is less than .50, then forecast NO. The decision is now reduced to a simple comparison between the probability forecast value and a test value called the threshold probability value (label this p^*). The use of the symbols p and p^* makes our decision rule:

If p exceeds p^* forecast YES; otherwise forecast NO. Simple? Yes, but is $p^* = .5$ the correct threshold value for the forecast problem? Here is where the utility of the forecasts must be considered. In a simple 2x2 contingency verification table, the frequency of forecast events can be altered by adjusting p^* to lower or higher values. Altering the verification table will alter the verification scores, optimism/pessimism (bias), and customer utility. Imagine what would happen if p^* was lowered to, say, 0.30. This means that more forecast probability values would exceed p^* under the new rule, thus permitting more YES forecasts to be made. This is what must be done if an unbiased verification table is sought (see Appendix A). This discussion deals with probability values, but scalar forecasts can also be altered to better fit an observed distribution of events. The procedure to do this is called inflation.

5.4.2 Inflation of Scalar Forecasts. Scalar forecasts seem to be easier to understand than probability forecasts. The output is a single, familiar value such as 78°F, 170° at 12 kts, 29.98 inches, and 7/10 cloud cover. These are forecasts already made in a categorical sense. For example, the 7/10 forecast is categorically a broken (BKN) condition. But if one was to think of the scalar forecasts in the same way probability forecasts are expected to behave, what is the scalar forecast's response to categorization? Unlike the distribution of probability forecasts where there is a clustering about two

means (those times where the event did not occur and where the event did) there is only one mean about which the scalar forecasts vary. This mean value is the same as the mean value of the observed events if the forecasts are unbiased. The principal difference between the forecast and observed events about this mean value is that the forecast values are normally tighter in their spread from the mean than are the observed events. This performance characteristic means that the odds of forecasting an outlier event (e.g., strong wind speeds) is very low. Conversely, the odds of having a valid forecast being in effect when an outlier event occurs is likewise low. To overcome this apparent weakness, scalar forecasts can be inflated to spread them to match the variability of the observed events distribution. The inflation formula is:

$$Y'' = C + (Y' - C)/R$$

where

Y'' is the inflated forecast

Y' is the original forecast

C is the mean of the event over the development sample

R is the multiple correlation of the equation that produced Y'

Practical applications of the inflation formula include spreading of wind speeds and cloud cover amounts. The typical problem with using unadjusted wind speed forecasts was mentioned above; and for cloud cover a sharper (more clear and cloudy) set of forecasts will result. Again, the application of the inflation formula is like the probability threshold applications: what is the desired result? If forecasts should match the observed event's distribution, use the inflation formula. If the error between the forecasts and observations is to be minimized, use the original uninflated forecast.

6. MOS FORECASTING HINTS ON USAGE

6.1 Interpreting Probabilities. Regardless of where a probability estimate of an event that is yet to occur (or not occur) is obtained, the user of this probability value is encumbered with a decision to be made. For example, if the probability of precipitation (POP) occurrence is 37% at the 24-hour forecast point, what will the yes/no forecast be for an important event such as a retirement parade. First, what are the situational odds? POP at 37% means that there is a 37% chance (i.e. 37 times out of 100) that it will precipitate, but there is no indication of intensity or duration. Second, should an arbitrary categorization rule be used to avoid a complex decision? For example, if POP exceeds 50% then forecast the occurrence of rain. That simple rule may not be true to the situation at hand, however. Reflect on this situation: POP = 37%. Forecast rain and it doesn't: disappointment (had to have the ceremony in a smelly hangar). Forecast no-rain and it does: anger (dumb Stormy). Forecast rain and it does: understanding disappointment (better a smelly hangar than wet people). Forecast no-rain and no-rain occurs: fresh-air happiness (nice Stormy). This situation makes the forecast a little more personal, doesn't it? The individual forecaster put under similar circumstances (since MOS doesn't account for everything), must use his/her meteorology and look at all the other available information. Got a storm radar-sensed band of precipitation coming into the area? This additional information can be used to raise the POP estimate. Got an upper level trough that will have passed through the area by parade time? That should lower the POP. MOS can provide a reliable probability estimate of future weather events, but on a practical (sometimes very practical) day-to-day use, the local forecaster is the best source of fine-tuning. There are only suggested ways to move the probability closer to zero or one, but even when the adjusted POP is say, up to 80%, is that high enough to say, "Yes, the parade will be a wash out?" One final note: The meaning of 37% was spelled out above, but occasionally this gets misinterpreted. Some have been told that a POP of 37% means that 37% of the area will be covered by precipitation--no!! The statistical relationship that produces the POP value was developed on the counts of precipitation occurrences found in surface observations--not in any near-miss sense. Therefore, the MOS forecasts estimate the probability of a "hit" at the station, not the areal coverage around the station.

6.2 Limits of Predictability. There are other features about the probability values that need to be known. One is that rare events (say, events with relative frequency of occurrence of less than 2%) are not handled well by the AWS MOS system. This is mostly due to the amount of events in the data archive with which the MOS equations are made (i.e., a sample size problem). A secondary, but just as valid, problem is the true predictive qualities of the available predictors. That is, if certain fields from the PE model are not well correlated with a sample of rare events, the statistical regression technique will not be able to find enough hooks to link up the prognoses fields to these rare events. A large part of this has to do with the scale of the phenomenon--the PE smooths out scales that are truly pertinent to thunderstorm forecasting, for example. On the other hand, the MOS equations do very well with the more synoptic scale features such as temperature,

altimeter setting, and wind. Another feature of the probability values is their feasible range. Boehm (1976) illustrates that the distribution of probability forecasts is a function of both the relative frequency of the event (call this C) and the correlation between the forecasts and the verifying observations (call this R). Experience shows, however, that MOS equations which attempt to predict low-frequency events have low correlations, and low correlations mean that the probabilities lose their sharpness (the ability to be close to zero and one) and tend to cluster about the value C. The binomial distribution can be used to illustrate the point for low values of R. The mean of the probability forecasts is some value between zero and one, and if the equations are reliable, this mean will be C. The standard deviation of forecasts about this mean is the square root of $C(1-C)$. Now, as an example, let $C=0.05$ and you will compute the standard deviation to be 0.2179. As a rough approximation, 95% of the forecast probabilities will be within ± 2 standard deviations of the mean, or in the interval 0 to 0.486. This means that a MOS forecast of an event that occurs at a climatological rate of 5% will be hard pressed to deliver a forecast probability in excess of 50%!! This is not the fault of the MOS system, because virtually any objective probability production procedure will have the same constraint. It's in the mathematics.

6.3 Adjusting MOS to Local Conditions. There are no secrets here, just hard-won experience and detailed local analysis of how MOS actually performed over the months. The use of large-scale area and time statistics are available but ideas are offered that might help to improve local terminal forecaster skills. The ideas that work the best may be different from place-to-place.

6.3.1 Golden Rules of MOS Support. Lowry (1980) describes some golden rules of MOS support that apply to NWS MOS. Those rules that are valid for AWS MOS products are paraphrased:

6.3.1.1 Watch for systematic dynamic model errors. Since MOS was derived on the relationship found between dynamic model outputs and surface observations, systematic model errors are accounted for through the statistical regression equations that generate the MOS forecasts. Since MOS already accounts for the long-haul average systematic error in the model, the MOS forecasts should not be adjusted to account for these differences. One can, however, remove smaller scale and daily deviations from the systematic errors to adjust MOS forecasts.

6.3.1.2 Check for models agreement. If more than one model is involved in the production of MOS forecasts, any disagreements will degrade the reliability of the probabilities. If one can determine which model might be the more accurate for the situation at hand, modification of MOS guidance in favor of that model is acceptable.

6.3.1.3 Watch the edges of spreading, or moving, meteorological events. For example, nearby or upwind stations begin observing rain as the 40% POP-line passes them--time the 40% POP-line passage at upstream locations. On another day this may be the 60% line, and so forth.

6.3.1.4 Watch out for tight forecast probability gradients. There may be significant differences in probability of occurrence values between relatively close stations; therefore, a slight shift in a weather-producing system may push a particular station rather quickly into a low or high threat region.

6.3.1.5 Add the local effects. Although local considerations such as station elevation, latitude, longitude, and climate are offered to the MOS system as potential predictors, not all local effects are quantified. Local forecasters know best how that nearby swamp, the urban heat island, or the valley orientation affects local weather to a degree that centralized generalization cannot match. Use this local knowledge to modify MOS forecasts accordingly.

6.3.1.6 Beware of rare events. A typical example is the occurrence of a tropical storm near the station of concern. Since very few of these events are likely to have been in the data upon which the MOS equations were derived, such future events may not initialize the MOS forecasts sufficiently well. Anticipate, for example, the underestimate of wind speeds and precipitation amounts when a tropical storm might be influencing the area.

6.3.1.7 Are there initialization errors in the basic models? MOS ties the dynamics together in sensible ways (e.g. higher relative humidities link to higher POP values, stronger low level winds link to higher surface wind forecasts, etc.). Therefore, any additional knowledge, such as poor models initialization, can be used to modify MOS forecasts accordingly.

6.3.1.8 Add later known data and meteorological information such as radar reports, PIREPS, satellite, local analyses, etc. All this information is not available to the MOS system directly nor is it as timely as the forecaster's access.

6.3.2 Tracking Biases. The 11WS (Alaska) has a very comprehensive program on MOS verification at individual stations and has documented ways to better take advantage of the MOS support. Completed analyses show, in part, the effect of NMC's model change from the PE to the spectral, because the MOS equations used in Alaska were developed originally from PE-based forecast fields. For example, the surface wind speed MOS equations include the mean boundary layer wind speed as a predictor. The change from PE to the spectral model redefined the boundary layer (as the MOS System defines it) as a deeper layer; hence stronger mean winds. Alaskan MOSVER shows a steady positive bias (overforecasting). Local biases documentation is important in order to adjust the MOS forecast. To do this, separate charts should be maintained for each cycle (00Z and 12Z) and for each projection. For example, if one wants to track local biases for temperature, you will need 2 cycles times 7 projections, or 14 charts would be needed. Plot (or log) forecast and verified temperatures everyday and refer to these charts to help determine bias trends. Because there are 14 different MOS equations involved, 14 charts are needed. In the case of ceilings with its 6 categories, there are $6 \times 14 = 84$ equations involved. Since manually keeping 84 charts would most likely be too large an administrative burden, identify one, or only a few, forecast criteria problems (perhaps ceilings less than 1000 feet and less than 3000 feet). Keep charts of the forecast "categories" (not the actual bulletin display values)

and the accompanying verification categories. This would reduce the numbers of charts needed. This charting technique is a subjective pattern recognition procedure of sorts. This idea comes from the early 1970's AWS/DN trajectory work where, for example, severe thunderstorm occurrences were often preceded by very characteristic trajectory forecast traces derived from charts plotted daily.

Crowley (1981) shows another approach to improve local forecasts by charting one MOS forecast element against another. He found a correlation between the MOS minimum temperature forecasts and MOS wind speed forecasts. He plotted the average temperature verification error (also called bias) as a function of the wind speed forecasts. He clearly shows a technique that can be applied to local MOS forecasts to enhance the original information. This idea can be used to find joint associations at any location.

6.3.3 Regional Verification. Verification of MOS forecasts (MOSVER) performed at the Statistical Systems Section (AFGWC/TSMS) also provides a means to assist local forecasters. For example, when the MOS bulletin indicates that a particular station will have a category 2 ceiling, what are the odds that the verifying ceiling will fall in category 1, category 2 (correct forecast), category 3, etc? These values can be computed from archives of past MOS forecasts and observations, but are not available for all locations. This problem is overcome to some degree by collecting a regional set of MOSVER statistics.

Table 9 is such a collection. This verification table was created by first noting what category the MOS forecast made (e.g., category 2) and then logging the category of the actual verifying observation. In Table 9, for example, in a sample of 960 MOS forecasts, 50 forecasts of category 2 were made and 11 of these verified exactly in category 2. This table of raw numbers can now be converted into a useful probability table for future use by the forecaster. Table 10 is such a table. This table displays the conditional probabilities of observing any particular category for all possible MOS forecast categories. For example, if the MOS forecast is for category 5, the probability of getting an exact category 5 verification is 35%, of verifying in category 6 is 51%, of verifying lower than category 5 is 14% (sum of categories 1 through 4 values), etc. Other information is also made available to the forecaster such as the sample size that was used in computing these probabilities and the sample climatology. These values are also computed from the raw data in Table 9. Every other MOS forecast can be analyzed and used in a manner similar to this.

Table 9. A Combined MOS Verification Contingency Table for the Stations at Beale, McClellan, Castle, Mather and Travis Air Force Bases.

		MOS FORECAST CATEGORY						TOTALS
		1	2	3	4	5	6	
OBSERVED CATEGORY	1	4	1	1	1	1	9	17
	2	14	11	3	4	3	6	41
	3	4	4	9	8	2	9	36
	4	3	4	11	27	17	7	69
	5	4	9	15	43	57	32	160
	6	7	21	12	27	82	488	637
	TOTS	36	50	51	110	162	551	960

Table 10. Table of Conditional Probabilities of Observed Event Category given the MOS Forecast Category. These values are computed from Table 9 values.

		MOS FORECAST CATEGORY						SAMPLE CLIMO
		1	2	3	4	5	6	
OBSERVED CATEGORY	1	.11	.02	.02	.01	.01	.02	.02
	2	.39	.22	.06	.04	.02	.01	.04
	3	.11	.08	.18	.07	.01	.02	.04
	4	.08	.08	.22	.25	.10	.01	.07
	5	.11	.18	.29	.39	.35	.06	.17
	6	.19	.42	.24	.25	.51	.89	.66
	SAMPLE SIZE	36	50	51	110	162	551	960

REFERENCES

- Barnes, S. L., 1964: A Technique for Maximizing Details in Numerical Weather Map Analysis, Journal of Applied Meteorology 3, 369-409.
- Bermowitz, R. J. and E. A. Zurndorfer, 1978: On the Use of the LFM Predictors in PE-based POPA Equations, National Weather Digest 3, 45-47.
- Boehm, A. R., 1976: Transnormalized Regression Probability. AWS/TR-75/259, Air Weather Service, Scott AFB, IL.
- Crowley, C., 1981: MOS Minimum Temperature Error Relative to Wind Speed, National Weather Digest 6, 18-21.
- Fye, F. K., 1978: The AFGWC Automated Cloud Analysis Model. AFGWC/TM-78/002, Air Force Global Weather Central, Offutt AFB, NE.
- Glahn, H. R. and D. A. Lowry, 1972: The Use of Model Output Statistics (MOS) in Objective Weather Forecasting. J. Appl. Meteor. 11, 1203-1211.
- Hoke, J. E., J. L. Hayes, and L. G. Renninger, 1981: Map Projections and Grid Systems for Meteorological Applications. AFGWC/TN-79/003, Air Force Global Weather Central, Offutt AFB, NE.
- Klein, W. H., 1971: Computer Prediction of Precipitation Probability in the United States. J. Appl. Meteor. 10, 903-915.
- Klein, W. H., 1978: Model Output Statistics in the Western United States, National Weather Digest, 3, 28-36.
- Klein, W. H. and H. R. Glahn, 1974: Forecasting Local Weather by Means of Model Output Statistics. Bulletin of the American Meteorological Soc. 55, 1217-1227.
- Lowry, D. A., 1980: How to Use and Not to Use MOS Guidance, Preprint from the Eighth AMS Conference on Weather Forecasting and Analysis, June 10-13, Denver Colorado, American Meteorological Society, Boston, MA, pp. 11-12.
- Panofsky, H. A. and G. W. Brier, 1965: Some Applications of Statistics to Meteorology. The Pennsylvania State University, University Park, PA.
- Snellman, L. W., 1977: Operational Forecasting Using Automated Guidance. Bulletin of the American Meteorological Soc. 58, 1036-1044.
- Tarbell, T. C., F. P. Lewis, L. G. Renninger, and A. M. Weiner, 1982: The Air Weather Service Primitive Equation Models. AFGWC/TN-82/001, Air Force Global Weather Central, Offutt AFB, NE.
- Wassall, R. B., 1977: A Study of the Significance of Forecaster Changes to MOS Temperature Guidance, National Weather Digest, 2, 27-30.

APPENDIX A

Miller-Best II Threshold Model by Lt Col D. L. Best

1. INTRODUCTION. This paper is a sequel to TDL Office Note 78-14, A Model for Converting Probability Forecasts to Categorical Forecasts, by R. G. Miller and D. L. Best. In the course of applying the original threshold model (now referred to as the MB-I model) described in TDL O.N. 78-14, results were unsatisfactory in those cases where the MOS equations contained a low correlation coefficient (R) and/or where the relative frequency (C) of the forecast event was low. Since there are many instances where a low R and/or C occurs, an investigation was launched to correct the problem. This paper illustrates this weakness and presents a modification to the original model that significantly reduces the low-end problem.

2. MB-II MODEL DEVELOPMENT.

a. ANALYSIS OF THE MB-I UNIT BIAS MODEL. The basic issue is to derive threshold probabilities that will convert a probability forecast into a categorical forecast in such a way as to obtain a ratio of forecasts to observed events (bias) of unity (i.e., forecast an event as often as it occurs). The original MB-I model was designed for this desired response and is solved by: $p^* = R(.5 - C) + C$. Considerable empirical evidence was collected before confidence was established that this model indeed gave satisfactory unit bias response. Upon reflection, however, the confidence-building cases dealt with forecast equations that had reasonably healthy correlations (R) and climatologies (C). Subsequent attempts to apply this model to certain rare events like total precipitation greater than 1 inch showed a significant underforecasting or less-than-one bias. To better understand what might have been underlying this apparent failure, 134 pairs of correlation and climatology (R,C) values from 134 MOS equations were run through special computer programs to establish what the optimum threshold probability value (p^*) actually should be. This was done over the dependent development sample. The equations' correlations (R) and climatologies (C) were then used to compute the MB-I values. To judge the MB-I values against the ground-truth values a simple ratio (MB-I values divided by optimum values) was chosen. Figures 1 and 2 are the results of this procedure. Each figure has both of the MB-I (labeled PM) and MB-II (labeled PB) model responses. Further discussion will follow the introduction of the MB-II model below.

b. MB-II UNIT BIAS MODEL. The actual evolution of the MB-II model was 90% inspiration and 10% derivation. Historically, Miller and Best had experimented with many forms of simple procedures and calculation schemes to convert probability forecasts into categorical choices. The first acceptable model and procedure was published in TDL ON 78-14. The earlier throw-away techniques were revisited in hopes that a clue might be found for a simple fix. Each was examined against the optimum p^* data file through plot analyses. One particular model had a curious effect when compared to the MB-I model response: it was practically the mirror image. In other words, where MB-I was producing p^* estimates too high, the other technique was producing p^* estimates too low, and vice versa. This model was a weighted-means technique:

$$p^* = C m_0 + (1-C) m_1 \quad (1)$$

where C was defined above, m_0 is the mean of the probability forecasts when the verifying observation showed non-occurrence ($Y=0$), and m_1 is the mean of probability forecasts when the verifying observation showed occurrence ($Y=1$).

Miller and Best (1981) showed that in terms of the forecast equations' R and C values:

$$m_0 = C(1-R^2) \text{ and} \quad (2)$$

$$m_1 = R^2 + C(1-R^2) \quad (3)$$

Entering (2) and (3) into (1) and with some manipulation yields.

$$p^*_0 = .2R^2 (.5-C)+C \quad (4)$$

The final inspiration that led to the MB-II version was that if two methods had opposite weaknesses and their responses bracketed the desired solution, why not simply take the mean of the two and define a new model (thus the MB-II):

$$p^* = .5 (R(.5-C)+C+.2R^2 (.5-C) +C)$$

which reduces to

$$p^* = (.5+R)R(.5-C)+C \quad (5)$$

Thus the MB-II model varies only by the correlation control factor and both have the same general form as the MB-I model:

$$p^* = F(.5-C)+C$$

where $F=R$ in MB-I and $F=(.5+R)R$ in MB-II.

3. DISCUSSION AND CONCLUSIONS. Figures 1 and 2 demonstrate that MB-II is better able to fit the optimum threshold values at lower R and C values than the MB-I. Figure 1 shows that over the range of possible correlations, MB-I loses its fit below $R=.3$, but the MB-II extends the fit down to $R=.1$ before failing. In the region below $R=.1$, MB-II provides p^* estimates closer to optimum than does MB-I even though both are weak there.

Figure 2 shows much the same effects as described above over the range of climatology (relative frequency of the event). Here, MB-I loses fit below $C=.05$ whereas MB-II is accurate down to a low $C=.01$.

It is difficult to rationalize why anyone would want to use probability forecasts that come from equations with correlations and climatologies in the low limits where MB-I breaks down. However, the business of weather forecasting in many instances, finds its benefit and value to the customers of weather support in the skills of forecasting the rarer events (i.e. low C).

The MB-II goes a long way, therefore, in meeting this need over MB-I, particularly if one is challenged to convert low-end probability forecasts to yes-no decisions.

CLOSING NOTE: This method has been improved upon by Miller and Best (1981) by a parameterization of the probability forecasts into betadistributions. This newer methodology permits a wide range of threshold values to be computed depending on desired categorical responses--a key to optimizing customer support.

4. REFERENCES.

Mason, I., 1979: On Reducing Probability Forecasts to Yes/No Forecast. Monthly Weather Review 107, 207-211.

Miller, R. G. and D. L. Best 1978; A Model for Converting Probability Forecasts to Categorical Forecasts. TDL Office Note 78-14, National Weather Service, NOAA, U.S. Department of Commerce.

Miller, R. G. and D. L. Best 1981; A Beta Classification Model. TDL Office Note 81-8, National Weather Service, NOAA, U.S. Department of Commerce.

THRESHOLD MODELS' SENSITIVITY

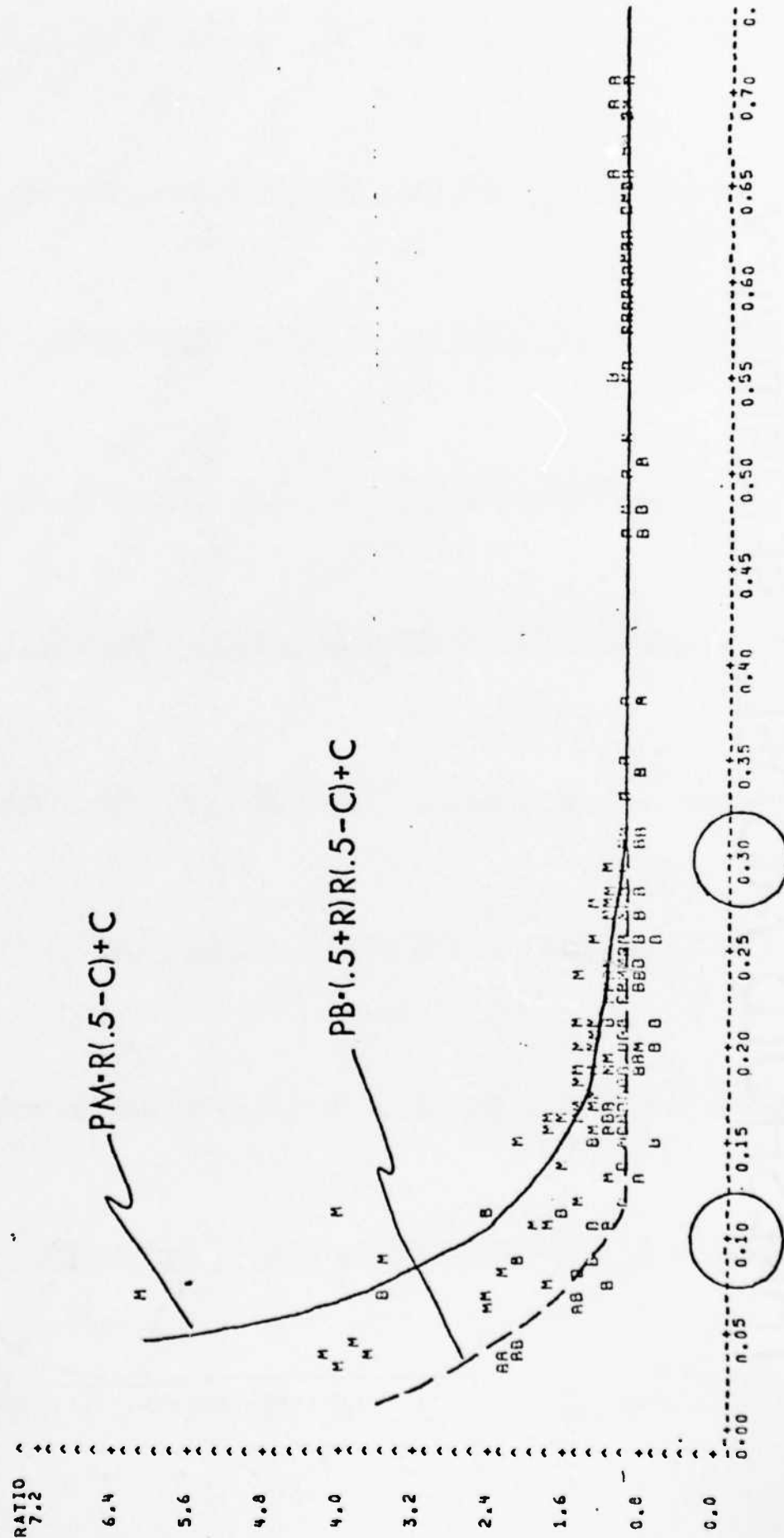


Figure 1. Comparison of MB-I (PM) and MB-II (PB) Model Responses Over the Range of Possible Correlations

THRESHOLD MODELS' SENSITIVITY

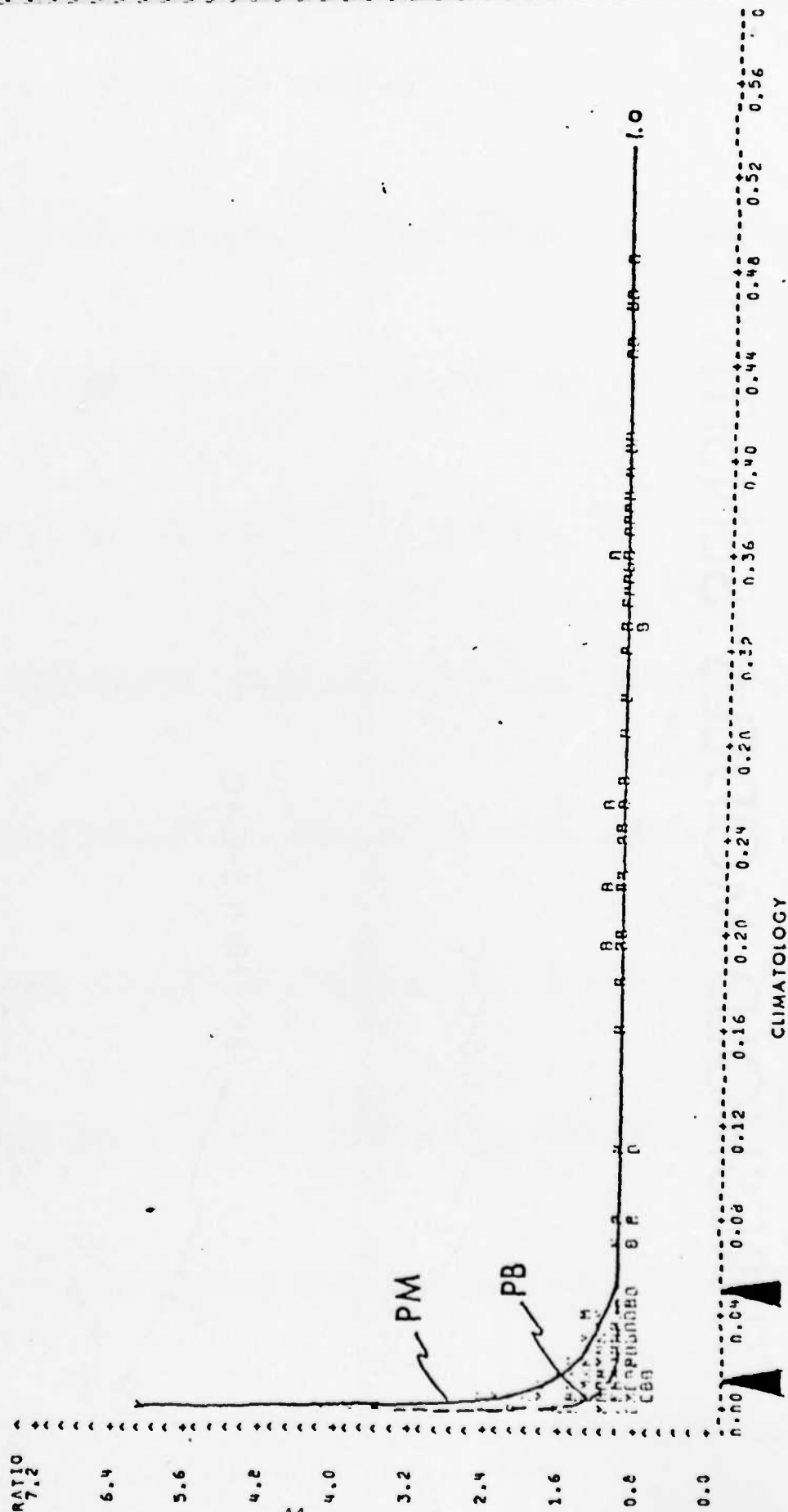


Figure 2. Comparison of MB-I (PM) and MB-II (PB) Model Responses Over the Range of Climatological Relative Frequency of the Event)

APPENDIX B

List of Overseas Operational and Development Stations

OPERATIONAL STATION LIST

EUROPE (EUR)

Region 1

<u>NUMBER</u>	<u>ICAO</u>	<u>NAME</u>	<u>LAT</u>	<u>LONG</u>
010100	ENAN	Andoya/Andenes, NO	69°18'N	16°07'E
010230	ENDU	Bardufoss, NO	69°04'N	18°32'E
011520	ENBO	Bodo, NO	67°17'N	14°25'E
011830	ENEV	Evenes, NO	68°30'N	16°41'E
012410	ENOL	Orland, NO	63°42'N	9°37'E
012710	ENVA	Vaernes, NO	63°28'N	10°56'E
013110	ENBR	Bergan/Flesland, NO	60°17'N	5°13'E
014150	ENZV	Stavanger/Sola, NO	58°53'N	5°38'E

Region 2

<u>NUMBER</u>	<u>ICAO</u>	<u>NAME</u>	<u>LAT</u>	<u>LONG</u>
030680	EGQS	Lossiemonth, UK	57°43'N	3°20'W
030750	EGPC	Wick, UK	58°27'N	3°05'W
030910	EGPD	Aberdeen/Dyce, UK	57°12'N	2°12'W
031300	EGOY	West Freugh, UK	54°51'N	4°57'W
032040	EGNS	Isle of Man/Ronald, UK	54°05'N	4°38'W
032570	EGXE	Leeming, UK	54°18'N	1°32'W
033600	EGXI	Finninglery, UK	53°29'N	1°00'W

Region 3

<u>NUMBER</u>	<u>ICAO</u>	<u>NAME</u>	<u>LAT</u>	<u>LONG</u>
033770	EGXN	Waddington, UK	53°10'N	0°31'W
033790	EGYD	Cranwell, UK	53°02'N	0°30'W
033910	EGXC	Coningsby, UK	53°05'N	0°10'W
033951	EGXA	Manby, UK	53°21'N	0°05'E
034620	EGXT	Wittering, UK	52°37'N	0°28'W
034700	EGYH	Holbeach Gun Range, UK	52°51'N	0°10'E
034701	EGUP	Sculthorpe, UK	52°50'N	0°45'E
034950	EGYC	Coltishall, UK	52°46'N	1°21'E
035580	EGVW	Bedford, UK	52°13'N	0°29'W
035621	EGWZ	Alconbury, UK	52°22'N	0°13'W
035771	EGUN	Mildenhall, UK	52°22'N	0°29'E
035831	EGUL	Lakenheath, UK	52°24'N	0°34'E
035951	EGVG	Woodbridge, UK	52°05'N	1°24'E
035961	EGVJ	Bentwaters, UK	52°08'N	1°26'E
036440	EGVA	Fairford, UK	51°41'N	1°46'W
036490	EGVN	Brize Norton, UK	51°45'N	1°35'W
036531	EGUD	Abingdon, UK	51°41'N	1°19'W

<u>NUMBER</u>	<u>ICAO</u>	<u>NAME</u>	<u>LAT</u>	<u>LONG</u>
036551	EGUA	Upper Heyford, UK	51°56'N	1°15'W
036580	EGUB	Benson, UK	51°37'N	1°05'W
036880	EGVT	Weathersfield, UK	51°58'N	0°30'E
037435	EGVI	Greenham Common, UK	51°23'N	1°17'W
037460	EGDM	Boscombe Down, UK	51°10'N	1°45'W
037610	EGVO	Odiham, UK	51°15'N	0°57'W
037660	EGUF	Farnborough, UK	51°17'N	0°45'W

Region 4

There are no operational stations in this region.

Region 5

<u>NUMBER</u>	<u>ICAO</u>	<u>NAME</u>	<u>LAT</u>	<u>LONG</u>
080870	LEBR	Bardenas Reales, SP	42°12'N	1°27'W
081605	LEZA	Zaragoza (USAF), SP	41°40'N	1°02'W
081810	LEBL	Barcelona/Munta, SP	41°17'N	2°04'E
082270	LETO	Madrid/Torrejon, SP	40°29'N	3°27'W
083970	LEMO	Moron De La Frontera, SP	37°09'N	5°36'W
084100	LEBA	Cordoba, SP	37°51'N	4°51'W
084490	LERT	Rota Naval Station, SP	36°39'N	6°21'W
084820	LEMG	Malaga, SP	36°39'N	4°28'W

Region 6

<u>NUMBER</u>	<u>ICAO</u>	<u>NAME</u>	<u>LAT</u>	<u>LONG</u>
060300	EKYT	Alborg, DN	57°06'N	9°52'E
060600	EKKA	Karup, DN	56°17'N	9°08'E
061000	EKVA	Vandel, DN	55°43'N	9°13'E
061100	EKSP	Skrydstrup, DN	55°14'N	9°16'E

Region 7

<u>NUMBER</u>	<u>ICAO</u>	<u>NAME</u>	<u>LAT</u>	<u>LONG</u>
062650	EHSB	Soesterberg, NL	52°08'N	5°16'E
062900	EHTW	Twenthe/Enshed, NL	52°16'N	6°54'E
063401	EHWO	Woensdrecht, NL	51°27'N	4°21'E
063500	EHGR	Gilze/Rijen, NL	51°34'N	4°56'E
063750	EHVK	Volkel, NL	51°39'N	5°42'E
063850	EHDP	De Peel/Venray, NL	53°31'N	5°52'E
064000	EBFN	Koksijde, BX	51°05'N	2°39'E
064320	EBCV	Chievres, BX	50°34'N	3°50'E
064560	EBFS	Florennes, BX	50°14'N	4°39'E
064790	EBBL	Klein-Brogel, BX	51°10'N	5°28'E
100220	EDNL	Leck, DL	54°48'N	8°57'E
100460	EDCK	Kiel/Holteau, DL	54°23'N	10°09'E
100380	EDNQ	Hohn/Rendsburg, DL	54°19'N	9°32'E
101220	EDNJ	Jever, DL	53°32'N	7°53'E
101360	EDCN	Nordhotz-Spieka, DL	53°46'N	8°40'E

NUMBER	ICAO	NAME	LAT	LONG
101470	EDDH	Hamburg, DL	53°38'N	9°59'E
102180	EDNA	Alhorn, DL	52°53'N	8°14'E
102340	EDCR	Rotenburg/Hannover, DL	53°08'N	9°21'E
102530	-	Luchow, DL	52°58'N	11°10'E
103370	EDCD	Hildesheim, DL	52°11'N	9°57'E
103430	EDCL	Celle, DL	52°36'N	10°02'E
104020	EDUW	Wildenrath, DL	51°07'N	6°13'E
104040	EDNZ	Goch, DL	51°41'N	6°10'E
104190	-	Ludenscheid, DL	51°14'N	7°36'E
104270	-	Kahler Asten, DL	51°11'N	8°29'E
104390	EDPF	Fritzlar, DL	51°07'N	9°17'E
104440	-	Gottinger, DL	51°33'N	9°57'E
104520	-	Braunlage, DL	51°43'N	10°37'E
105010	EDCM	Aachen, DL	50°47'N	6°06'E
105020	EDNN	Norvenich, DL	50°50'N	6°40'E
105090	EDCU	Butzweilerhof, DL	50°59'N	6°53'E
105260	-	Marienberg, DL	50°40'N	7°58'E
105325	EDEV	Friedburg AAF, DL	50°20'N	8°44'E
105420	-	Bad Hersfeld, DL	50°52'N	9°42'E
105445	EDEX	Fulda AAF, DL	50°33'N	9°39'E
106070	EDAD	Spangdalem, DL	49°58'N	6°42'E
106100	EDAB	Bitburg, DL	49°57'N	6°34'E
106160	EDAH	Hahn, DL	49°57'N	7°16'E
106190	EDZJ	Baumholder, DL	49°38'N	7°18'E
106265	EDEH	Bad Kreuznach AAF, DL	49°51'N	7°53'E

Region 8

There are no operational stations in this region.

Region 9

NUMBER	ICAO	NAME	LAT	LONG
091770	-	Teterow, DD	53°46'N	12°37'E
091800	ETBH	Barth, DD	54°20'N	12°43'E
092700	-	Neuruppin, DD	52°54'N	12°49'E
093610	-	Magdeburg, DD	52°06'N	11°35'E
094690	ETLS	Leipzig/Schkeuditz, DD	51°25'N	12°14'E
103840	EDBB	Berlin, DL	52°28'N	13°24'E

Region 10

NUMBER	ICAO	NAME	LAT	LONG
095540	ETEF	Erfut/Bindersleben, DD	50°59'N	10°58'E
095780	-	Fichtelberg, DD	50°26'N	12°57'E
106140	EDAR	Ramstein, DL	49°26'N	7°35'E
106145	EDIV	Pirmassens AAF, DL	49°13'N	7°37'E
106335	EDOT	Finthen AAF/Mainz, DL	49°58'N	8°09'E
106370	EDDF	Frankfurt/Main, DL	50°03'N	8°35'E
106405	EDEN	Maurice Rose AF, DL	50°11'N	8°40'E

NUMBER	ICAO	NAME	LAT	LONG
106420	EDID	Hanau, DL	50°10'N	8°57'E
106570	EDOF	Wertheim AAF, DL	49°46'N	9°29'E
106585	EDEG	Bad Kissingen, DL	50°12'N	10°06'E
106590	EDIN	Kitzingen AAF, DL	49°45'N	10°12'E
106595	EDEU	Giebelstadt AAF, DL	49°39'N	9°58'E
106710	-	Coburg, DL	50°16'N	10°57'E
106755	EDEJ	Bamburg AAF, DL	49°55'N	10°55'E
106850	EDQM	Hof, DL	50°19'N	11°53'E
106870	EDIC	Grafenwohr, DL	49°42'N	11°57'E
107120	EDAS	Sembach, DL	49°31'N	7°52'E
107140	EDAM	Zwiebrucken, DL	49°13'N	7°25'E
107220	EDAL	Sollingen, DL	48°47'N	8°05'E
107295	EDOR	Coleman AAF, DL	49°34'N	8°28'E
107340	EDIE	Heidelberg, DL	49°24'N	8°39'E
107380	EDDS	Stuttgart/Echter, DL	48°41'N	9°12'E
107382	-	Goppingen AAF, DL	48°43'N	9°41'E
107450	EDOP	Schwabisch Hall, DL	49°07'N	9°47'E
107520	EDIK	Illesheim AAF, DL	49°28'N	10°23'E
107550	EDEB	Ansbach/Katterbach, DL	49°19'N	10°38'E
107640	EDIG	Feucht AAF, DL	49°23'N	11°11'E
107715	EDIH	Hohenfels AAF, DL	49°13'N	11°50'E
107880	EDPS	Straubing, DL	48°49'N	12°35'E
107960	-	Zwiesel, DL	49°01'N	13°15'E
108050	EDAN	Lahr, DL	48°22'N	7°50'E
108450	EDSD	Leipheim Donau, DL	48°26'N	10°14'E
108530	EDSU	Neuberg/Donau, DL	48°43'N	11°13'E
108560	EDSL	Lechfeld, DL	48°11'N	10°52'E
108570	EDSA	Landsberg/Lech, DL	48°04'N	10°54'E
108600	EDSI	Ingolstadt, DL	48°43'N	11°32'E
108620	EDAV	Siegenberg GR, DL	48°45'N	11°48'E
108660	EDDM	Munchen/Rien, DL	48°08'N	11°43'E
108690	EDSE	Erding, DL	48°19'N	11°57'E
109000	EDSG	Bremgarten, DL	47°54'N	7°37'E
109080	-	Feldberg/Schwarz, DL	47°52'N	8°00'E
109210	EDPH	Neuhausen Ob Eck, DL	47°59'N	8°54'E
109470	EDSM	Memmingen, DL	47°59'N	10°14'E
109530	EDSK	Kaufbeuren, DL	47°52'N	10°37'E
114140	LKKV	Karlovy Vary, CZ	50°12'N	12°54'E
114480	-	Plzen/Dobruany, CZ	49°40'N	13°17'E
115180	LKPR	Prague/Ruzyne, CZ	50°06'N	14°15'E
115351	-	Bechyne, CZ	49°16'N	14°30'E
116360	-	Kostelni Myslov, CZ	49°11'N	15°28'E

Region 11

NUMBER	ICAO	NAME	LAT	LONG
109711	EDOV	Bad Tolz, DL	47°46'N	11°36'E
110100	LOWL	Linz/Horsching, OS	48°14'N	14°11'E
160365	LIYW	Aviano (USAF), IY	46°02'N	12°36'E

Region 12

<u>NUMBER</u>	<u>ICAO</u>	<u>NAME</u>	<u>LAT</u>	<u>LONG</u>
160660	LIMC	Milano/Malpensa, IY	45°37'N	8°44'E
160840	LIMS	Piacenza, IY	44°55'N	9°44'E
160880	LIPL	Brescia/Ghedì, IY	45°25'N	10°17'E
160900	LIPX	Verona, IY	45°23'N	10°52'E
161490	LIPR	Rimini, IY	44°01'N	12°38'E
163120	LIBV	Gioia Del Colle, IY	40°46'N	16°56'E
163180	LIBX	Martina Franca, IY	40°42'N	17°20'E

Region 13

<u>NUMBER</u>	<u>ICAO</u>	<u>NAME</u>	<u>LAT</u>	<u>LONG</u>
161580	LIRP	Pisa/San Guisto, IY	43°40'N	10°23'E
162390	LIRA	Rome, IY	41°48'N	12°35'E
162530	LIRM	Grazzanise, IY	41°04'N	14°05'E
162890	LIRN	Naples/Capodich, IY	40°53'N	14°18'E
164220	LICR	Reggio/Calabria, IY	38°05'N	15°39'E
164590	LICZ	Catania/Sigonel, IY	37°24'N	14°55'E
165310	LIEO	Olbia/Costa Smerald, IY	40°54'N	9°31'E
165460	LIED	Decimomannu, IY	39°21'N	8°58'E
603900	DAAG	Algiers, AL	36°43'N	3°15'E
607150	DTTA	Tunis, TS	36°50'N	10°14'E
620100	HLLT	Tripoli, LY	32°41'N	13°10'E

Region 14

<u>NUMBER</u>	<u>ICAO</u>	<u>NAME</u>	<u>LAT</u>	<u>LONG</u>
110360	LOWW	Wien/Schwechat, OS	48°07'N	16°34'E

Region 15

There are no operational stations in this region.

Region 16

<u>NUMBER</u>	<u>ICAO</u>	<u>NAME</u>	<u>LAT</u>	<u>LONG</u>
166480	LGLR	Larisa, GR	39°39'N	22°27'E
166651	LGBL	Nea Ankhialos, GR	39°13'N	22°48'E
166220	LGTS	Thessaloniki, GR	40°30'N	22°58'E
166990	LGTC	Tanagra, GR	38°19'N	23°32'E
167160	LGAT	Athens/Hellinikon, GR	37°54'N	23°44'E
170600	LTBA	Istanbul/Yeslik, TU	40°58'N	28°49'E
171150	LTBG	Bandirma, TU	40°21'N	27°58'E
171500	LTBF	Balikesir, Tu	39°39'N	27°52'E
172180	LTBL	Izmir/Cigli, TU	38°30'N	27°01'E

Region 17

<u>NUMBER</u>	<u>ICAO</u>	<u>NAME</u>	<u>LAT</u>	<u>LONG</u>
170290	LTAQ	Samsun, TU	41°16'N	36°18'E
170820	LTAP	Merzifon, TU	40°51'N	35°35'E
170965	LTCE	Erzurum, TU	39°57'N	41°10'E
171240	LTBI	Eskisehir, TU	39°46'N	30°31'E
171270	LTAE	Ankara/Murted, TU	40°05'N	32°34'E
171950	LTAU	Kayseri/Erkilet, TU	38°43'N	35°29'E
172000	LTAT	Malatya/Erhac, TU	38°21'N	38°18'E
172440	LTAN	Konya, TU	37°52'N	32°30'E
172800	LTCC	Diyarbakir, TU	37°55'N	40°20'E
172805	LTCJ	Batman, TU	37°56'N	41°07'E
173000	LTAI	Antalya, TU	36°53'N	30°42'E
173500	LTAG	Adana/Incirlik, TU	36°59'N	35°18'E

Region 18

<u>NUMBER</u>	<u>ICAO</u>	<u>NAME</u>	<u>LAT</u>	<u>LONG</u>
013840	ENGM	Oslo/Gardermoen, NO	60°12'N	11°05'E
014880	ENFB	Oslo/Fornebu, NO	59°54'N	10°37'E
014940	ENRY	Rygge, NO	59°23'N	10°47'E
021280	ESPD	Gunnarn, SN	65°01'N	17°41'E
023660	ESNN	Sundsvall/Harnosand, SN	62°32'N	17°27'E
024690	ESCN	Stockholm/Tullinge, SN	59°11'N	17°55'E
025500	ESSJ	Jonkoping, SN	57°46'N	14°05'E

ASIA (ASN)

Region 1

<u>NUMBER</u>	<u>ICAO</u>	<u>NAME</u>	<u>LAT</u>	<u>LONG</u>
470700	-	Kaesong, KO	37°58'N	126°33'E
471060	RKSB	Uijongbu Arpt, KO	37°44'N	127°03'E
471064	RKSX	Camp Stanley, KO	37°47'N	126°51'E
471065	RKSR	Sinsan Ni, KO	37°47'N	126°51'E
471066	RKST	Tong Du Chon, KO	37°55'N	127°03'E
471105	RKSY	Yongsan, KO	37°31'N	127°00'E
471200	RKSW	Suwon AB, KO	37°15'N	127°00'E
471204	RKSN	Koon-ni Range, KO	37°02'N	126°45'E
471220	RKSO	Osan AB, KO	37°05'N	127°02'E
471270	RKSG	Pyongtaek, KO	36°57'N	127°02'E
471410	RKJK	Kunsan AB, KO	35°54'N	126°37'E

Region 2

<u>NUMBER</u>	<u>ICAO</u>	<u>NAME</u>	<u>LAT</u>	<u>LONG</u>
470610	-	Changjon, KO	38°44'N	128°11'E
470750	-	Pyonggang, KO	38°24'N	127°18'E
470900	-	Sogcho, KO	38°12'N	128°36'E

Region 3

<u>NUMBER</u>	<u>ICAO</u>	<u>NAME</u>	<u>LAT</u>	<u>LONG</u>
471026	RKXX	Nightmare Range, KO	38°04'N	127°21'E
471040	RKNC	Chunchon, KO	37°52'N	127°43'E
471223	RKNR	Kotar Range, KO	37°06'N	128°54'E
471280	RKTU	Chongju AB, KO	36°42'N	125°30'E
471320	RKTD	Taejon AB, KO	36°20'N	127°23'E
471340	RKTY	Yechon, KO	36°38'N	128°21'E
471390	RKTH	Pohang AB, KO	35°59'N	129°25'E
471420	RKTG	Taegu AB/Toncho, KO	35°54'N	128°39'E
471425	RKTG	Taegu South, KO	35°50'N	128°35'E
471530	RKPK	Pusan/Kimhae, KO	35°11'N	128°56'E
471540	RKPP	Pusan Intl Arpt, KO	35°10'N	129°08'E
471580	RKJJ	Kwangju, KO	35°07'N	126°49'E
471610	RKPS	Sachon AB, KO	35°05'N	128°05'E

Region 4

<u>NUMBER</u>	<u>ICAO</u>	<u>NAME</u>	<u>LAT</u>	<u>LONG</u>
475800	RJSM	Misawa AB, JP	40°41'N	141°23'E

Region 5

There are no operational stations in this region.

Region 6

There are no operational stations in this region.

Region 7

<u>NUMBER</u>	<u>ICAO</u>	<u>NAME</u>	<u>LAT</u>	<u>LONG</u>
476420	RJTY	Yokota AB, JP	35°45'N	139°21'E

Region 8

There are no operational stations in this region.

Region 9

There are no operational stations in this region.

Region 10

There are no operational stations in this region.

Region 11

<u>NUMBER</u>	<u>ICAO</u>	<u>NAME</u>	<u>LAT</u>	<u>LONG</u>
479300	ROAH	Naha AB/Okinawa, JP	26°12'N	127°39'E
479310	RODN	Kadena AB/Okinawa, JP	26°21'N	127°45'E
479380	RODE	Ie Shima Aux AB, JP	26°43'N	127°47'E

SOUTH CHINA SEA (SCS)

Region 1

There are no operational stations in this region.

Region 2

There are no operational stations in this region.

Region 3

There are no operational stations in this region.

Region 4

<u>NUMBER</u>	<u>ICAO</u>	<u>NAME</u>	<u>LAT</u>	<u>LONG</u>
983220	RPXC	Crow Valley Gunnery Range, PH	15°19'N	120°25'E
983270	RPMK	Clark AB/Angeles, PH	15°11'N	120°33'E
984260	RPMB	Cubi Point NAS, PH	14°48'N	120°16'E

Region 5

There are no operational stations in this region.

MIDDLE EAST (OILP5)

Region 1

<u>NUMBER</u>	<u>ICAO</u>	<u>NAME</u>	<u>LAT</u>	<u>LONG</u>
403610	OESK	Al Jouf/Sakawa, SD	29°56'N	40°12'E
404160	OEDR	Dhahran, SD	26°16'N	50°10'E
404380	OERY	Riyadh Intl, SD	24°42'N	46°44'E
405820	OKBK	Kuwait Int, KW	29°13'N	47°59'E
411500	OBBI	Bahrain, BN	26°16'N	50°37'E
411700	OTBD	Doha Intl Arpt, QT	25°15'N	51°34'E

Region 2

<u>NUMBER</u>	<u>ICAO</u>	<u>NAME</u>	<u>LAT</u>	<u>LONG</u>
401650	LLRD	Haifa/Ramat David, IS	32°40'N	35°11'E
401800	LLBG	Tel Aviv/Ben Gurion, IS	32°00'N	34°54'E

Region 3

<u>NUMBER</u>	<u>ICAO</u>	<u>NAME</u>	<u>LAT</u>	<u>LONG</u>
400800	OSDI	Damascus New Intl, SY	33°25'N	36°31'E
402700	OJAM	Amman/King Abdullah, TJ	31°59'N	35°59'E

Region 4

<u>NUMBER</u>	<u>ICAO</u>	<u>NAME</u>	<u>LAT</u>	<u>LONG</u>
406500	ORBB	Baghdad, IQ	33°14'N	44°14'E
408310	OIAA	Abadan Intl, IQ	30°22'N	48°15'E

Region 5

<u>NUMBER</u>	<u>ICAO</u>	<u>NAME</u>	<u>LAT</u>	<u>LONG</u>
407950	OIAD	Ezful/Vahdati AB, IR	32°26'N	48°24'E
408480	OISS	Shiraz Intl, IR	29°32'N	52°35'E
408999	OIFM	Hatami, IR	32°45'N	51°51'E

Region 6

<u>NUMBER</u>	<u>ICAO</u>	<u>NAME</u>	<u>LAT</u>	<u>LONG</u>
407060	OITT	Tabriz, IR	38°08'N	46°15'E
407450	OIMM	Mashhad, IR	36°16'N	59°38'E
407540	OIII	Tehran/Mehrabad, IR	35°41'N	51°19'E
407660	OIRR	Kermanshah, IR	34°21'N	47°09'E

Region 7

<u>NUMBER</u>	<u>ICAO</u>	<u>NAME</u>	<u>LAT</u>	<u>LONG</u>
407180	-	Pahlavi, IR	37°28'N	49°28'E
407360	-	Babulsar, IR	36°43'N	52°39'E

MIDDLE EAST (OILPT)

Region 1

<u>NUMBER</u>	<u>ICAO</u>	<u>NAME</u>	<u>LAT</u>	<u>LONG</u>
411140	OEKM	Khamis Mushait, SD	18°18'N	42°48'E
412560	OOMS	Muscat/Seeb Intl, OM	23°35'N	58°17'E
412880	OOMA	Masirah, SD	20°40'N	58°54'E
413140	OOTH	Thumrait, OM	17°44'N	53°56'E
413160	OOSA	Salalah, OM	17°02'N	54°05'E

Region 2

<u>NUMBER</u>	<u>ICAO</u>	<u>NAME</u>	<u>LAT</u>	<u>LONG</u>
404000	OEJW	El Weijh, SD	26°14'N	36°26'E
410260	OEJD	Jeddah Intl, SD	21°30'N	39°12'E
629999	-	Ras Banas, UB	23°35'N	35°17'E

Region 3

<u>NUMBER</u>	<u>ICAO</u>	<u>NAME</u>	<u>LAT</u>	<u>LONG</u>
408750	OIKB	Bandar Abbas, IR	27°11'N	56°17'E
411940	OMDB	Dubai, ER	25°15'N	55°20'E
412160	OMAD	Abu Dhabi Intl, ER	24°26'N	54°28'E
417800	OPKC	Karachi Arpt, PK	24°54'N	67°09'E

Region 4

<u>NUMBER</u>	<u>ICAO</u>	<u>NAME</u>	<u>LAT</u>	<u>LONG</u>
409480	OAKB	Kabul Intl, AH	34°33'N	69°13'E
409900	OAKN	Kanahar, AH	31°30'N	65°51'E
415300	OPPS	Eshawar, PK	34°00'N	71°31'E

Region 5

There are no operational stations in this region.

Region 6

<u>NUMBER</u>	<u>ICAO</u>	<u>NAME</u>	<u>LAT</u>	<u>LONG</u>
621760	-	Giarabub, LY	29°45'N	24°32'E
623660	HECA	Cairo Intl, UB	30°08'N	31°24'E
623999	HECW	Cairo West, UB	30°08'N	30°43'E
624020	-	Kena/Quina, UB	26°11'N	32°44'E
624050	HELX	Luxor, UB	25°40'N	32°42'E
624140	HESN	Aswan, UB	23°58'N	32°47'E

AFRICA (AFRPT)Region 1

<u>NUMBER</u>	<u>ICAO</u>	<u>NAME</u>	<u>LAT</u>	<u>LONG</u>
411400	OEGN	Gezan/Gizan, SD	16°52'N	42°35'E
620530	HLLB	Benina, LY	32°05'N	20°16'E
621240	HLLS	Shebha, LY	27°01'N	14°26'E
622710	-	Kufra, LY	24°13'N	23°18'E
627210	HSSS	Khartoum, LY	15°36'N	32°33'E

Region 2

<u>NUMBER</u>	<u>ICAO</u>	<u>NAME</u>	<u>LAT</u>	<u>LONG</u>
626410	HSSP	Port Sudan, SU	19°35'N	37°13'E

AFRICA (AFRNO)

<u>NUMBER</u>	<u>ICAO</u>	<u>NAME</u>	<u>LAT</u>	<u>LONG</u>
414670	ODAA	Aden Khormaksar, AD	12°50'N	45°02'E
631250	HFFF	Djbouti/Ambowl, DJ	11°33'N	43°09'E
632600	HCMM	Mogadiscio, SI	2°02'N	45°21'E
634500	HAAB	Addis Ababa, ET	8°59'N	38°48'E
634710	HADR	Dire Dawa Intl, ET	9°36'N	41°52'E
636800	-	Kampala, UG	0°19'N	32°37'E
637400	HKNA	Nairobi, Kenya	1°19'S	36°55'E

DEVELOPMENT STATION LIST

EUROPE (EUR)

Region 1

<u>NUMBER</u>	<u>ICAO</u>	<u>NAME</u>	<u>LAT</u>	<u>LONG</u>
010330	-	Torsvag, NO	70°15'N	19°30'E
010610	-	Brennelv, NO	70°04'N	25°07'E
010780	-	Sletnes Fyr, NO	71°05'N	28°14'E
010890	ENKR	Kirkennes Lufthavn, NO	69°43'N	29°53'E
011020	-	Sklinna Fyr, NO	65°12'N	11°00'E
011150	-	Myken, NO	66°46'N	12°29'E
011600	-	Skrova, NO	68°09'N	14°39'E
012150	-	Hustad, NO	62°58'N	7°09'E
012380	-	Fokstua, NO	62°07'N	9°18'E
012710	ENVA	Vaernes, NO	63°28'N	10°56'E
013170	-	Bergen/Florida, NO	60°23'N	5°20'E
014150	ENZV	Stavanger/Sola, NO	58°53'N	5°38'E
060110	-	Thorshavn, FA	62°01'N	6°46'W

Region 2

<u>NUMBER</u>	<u>ICAO</u>	<u>NAME</u>	<u>LAT</u>	<u>LONG</u>
030050	-	Lerwick, UK	60°08'N	1°11'W
030220	EGPL	Benbecula, UK	57°28'N	7°22'W
030490	-	Cape Wrath, UK	58°37'N	5°00'W
030590	EGPE	Inverness/Delcross, UK	57°32'N	4°03'W
030930	-	Fraserburgh, UK	57°42'N	2°00'W
031310	-	Mull of Galway, UK	54°38'N	4°51'W
031850	-	St Abbas Head, UK	55°55'N	2°08'W
032220	EGNC	Carlisle, UK	54°56'N	2°57'W
032820	-	Whitby C.G. UK	54°29'N	0°36'W
033180	EGNH	Blackpool Aprt, UK	53°46'N	3°02'W
034000	-	Bardsey Island, UK	52°45'N	4°48'W
035340	EGBB	Birmingham Aprt, UK	52°27'N	1°44'W
039530	-	Valentia Obs, IE	51°56'N	10°15'W
039600	-	Kilkenny, IE	52°40'N	7°16'W
039690	EIDW	Dublin Arpt, IE	53°26'N	6°15'W
039760	-	Belmullet, IE	54°14'N	10°00'W
039800	-	Malin Head, IE	55°22'N	7°20'W

Region 3

<u>NUMBER</u>	<u>ICAO</u>	<u>NAME</u>	<u>LAT</u>	<u>LONG</u>
033910	EGXC	Coningsby, UK	53°05'N	0°10'W
036580	EGUB	Benson, UK	51°37'N	1°05'W
036960	-	Walton-on-Naze, UK	51°51'N	1°17'E
037150	EGFF	Glamorgan/Rhoose, UK	51°24'N	3°21'W

<u>NUMBER</u>	<u>ICAO</u>	<u>NAME</u>	<u>LAT</u>	<u>LONG</u>
038170	EGDG	St Mawgan, UK	50°26'N	5°00'W
038650	EGHI	Southampton, UK	50°54'N	1°24'W
038940	EGJB	Guernsey, UK	49°26'N	2°36'W

Region 4

<u>NUMBER</u>	<u>ICAO</u>	<u>NAME</u>	<u>LAT</u>	<u>LONG</u>
063200	-	Goree Lgt Platform, NL	51°56'N	3°40'E
070020	-	Boulogne, FR	50°44'N	1°36'E
070050	LFOI	Abbeville, FR	50°08'N	1°50'E
070240	LFRG	Cherbourg, FR	49°39'N	1°28'W
070270	LFRK	Caen/Carpique, FR	49°11'N	0°27'W
070370	LFOP	Roven/Boos, FR	49°23'N	1°11'E
070610	LFOW	St. Quentin/Roupy, FR	49°49'N	3°12'E
070700	LFSR	Reims/Champagne, FR	49°18'N	4°02'E
071100	LFRB	Brest/Guipavas, FR	48°27'N	4°25'W
071300	LFRN	Rennes/St Jacques, FR	48°04'N	1°44'W
071390	LFOF	Alencon/Valframber, FR	48°27'N	0°06'E
071570	LFPG	Paris/C. DeGaulle, FR	49°02'N	2°32'E
071680	LFQB	Troyes/Barberey, FR	48°20'N	4°01'E
071690	LFSI	St. Dizier/Robinson, FR	48°38'N	4°54'E
072070	-	Le Talut, FR	47°18'N	3°13'W
072220	LFRS	Nantes/Chateau/Boug, FR	47°10'N	1°36'W
072300	LFRA	Angers Avrille, FR	47°30'N	0°34'W
072490	LFOJ	Orleans/Bricy, FR	47°59'N	1°45'E
073140	-	Chassiron, FR	46°02'N	1°25'W
073350	LFBI	Poitiers/Biard, FR	46°35'N	0°19'E
073540	LFLX	Chateauroux/Deols, FR	46°51'N	1°43'E
075100	LFBD	Bordeaux/Merignac, FR	44°50'N	0°42'W
075240	LFBA	Agen/LaGarenne, FR	44°11'N	0°36'E
075350	-	Gourdon, FR	44°45'N	1°24'E
076020	LFBZ	Biarritz/Bayonne, FR	43°28'N	1°32'W

Region 5

<u>NUMBER</u>	<u>ICAO</u>	<u>NAME</u>	<u>LAT</u>	<u>LONG</u>
077200	-	Pic Du Midi, FR	42°56'N	0°09'E
080150	-	Oviedo, SP	43°22'N	5°51'W
080420	LEST	Santiago, SP	42°54'N	8°26'W
080750	LEBG	Burgos/Villafria, SP	42°21'N	3°37'W
081600	LEZG	Zaragoza, SP	41°40'N	1°01'W
081810	LEBL	Barcelona/Muntadas, SP	41°17'N	2°04'E
082020	LESA	Salamanca/Matacan, SP	40°57'N	5°29'W
082210	LEMD	Madrid/Barajas, SP	40°28'N	3°34'W
082330	LECH	Calamocha, SP	40°53'N	1°17'W
082610	-	Caceres, SP	39°29'N	6°22'W
082800	LEAB	Albacete/Los Llano, SP	38°57'N	1°51'W
082840	LEVC	Valencia/Manises, SP	39°29'N	0°28'W
083480	-	Ciudad Real, SP	38°59'N	3°56'W
084100	LEBA	Cordoba, SP	37°51'N	4°51'W

NUMBER	ICAO	NAME	LAT	LONG
084490	LERT	Rota NS, SP	36°39'N	6°21'W
084820	LEMG	Malaga, SP	36°39'N	4°28'W
034870	LEAM	Almeria, SP	36°50'N	2°27'W
085360	LPP1	Lisbon/Portella, PO	38°46'N	9°08'W
085490	-	Coimbra, PO	40°12'N	8°25'W
085540	LPFR	Faro, PO	37°01'N	7°58'W
085620	LPBJ	Beja, PO	38°01'N	7°52'W
085750	-	Braganca, PO	41°49'N	6°46'W

Region 6

NUMBER	ICAO	NAME	LAT	LONG
014480	-	Oksoy, NO	58°04'N	8°03'E
014820	-	Ferder, NO	59°02'N	10°32'E
020600	-	Naimakka, SN	68°41'N	21°32'E
060410	-	Skagen, DN	57°46'N	10°39'E
060590	-	Lyngvig, DN	56°03'N	8°06'E
060710	-	Fornaes, DN	56°27'N	10°58'E
061520	-	Glumso, DN	55°21'N	11°41'E
061930	-	Hammerode, DN	55°18'N	14°47'E
090910	-	Arkona, DD	54°41'N	13°26'E

Region 7

NUMBER	ICAO	NAME	LAT	LONG
062400	EHAM	Amsterdam/Schiphol, NL	52°18'N	4°46'E
062700	EHLW	Leeuwarden, NL	53°13'N	5°46'E
062800	EHGG	Eelde/Gronigen, NL	53°08'N	6°35'E
062900	EHTW	Twenthe/Enschede, NL	52°16'N	6°54'E
063500	EHGR	Gilze-Rijen, NL	51°34'N	4°56'E
064070	EBOS	Ostend/Middelkerke, NL	51°12'N	2°52'E
064510	EBBR	Brussels Intl, BX	50°54'N	4°28'E
064560	EBFS	Florennes, BX	50°14'N	4°39'E
064900	-	Spa/La Sauveniere, BX	50°29'N	5°55'E
065900	ELLX	Luxembourg/Findel, BX	49°37'N	6°13'E
094530	-	Brocken, DD	51°48'N	10°37'E
095460	-	Kaltenordheim, DD	50°38'N	10°09'E
100050	-	Elbe 1/Ship, DL	54°00'N	8°07'E
100350	-	Schleswig, DL	54°32'N	9°33'E
101470	EDDH	Hamburg/Fuhlsbutte, DL	53°38'N	9°59'E
102150	EDNO	Oldenburg, DL	53°11'N	8°10'E
103130	-	Munster, DL	51°58'N	7°36'E
103380	EDVV	Hannover, DL	52°28'N	9°42'E
104000	EDDL	Dusseldorf, DL	51°17'N	6°46'E
104270	-	Kahler Asten, DL	51°11'N	8°29'E
105320	-	Giessen, DL	50°34'N	8°42'E
106160	EDAH	Hahn, DL	49°57'N	7°16'E

Region 8

<u>NUMBER</u>	<u>ICAO</u>	<u>NAME</u>	<u>LAT</u>	<u>LONG</u>
067000	LSGG	Geneva/Cointrin, SW	46°15'N	6°08'E
072700	-	Chateau Chinon, FR	47°04'N	3°56'E
072830	-	Langres, FR	47°50'N	5°19'E
072880	-	Besancon, FR	47°15'N	5°59'E
074340	LFBL	Limoges/Bellegarde, FR	45°52'N	1°11'E
074600	LFLC	Clermont-Ferrand, FR	45°47'N	3°10'E
074700	LFHP	Le Puy, FR	45°03'N	3°54'E
074810	LFLI	Lyon/Safolas, FR	45°44'N	5°05'E
075580	-	Millau, FR	44°07'N	3°01'E
076430	LFMT	Montpellier, FR	43°35'N	3°58'E
076600	-	Toulon, FR	43°06'N	5°56'E
076900	LFMN	Nice/Cote Daazur, FR	43°39'N	7°12'E
077470	LFMP	Perpignan/Llabanere, FR	42°44'N	2°52'E

Region 9

<u>NUMBER</u>	<u>ICAO</u>	<u>NAME</u>	<u>LAT</u>	<u>LONG</u>
091620	-	Schwerin, DD	53°38'N	11°25'E
091700	-	Warnemunde, DD	54°11'N	12°05'E
091930	-	Ueckermunde, DD	53°45'N	14°04'E
092610	-	Seehausen, DD	52°54'N	11°44'E
092800	-	Neubrandenburg, DD	53°33'N	13°12'E
093610	-	Magdeburg, DD	52°06'N	11°35'E
093850	ETBS	Berlin/Schonefeld, DD	52°23'N	13°31'E
094690	ETLS	Liepzig/Schkeuditz, DD	51°25'N	12°14'E
094960	-	Cottbus, DD	51°47'N	14°19'E
121050	-	Koszalin, PL	54°12'N	16°09'E
121350	-	Hel, PL	54°36'N	18°49'E
121850	-	Ketrzyn, PL	54°01'N	21°22'E
122350	-	Chojnice, PL	53°42'N	17°33'E
122700	-	Mlawa, PL	53°06'N	20°21'E
122950	-	Bialystok, PL	53°06'N	23°10'E
123000	-	Gorzow Wlkp, PL	52°44'N	15°15'E
123300	EPPO	Poznan/Lawica, PL	52°25'N	16°50'E
123750	EPWA	Warsaw/Okecie, PL	52°11'N	20°59'E
124240	-	Wroclaw/Strachowice, PL	51°06'N	16°53'E
124350	-	Kalisz, PL	51°44'N	18°05'E
124950	-	Lublin, PL	50°14'N	22°34'E
125600	-	Katowice, PL	50°14'N	19°02'E
125700	-	Kielce, PL	50°51'N	20°37'E
126950	-	Przemysl, PL	49°48'N	22°46'E

Region 10

<u>NUMBER</u>	<u>ICAO</u>	<u>NAME</u>	<u>LAT</u>	<u>LONG</u>
071900	LFST	Stasbourg/Entzheim, FR	48°33'N	7°38'E
106550	-	Wurzburg, DL	49°48'N	9°54'E
106850	EDQM	Hof, DL	50°19'N	11°53'E
107380	EDDS	Stuttgart/Echter, D1	48°41'N	9°12'E
107760	-	Regensburg, DL	49°01'N	12°04'E
108520	-	Augsburg, DL	48°23'N	10°51'E
109000	EDSG	Bremgarten, DL	47°54'N	7°37'E
115180	LKPR	Prague/Ruzyne, CZ	50°06'N	14°15'E
115410	-	Ceske Budejovice, CZ	48°57'N	14°27'E
116030	LKLB	Leberec, CZ	50°46'N	15°01'E
116590	-	Pribyslav, CZ	49°35'N	15°46'E
117350	-	Praded, CZ	50°04'N	17°14'E
117740	LKHO	Holesov, CZ	49°19'N	17°34'E

Region 11

<u>NUMBER</u>	<u>ICAO</u>	<u>NAME</u>	<u>LAT</u>	<u>LONG</u>
069900	-	Vaduz Liechtenstein, LT	47°08'N	9°32'E
075910	-	Embrun, FR	44°34'N	6°30'E
109800	-	Wendelstein, FR	47°42'N	12°01'E
111570	LOXA	Aigen Im Ennstal, OS	47°32'N	14°08'E
112400	LOWG	Graz-Thalerhof, OS	47°00'N	15°27'E
160200	LIPB	Bolzano, IY	46°28'N	11°20'E
160400	LIVO	Tarvisio, IY	46°30'N	13°35'E
160520	LIMH	Pian Rosa, IY	45°56'N	7°42'E
161120	LIMX	Monte Fraiteve, IY	44°59'N	6°51'E
161340	LIVC	Monte Cimone, IY	44°12'N	10°42'E
161810	LIRZ	Perugia/S.Egidio, IY	43°05'N	12°30'E

Region 12

<u>NUMBER</u>	<u>ICAO</u>	<u>NAME</u>	<u>LAT</u>	<u>LONG</u>
160900	LIPX	Verona/Villafranca, IY	45°23'N	10°52'E
162520	LTBS	Campobasso, IY	41°34'N	14°39'E
162700	LIBD	Bari/Palese Macchie, IY	41°08'N	16°47'E
163600	LIBY	S. Maria Di Leuca, IY	39°49'N	18°21'E
166410	LGKR	Kerkira/Corfu, GR	39°37'N	19°55'E

Region 13

<u>NUMBER</u>	<u>ICAO</u>	<u>NAME</u>	<u>LAT</u>	<u>LONG</u>
083060	LEPA	Palma De Mallorca, SP	39°33'N	2°44'E
162060	LIRS	Grosseto, IY	42°45'N	11°04'E
162390	LIRA	Rome/Ciampino, IY	41°48'N	12°35'E
163100	LIQK	Capo Palinuro, IY	40°01'N	15°17'E
163500	LIBC	Crotone/Sanna, IY	39°00'N	17°05'E
164000	LICU	Ustica, IY	38°42'N	13°11'E
164600	LICC	Catania/Fontanarosa, IY	37°28'N	15°03'E

<u>NUMBER</u>	<u>ICAO</u>	<u>NAME</u>	<u>LAT</u>	<u>LONG</u>
164700	LICG	Pantelleria, IY	36°49'N	11°58'E
165200	LIEA	Alghero, IY	40°38'N	8°17'E
165600	LIEE	Cagliari/Elmas, IY	39°15'N	9°03'E
165970	LMML	Luqa/Valletta, ML	35°51'N	14°29'E

Region 14

<u>NUMBER</u>	<u>ICAO</u>	<u>NAME</u>	<u>LAT</u>	<u>LONG</u>
110350	-	Wien/Hohe Warte, OS	48°15'N	16°22'E
119030	LKSL	Sliac, CZ	48°38'N	19°09'E
119680	LKKZ	Kosice, CZ	48°42'N	21°16'E
128220	-	Gyor, HU	47°42'N	17°41'E
128430	-	Budapest/Lorinc, HU	47°26'N	19°11'E
128820	-	Debrecen, HU	47°29'N	21°38'E
129350	-	Sifok, HU	46°55'N	18°03'E
129820	-	Szeged, HU	46°15'N	20°06'E
131500	-	Slavonski Bord, YG	45°10'N	18°00'E
132720	LYBE	Belgrade Intl, YG	44°49'N	20°17'E
150040	-	Sighetu Marmatiei, RO	47°58'N	23°55'E
150200	-	Botosani, RO	47°41'N	26°40'E
151200	-	Cluj-Napoco, RO	46°47'N	23°34'E
151500	LRBC	Bacau, RO	46°35'N	26°59'E
152350	-	Fagaras, RO	45°51'N	24°59'E
152920	LRCS	Caransebes, RO	45°25'N	22°15'E
153500	-	Buzau, RO	45°09'N	26°49'E
153600	-	Sulina, RO	45°09'N	29°40'E
154500	LRCV	Craiova, RO	44°19'N	23°52'E
155350	-	Rousse, BU	43°52'N	25°57'E
155561	LBWN	Varna, BU	43°14'N	27°50'E
156550	LBBG	Burgas, Bu	42°29'N	27°29'E

Region 15

<u>NUMBER</u>	<u>ICAO</u>	<u>NAME</u>	<u>LAT</u>	<u>LONG</u>
131160	LYRI	Rijeka/Omisalj, YG	45°13'N	14°35'E
131310	LYZA	Zagreb-Pleso, YG	45°44'N	16°04'E
132280	-	Bihac, YG	44°49'N	15°53'E
133330	LYSP	Split Intl, YG	43°32'N	16°18'E
133530	LYSA	Sarajevo/Butmir, YG	43°49'N	18°20'E
133880	-	Nis, YG	43°20'N	21°54'E
134570	LYTV	Tivat, YG	42°44'N	18°44'E
134730	-	Pec, YG	42°40'N	20°18'E
156150	-	Mussala/Mt Top, BU	42°10'N	23°35'E
156270	-	Botev Vrah/Mt Top, BU	42°43'N	24°55'E
157300	-	Kurdjali, BU	41°38'N	25°24'E

Region 16

<u>NUMBER</u>	<u>ICAO</u>	<u>NAME</u>	<u>LAT</u>	<u>LONG</u>
166130	-	Florina, GR	40°48'N	21°25'E
166220	LGTS	Thessaloniki/Mikra, GR	40°31'N	22°58'E
166500	LGLM	Limnos/Lichma, GR	39°55'N	25°14'E
166750	-	Lamia, GR	38°54'N	22°24'E
166820	LGAD	Andravida, GR	37°55'N	21°18'E
167160	LGAT	Athens/Hellenikon, GR	37°54'N	23°44'E
167230	LGSM	Samos Aprt, GR	37°45'N	26°52'E
167320	-	Naxos, GR	37°06'N	25°23'E
167340	-	Methoni, GR	36°50'N	21°42'E
167494	LGRP	New Rodos Aprt, GR	36°25'N	28°05'E
167540	LGIR	Iraklion-Crete, GR	35°20'N	25°11'E
171150	LTBG	Bandirma, Tu	40°21'N	27°58'E
172180	LTBL	Izmir/Cigli, TU	38°30'N	27°01'E

Region 17

<u>NUMBER</u>	<u>ICAO</u>	<u>NAME</u>	<u>LAT</u>	<u>LONG</u>
170220	-	Zonguldak, TU	41°27'N	31°48'E
170380	LTCG	Trabzon, TU	41°00'N	39°43'E
170820	LTAP	Merzifon, TU	40°51'N	35°35'E
170900	-	Sivas, TU	39°45'N	37°01'E
170960	-	Erzurum, TU	39°55'N	41°16'E
171240	LTBI	Eskisehir, TU	39°46'N	30°31'E
171280	LTAC	Ankara/Esenboga, TU	40°07'N	32°59'E
171880	LTBO	Usak, TU	38°40'N	29°25'E
171950	LTAU	Kayseri/Erkilet, TU	38°43'N	35°29'E
172000	LTAT	Malatya/Erhac, TU	38°21'N	38°18'E
172440	LTAN	Konya, TU	37°52'N	32°30'E
172800	LTCC	Diyarbakir, TU	37°55'N	40°13'E
173000	LTAI	Antalya, TU	36°53'N	30°42'E
173500	LTAG	Adana/Incirlik AB, TU	36°59'N	35°18'E
176090	LCLK	Larnaca Aprt, CY	34°53'N	33°38'E

Region 18

<u>NUMBER</u>	<u>ICAO</u>	<u>NAME</u>	<u>LAT</u>	<u>LONG</u>
013820	-	Kise Pa Hedmark, NO	60°46'N	10°49'E
020200	-	Katterjakk, SN	68°25'N	18°10'E
021080	-	Klimpfjall, SN	65°04'N	14°48'E
021200	-	Kvikkjokk, SN	66°57'N	17°45'E
021240	-	Arjeplog, SN	66°02'N	17°52'E
021860	ESPA	Lulea/Kallax, SN	65°33'N	22°08'E
022260	ESPC	Ostersund/Froson, SN	63°11'N	14°30'E
022540	-	Aselle, SN	64°10'N	17°22'E
022590	ESNK	Kramfors Flygplats, SN	63°03'N	17°46'E
023160	-	Sarna, SN	61°41'N	13°08'E
023760	ESCL	Soderhamn, SN	61°16'N	17°06'E
024120	-	Gustavsfors, SN	60°09'N	13°48'E

NUMBER	ICAO	NAME	LAT	LONG
024580	ESCM	Uppsala, SN	59°53'N	17°36'E
025410	-	Snavlunda, SN	58°58'N	14°54'E
025500	ESSJ	Jonkoping, SN	57°46'N	14°05'E
025840	-	Gotska Sandon, SN	58°24'N	19°12'E
025920	-	Olands Norra Udde, SN	57°22'N	17°06'E
026500	-	Hano, SN	56°01'N	14°51'E
028070	EFIV	Ivalo, FI	68°36'N	27°25'E
028230	-	Muonio, FI	67°58'N	23°41'E
028440	EFPE	Pello, FI	66°48'N	24°00'E
028690	EFKS	Kuusamo, FI	65°58'N	29°11'E
028740	EFHL	Hailuoto, FI	65°02'N	24°48'E
028790	EFSU	Suomussalmi, FI	64°54'N	29°01'E
029030	EFKK	Kruununkyla, FI	63°43'N	23°09'E
029170	EFKU	Kuopio/Rissala, FI	63°01'N	27°48'E
029350	EFJY	Jyvaskyla, FI	62°24'N	25°40'E
029420	-	Niinisalo, FI	61°51'N	22°28'E
029490	-	Punkaharju, FI	61°48'N	29°19'E
029660	EFUT	Utti, FI	60°53'N	26°56'E
029810	-	Uto, FI	59°47'N	21°23'E
029840	-	Bagaskar, FI	59°56'N	24°01'E

MIDDLE EAST (OILP5)

Region 1

<u>NUMBER</u>	<u>ICAO</u>	<u>NAME</u>	<u>LAT</u>	<u>LONG</u>
402500	-	Hotel Four, TJ	32°30'N	38°12'E
403560	OETR	Turaif/Al Turay, SD	31°41'N	38°40'E
403570	OEBD	Badanah, SD	30°58'N	40°59'E
403610	OESK	Al Jouf/Sakaka, SD	29°56'N	40°12'E
403620	OERF	Rafha, SD	29°38'N	43°29'E
403730	OEPA	Quaisumah, SD	28°20'N	46°07'E
403940	OEHL	Hail, SD	27°31'N	41°44'E
404050	OEGS	Gassim, SD	26°18'N	43°48'E
404160	OEDR	Dhahram, SD	26°16'N	50°10'E
404380	OERY	Riyadh Intl, SD	24°42'N	46°44'E
405820	OKBK	Kuwait Intl/Mag, KW	29°13'N	47°59'E
406420	-	Rutbah, IQ	33°02'N	40°17'E
406440	-	Hotel One, IQ	33°47'N	41°28'E
406580	-	Nukhayb, IQ	32°02'N	42°15'E
406840	-	As Salman, IQ	30°30'N	44°32'E
406860	-	Al Busayyah, IQ	30°07'N	46°07'E
408580	OIAB	Bushehr, IR	28°57'N	50°50'E
411700	OTBD	Doha Intl Arpt, QT	25°15'N	51°34'E

Region 2

<u>NUMBER</u>	<u>ICAO</u>	<u>NAME</u>	<u>LAT</u>	<u>LONG</u>
400220	-	Latakia, SY	35°30'N	35°47'E
401000	OLBA	Beirut Intl/Khalde, LB	33°49'N	35°29'E
401650	LLRD	Haifa/Ramat David, IS	32°40'N	35°11'E
401800	LLBG	Tel Aviv/Ben Gurion, IS	32°00'N	34°54'E
401910	-	Beer-Sheva, IS	31°14'N	34°47'E

Region 3

<u>NUMBER</u>	<u>ICAO</u>	<u>NAME</u>	<u>LAT</u>	<u>LONG</u>
400010	OSKL	Kamishly/Omaich, SY	37°03'N	41°13'E
400070	OSAP	Aleppo/Neirab, SY	36°11'N	37°13'E
400090	-	Tel Abiad, SY	36°42'N	38°57'E
400300	-	Hama, SY	35°08'N	36°45'E
400390	-	Raqqa, SY	35°56'N	39°01'E
400610	OSPR	Palmyra/Tudmur, SY	34°33'N	38°18'E
400800	OSDI	Damascus New Intl, SY	33°25'N	36°31'E
401530	-	Mt Kenaan, IS	32°59'N	35°30'E
402600	-	Hotel Five, TJ	32°12'N	37°08'E
402700	OJAM	Amman/King Abdullah, TJ	31°59'N	35°59'E
406020	-	Rabiah, IQ	36°48'N	42°06'E

Region 4

<u>NUMBER</u>	<u>ICAO</u>	<u>NAME</u>	<u>LAT</u>	<u>LONG</u>
400450	-	Dier Zzor, SY	35°19'N	40°09'E
400720	-	Abu Kamal, SY	34°25'N	40°55'E
406080	ORBM	Mosul/Mossoul, IQ	36°19'N	43°09'E
406340	-	Haditha/Haqlani, IQ	34°04'N	42°22'E
406370	-	Khanaqin, IQ	34°18'N	45°26'E
406500	ORBB	Baghdad, IQ	33°14'N	44°14'E
406560	-	Karbalaa, IQ	32°37'N	44°01'E
406650	-	Kut-Al-Hai, IQ	32°10'N	46°03'E
406740	-	Semawa, IQ	31°18'N	45°16'E
406760	ORMN	Nasiriya, IQ	31°05'N	46°14'E
406800	-	Amarah, IQ	31°51'N	47°10'E
406890	-	Basrah/Maqal, IQ	30°43'N	47°47'E
408310	OIAA	Abadan Intl, IR	30°22'N	48°15'E

Region 5

<u>NUMBER</u>	<u>ICAO</u>	<u>NAME</u>	<u>LAT</u>	<u>LONG</u>
406110	-	Salahaddin, IQ	36°27'N	44°13'E
406210	-	Kiruk, IQ	35°28'N	44°24'E
406230	-	Sulaimaniya, IQ	35°33'N	45°27'E
407620	-	Torbat-Meydariah, IR	35°16'N	59°13'E
407950	OIAD	Dezful/Vahdati, IR	32°26'N	48°24'E
407980	-	Shahre-Kord, IR	32°19'N	50°51'E
408000	OIFF	Esfahan, IR	32°37'N	51°40'E
408090	-	Birjand, IR	32°52'N	59°12'E
408410	OIKK	Kerman, IR	30°15'N	56°58'E
408480	OISS	Shiraz Intl, IR	29°32'N	52°35'E
408590	-	Fasa, IR	28°58'N	53°41'E
409380	OAHR	Herat, AH	34°13'N	62°13'E

Region 6

<u>NUMBER</u>	<u>ICAO</u>	<u>NAME</u>	<u>LAT</u>	<u>LONG</u>
407030	-	Khoy, IR	38°33'N	44°58'E
407060	OITT	Tabriz, IR	38°08'N	46°15'E
407080	-	Ardebil, IR	38°15'N	48°17'E
407120	OITR	Rezaiyeh, IR	37°40'N	45°04'E
407270	-	Saghez, IR	36°15'N	46°16'E
407290	-	Zanjan, IR	36°41'N	48°29'E
407310	-	Ghazvin, IR	36°15'N	50°00'E
407430	-	Sabzevar, IR	36°13'N	57°40'E
407450	OIMM	Mashhad, IR	36°16'N	59°38'E
407470	OICS	Sanandaj, IR	35°20'N	47°00'E
407540	OIII	Tehran/Mehrabad, IR	35°41'N	51°19'E
407570	-	Semnan, IR	35°33'N	53°23'E
407660	OIRR	Kermanshah, IR	34°21'N	47°09'E
407670	OIHII	Hamadan, IR	34°52'N	48°33'E
407690	-	Arak, IR	34°08'N	49°42'E

<u>NUMBER</u>	<u>ICAO</u>	<u>NAME</u>	<u>LAT</u>	<u>LONG</u>
407820	-	Korramabad, IR	33°29'N	48°22'E
407850	-	Kashan, IR	33°59'N	51°27'E
407910	-	Tabas, IR	33°36'N	56°54'E
408210	OIYY	Yazd, IR	31°54'N	54°17'E

Region 7

<u>NUMBER</u>	<u>ICAO</u>	<u>NAME</u>	<u>LAT</u>	<u>LONG</u>
407180	-	Pahlavi, IR	37°28'N	49°28'E
407320	OIER	Ramsar, IR	36°55'N	50°40'E
407360	-	Babulsar, IR	36°43'N	52°39'E
407380	-	Gorgan, IR	36°51'N	54°28'E

ASIA (ASN)

Region 1

<u>NUMBER</u>	<u>ICAO</u>	<u>NAME</u>	<u>LAT</u>	<u>LONG</u>
470580	-	Pyongyang, KO	39°02'N	125°47'E
470680	-	Ryongyon, KO	38°12'N	124°53'E
470690	-	Haeju, KO	38°02'N	125°42'E
471120	-	Inchon, KO	37°29'N	126°38'E
471270	RKSG	Pyongtaek, KO	36°57'N	127°02'E
471410	RKJK	Kunsan AB, KO	35°54'N	126°37'E
471650	-	Mokpo/Yong Dang, KO	34°47'N	126°23'E
471870	RKPM	Mosulpo, KO	33°19'N	126°16'E

Region 2

<u>NUMBER</u>	<u>ICAO</u>	<u>NAME</u>	<u>LAT</u>	<u>LONG</u>
470030	-	Unggi, KO	42°19'N	130°24'E
470050	-	Samjiyon, KO	41°49'N	128°19'E
470080	-	Chongjin, KO	41°47'N	129°49'E
470140	-	Chunggang, KO	41°47'N	126°53'E
470220	-	Pungsan, KO	40°49'N	128°09'E
470250	-	Kimchack, KO	40°40'N	129°12'E
470350	-	Sinuiju, KO	40°06'N	124°23'E
470370	-	Kusong, KO	39°59'N	125°15'E
470390	-	Huichon, KO	40°10'N	126°17'E
470410	-	Hamhung, KO	39°56'N	127°33'E
470550	-	Wonsan, KO	39°10'N	127°26'E
470610	-	Changjon, KO	38°44'N	128°11'E
470670	-	Singye, KO	38°30'N	126°32'E

Region 3

<u>NUMBER</u>	<u>ICAO</u>	<u>NAME</u>	<u>LAT</u>	<u>LONG</u>
471010	-	Chun Chon, KO	37°52'N	127°44'E
471070	RKNN	Kangnung AB, KO	37°45'N	128°57'E
471320	RKTD	Taejon AB, KO	36°20'N	127°23'E

<u>NUMBER</u>	<u>ICAO</u>	<u>NAME</u>	<u>LAT</u>	<u>LONG</u>
471340	RKTY	Yechon AB, KO	36°38'N	128°21'E
471420	RKTN	Taegu AB, KO	35°54'N	128°39'E
471520	RKPU	Ulsan, KO	35°33'N	129°19'E
471560	-	Kwangju, KO	35°08'N	126°55'E
471920	-	Jinju, KO	35°11'N	128°05'E

Region 4

<u>NUMBER</u>	<u>ICAO</u>	<u>NAME</u>	<u>LAT</u>	<u>LONG</u>
474010	-	Wakkanai, JP	45°25'N	141°41'E
474070	-	Asahikawa, JP	43°46'N	142°22'E
474090	-	Abashiri, JP	44°01'N	144°17'E
474120	-	Sapporo, JP	43°03'N	141°20'E
474180	-	Kushiro, JP	42°59'N	144°24'E
474200	-	Nemuro, JP	43°20'N	145°35'E
474260	-	Urakawa, JP	42°10'N	142°47'E
474300	-	Hakodate, JP	41°49'N	140°45'E
475150	RJSH	Hachinohe AB, JP	40°33'N	141°28'E
475750	-	Aomori, JP	40°49'N	140°47'E
475840	-	Morioka, JP	39°42'N	141°10'E
475850	-	Miyako, JP	39°39'N	141°58'E
475910	RJST	Matsushima AB, JP	38°24'N	141°13'E

Region 5

<u>NUMBER</u>	<u>ICAO</u>	<u>NAME</u>	<u>LAT</u>	<u>LONG</u>
471150	-	Ullungdo Isl, KO	37°29'N	130°54'E
474210	-	Suttsu, JP	42°47'N	140°14'E
475820	-	Akita, JP	39°43'N	140°06'E
475870	-	Sakata, JP	38°54'N	139°50'E
476000	-	Wajima, JP	37°23'N	136°54'E
476020	-	Aikawa, JP	38°01'N	138°15'E
476040	-	Niigata, JP	37°55'N	139°03'E
477040	RJNK	Komatsu AB, JP	36°23'N	136°25'E
477400	-	Saigo, JP	36°12'N	133°20'E
477410	-	Matsue, JP	35°27'N	133°04'E
477460	-	Tottori, JP	35°31'N	134°11'E
477500	-	Maizuru, JP	35°28'N	135°23'E
477550	-	Hamada, JP	34°54'N	132°04'E

Region 6

<u>NUMBER</u>	<u>ICAO</u>	<u>NAME</u>	<u>LAT</u>	<u>LONG</u>
475700	-	Wakamatsu, JP	37°29'N	139°55'E
475880	-	Yamagata, JP	38°15'N	140°21'E
476180	-	Matsumoto, JP	36°15'N	137°58'E
476340	RJNG	Gifu AB, JP	35°23'N	136°53'E
476380	-	Kofu, JP	35°40'N	138°33'E

Region 7

<u>NUMBER</u>	<u>ICAO</u>	<u>NAME</u>	<u>LAT</u>	<u>LONG</u>
475980	-	Onahama, JP	36°57'N	140°54'E
476240	-	Maebashi, JP	36°24'N	139°04'E
476480	-	Choshi, JP	35°43'N	140°51'E
476620	RJTD	Tokyo, JP	35°41'N	139°46'E

Region 8

<u>NUMBER</u>	<u>ICAO</u>	<u>NAME</u>	<u>LAT</u>	<u>LONG</u>
476750	-	Oshima, JP	34°46'N	139°23'E
476780	-	Hachijojima, JP	33°06'N	139°47'E
476810	RJNH	Hamamatsu, JP	34°44'N	137°40'E
477780	-	Shionomisaki, JP	33°27'N	135°46'E
478270	-	Kagoshima, JP	31°34'N	130°33'E
478370	-	Tanegashima, JP	30°44'N	131°00'E
478540	RJFN	Nyutabaru AB, JP	32°05'N	131°27'E
478980	-	Shimizu/Ashizuri, JP	32°43'N	133°01'E
478990	-	Muruotomisaki, JP	33°15'N	134°11'E

Region 9

<u>NUMBER</u>	<u>ICAO</u>	<u>NAME</u>	<u>LAT</u>	<u>LONG</u>
477650	-	Hiroshima, JP	34°22'N	132°26'E
477720	-	Osaka, JP	34°41'N	135°31'E
478150	-	Oita, JP	33°14'N	131°37'E
478810	RJOS	Tokushima AB, JP	34°08'N	134°36'E
478870	-	Matsuyama, JP	33°50'N	132°47'E

Region 10

<u>NUMBER</u>	<u>ICAO</u>	<u>NAME</u>	<u>LAT</u>	<u>LONG</u>
477620	-	Shimonoseki, JP	33°57'N	130°56'E
478000	-	Izuhara, JP	34°12'N	129°18'E
478080	RJFF	Fukuoka/Itazuke, JP	33°35'N	130°27'E
478170	-	Nagasaki, JP	32°44'N	129°52'E
478190	-	Kumamoto, JP	32°49'N	130°43'E
478430	-	Fukue, JP	32°42'N	128°50'E

Region 11

<u>NUMBER</u>	<u>ICAO</u>	<u>NAME</u>	<u>LAT</u>	<u>LONG</u>
479090	-	Naze/Funchatogere, JP	28°23'N	129°30'E
479300	ROAH	Naha AB/Okinawa, JP	26°12'N	127°39'E
479450	ROMD	Minami Daito, JP	25°50'N	131°14'E

SOUTH CHINA SEA (SCS)Region 1

<u>NUMBER</u>	<u>ICAO</u>	<u>NAME</u>	<u>LAT</u>	<u>LONG</u>
466970	RCGM	Tao-Yuan, TW	25°04'N	121°14'E
467340	RCQC	Ma-Kung, TW	23°34'N	119°37'E
467450	RCAY	Kangshan/Okayama, TW	22°47'N	120°15'E
467460	RCKU	Chiayi, TW	23°28'N	120°23'E
467510	RCLG	Taichung, TW	24°11'N	120°39'E

Region 2

<u>NUMBER</u>	<u>ICAO</u>	<u>NAME</u>	<u>LAT</u>	<u>LONG</u>
467520	RCKW	Heng Chun, TW	22°02'N	120°43'E
467600	RCQS	Chih Hong, TW	22°48'N	121°11'E
467630	RCYU	Hua-Lien, TW	24°01'N	121°37'E
468100	RCLM	Tung-Sha Tao, TW	20°42'N	116°43'E
479180	ROIG	Ishigaki Jima, JP	24°20'N	124°10'E
479270	ROMY	Miyakojima, JP	24°47'N	125°17'E

Region 3

<u>NUMBER</u>	<u>ICAO</u>	<u>NAME</u>	<u>LAT</u>	<u>LONG</u>
982220	RPUQ	Vigan/Quirolgico, PH	17°34'N	120°23'E
982230	RPML	Laoag, PH	18°11'N	120°32'E
983280	RPUB	Baguio, PH	16°25'N	120°36'E
983360	-	Casiguran, PH	16°17'N	122°07'E

Region 4

<u>NUMBER</u>	<u>ICAO</u>	<u>NAME</u>	<u>LAT</u>	<u>LONG</u>
983250	-	Dagupan, PH	16°03'N	120°20'E
983270	RPMK	Clark AB, PH	15°11'N	120°33'E
983330	-	Baler, PH	15°46'N	121°34'E
984260	RBMB	Cubi Point NAS, PH	14°48'N	120°16'E
984290	RPMM	Manila Intl, PH	14°31'N	121°00'E
984340	-	Infanta, PH	14°45'N	121°39'E

Region 5

<u>NUMBER</u>	<u>ICAO</u>	<u>NAME</u>	<u>LAT</u>	<u>LONG</u>
984270	-	Tayabas, PH	14°02'N	121°35'E
984310	-	Calapan, PH	13°25'N	121°11'E
984400	RPUD	Daet/Bagasbas, PH	14°08'N	122°59'E
984440	RPMP	Legaspi/Cruzada, PH	13°08'N	123°44'E
984470	-	Catadunes Radar, PH	13°59'N	124°19'E

AFRICA - 3DNEPH ONLY (AFRNO)

Single Region

<u>NUMBER</u>	<u>ICAO</u>	<u>NAME</u>	<u>LAT</u>	<u>LONG</u>
414670	ODAA	Aden Khormaksar, AD	12°50'N	45°02'E
627600	HSFS	El Fasher, SU	13°37'N	25°20'E
627710	HSOB	El Obeid, SU	13°10'N	30°14'E
628050	-	Damazine, SU	11°47'N	34°23'E
628100	-	Kadugli, SU	11°00'N	29°43'E
631250	HFFF	Djibouti/Ambouli, DJ	11°33'N	43°09'E
632400	-	Belet Uen, SI	4°44'N	45°12'E
632600	HCMM	Mogadishu, SI	2°02'N	45°21'E
633320	HABD	Bahar Dar, ET	11°36'N	37°24'E
633330	HADC	Dessie/Combolcha, ET	11°05'N	39°43'E
633340	HADM	Debremarcos, ET	10°19'N	37°45'E
634020	HAJM	Jimma/Aba Segud, ET	7°39'N	36°49'E
634500	HAAB	Addis Ababa/Bole, ET	8°59'N	38°48'E
634600	-	Awassa, ET	7°04'N	38°30'E
634710	HADR	Dire Dawa Intl, ET	9°36'N	41°52'E
634740	HAGB	Goba, ET	7°01'N	40°00'E
635330	HANG	Neghelli, ET	5°18'N	39°42'E
636020	HUAR	Arua, UG	3°03'N	30°55'E
636120	HKLO	Lodwar, KN	3°07'N	35°37'E
636240	-	Mandera, KN	3°56'N	41°52'E
636300	-	Gulu, UG	2°45'N	32°20'E
636410	-	Marsabit, KN	2°18'N	37°54'E
636540	-	Masindi, UG	1°41'N	31°43'E
636610	HKKT	Kitale, KN	1°01'N	35°00'E
636820	HUJI	Jinja, UG	00°27'N	33°11'E
636950	-	Meru, KN	00°05'N	37°39'E

MIDDLE EAST (OILPT)

Region 1

<u>NUMBER</u>	<u>ICAO</u>	<u>NAME</u>	<u>LAT</u>	<u>LONG</u>
401990	LLET	Elat, IS	29°33'N	34°57'E
403100	OJMN	Ma'an, TJ	30°10'N	35°47'E
403750	OETB	Tabouk, SD	28°22'N	36°35'E
404300	OEMA	Medina/Al Madinah, SD	24°33'N	39°43'E
410360	OETF	Taif/At Taif, SD	21°29'N	40°32'E
410620	OESL	Sulayil/Assulay, SD	20°28'N	45°40'E
410840	OEBH	Bisha, SD	19°58'N	42°40'E
411140	OEKM	Khamis Mushait, SD	18°18'N	42°48'E
412560	OOMS	Muscat/Seeb Intl, OM	23°35'N	58°17'E
412880	OOMA	Masirah, SD	20°40'N	58°54'E
413160	OOSA	Salalah, OM	17°02'N	54°05'E

Region 2

<u>NUMBER</u>	<u>ICAO</u>	<u>NAME</u>	<u>LAT</u>	<u>LONG</u>
404000	OEWJ	El Wejh, SD	26°14'N	36°26'E
404390	OEYN	Yenbo/Yembo, SD	24°07'N	38°03'E
410260	OEJD	Jeddah Intl, SD	21°30'N	39°12'E
624650	-	Kosseir, UB	26°06'N	34°17'E

Region 3

<u>NUMBER</u>	<u>ICAO</u>	<u>NAME</u>	<u>LAT</u>	<u>LONG</u>
408750	OIKB	Bandar Abbas, IR	27°11'N	56°17'E
408830	-	Bander Lengeh, IR	26°33'N	54°52'E
411940	OMDB	Dubai, ER	25°15'N	55°20'E
412160	OMAA	Abu Dhabi Intl, ER	24°26'N	54°39'E
417560	OPJI	Jiwani, PK	25°04'N	61°48'E
417650	-	Hyderabad, PK	25°23'N	68°25'E
417800	OPKC	Karachi, Arpt PK	24°54'N	67°09'E

Region 4

<u>NUMBER</u>	<u>ICAO</u>	<u>NAME</u>	<u>LAT</u>	<u>LONG</u>
408290	-	Zabol, IR	31°01'N	61°29'E
408540	-	Bam, IR	29°06'N	58°24'E
408560	OIZH	Zahedan, IR	29°28'N	60°53'E
409040	-	Faizabad, AH	37°07'N	70°31'E
409110	OAMS	Mazari-Sharif, AH	36°42'N	67°12'E
409130	OAUZ	Kunduz, AH	36°40'N	68°55'E
409300	-	Northsalang, AH	35°19'N	69°01'E
409410	-	Ghelmin, AH	34°53'N	65°18'E
409430	-	Shahrak, AH	34°06'N	64°18'E
409450	-	Bamiyan, AH	34°49'N	67°49'E
409480	OAKB	Kabul Intl, AH	34°33'N	69°13'E
409540	OAJL	Jalalabad, AH	34°26'N	70°28'E
409680	-	Ghazni, AH	33°32'N	68°25'E
409700	-	Gerdiz/Gardez, AH	33°37'N	69°14'E
409740	-	Farah, AH	32°22'N	62°11'E
409790	-	Kalat, AH	32°07'N	66°54'E
409880	-	Bust/Laskar Gan, AH	31°33'N	64°22'E
409900	OAKN	Kanahar, AH	31°30'N	65°51'E
415150	-	Drosh, AH	35°33'N	71°48'E
415300	OPPS	Peshawar, PK	34°00'N	71°31'E
416200	-	Ft Sandeman, PK	31°21'N	69°28'E
416600	OPQT	Quetta/Samungli, PK	30°15'N	66°56'E
416850	-	Barkhan, PK	39°54'N	69°31'E
417120	-	Dalbandin, PK	28°53'N	64°24'E
417440	-	Khuzdar, PK	27°50'N	66°38'E

Region 5

<u>NUMBER</u>	<u>ICAO</u>	<u>NAME</u>	<u>LAT</u>	<u>LONG</u>
415710	OPRN	Rawalpindi/Islamaba, PK	33°37'N	73°06'E
415940	OPSR	Sargodha, PK	32°03'N	72°40'E
415980	-	Jhelum, PK	32°56'N	73°43'E
416400	-	Lahore, PK	31°33'N	74°20'E
416750	OPMT	Multan, PK	30°12'N	71°26'E
417150	OPJA	Jacobabad, PK	28°18'N	68°28'E

Region 6

<u>NUMBER</u>	<u>ICAO</u>	<u>NAME</u>	<u>LAT</u>	<u>LONG</u>
621760	-	Giarabub, LY	29°45'N	24°32'E
622710	-	Kufra, LY	24°13'N	23°18'E
623660	HECA	Cairo Intl, UB	30°08'N	31°24'E
623930	HEAT	Makabad/Asyut, UB	27°11'N	31°06'E
624050	HELX	Luxor, UB	25°40'N	32°42'E

AFRICA (AFRPT)Region 1

<u>NUMBER</u>	<u>ICAO</u>	<u>NAME</u>	<u>LAT</u>	<u>LONG</u>
413440	OYSN	Sanaa Intl/Rahaba, YE	15°31'N	44°11'E
626000	-	Wadi Halfa, SU	21°48'N	31°31'E
626400	-	Abu Hamed, SU	19°32'N	33°19'E
626500	HSDN	Dongola, SU	19°10'N	30°29'E
626800	-	Atbara, SU	17°42'N	33°58'E
627210	HSSS	Khartoum, SU	15°36'N	32°33'E
627300	-	Kassala, SU	15°28'N	36°24'E
627520	-	Gedaref/Azaza, SU	14°02'N	35°24'E
627720	-	Kosti, SU	13°10'N	32°40'E
627950	-	Abu Na' ama, SU	12°44'N	34°08'E

Region 2

<u>NUMBER</u>	<u>ICAO</u>	<u>NAME</u>	<u>LAT</u>	<u>LONG</u>
626410	HSSP	Port Sudan, ET	19°35'N	37°13'E
630210	HAAS	Asmara/Yohannes, ET	15°17'N	38°55'E

APPENDIX C

List of CONUS and Alaska Operational Stations (SOFTRIX Support)

STATION LIST FOR SOFTRIX DATA BASE

<u>CALL</u>	<u>LOCATION</u>	<u>STATE</u>	<u>LAT</u>	<u>LONG</u>
ABE	Allentown	PA	40°39'N	75°26'W
ABI	Abilene	TX	32°25'N	99°41'W
ABQ	Albuquerque	NM	35°03'N	106°37'W
ABR	Aberdeen	SD	45°27'N	98°26'W
ACT	Waco	TX	31°37'N	97°13'W
ACV	Arcata	CA	40°59'N	124°06'W
ACY	Atlantic City	NJ	39°27'N	74°34'W
ADW	Andrews AFB	MD	38°49'N	76°51'W
AEX	England AFB	LA	31°19'N	92°33'W
AGR	Avon Park AFR	FL	27°39'N	81°20'W
AGS	Augusta	GA	33°22'N	81°58'W
AHN	Athens	GA	33°57'N	83°19'W
ALB	Albany	NY	42°45'N	73°48'W
ALO	Waterloo	IA	42°33'N	92°24'W
ALW	Walla Walla	WA	46°06'N	118°17'W
AMA	Amarillo	TX	35°14'N	101°42'W
APN	Alpena	MI	45°04'N	83°34'W
AST	Astoria	OR	46°09'N	123°53'W
ATL	Atlanta	GA	33°39'N	84°26'W
AT2	Atterbury AFR	IN	39°18'N	86°06'W
AUS	Austin	TX	30°18'N	97°42'W
AVL	Asheville	NC	35°26'N	82°32'W
AVP	Scranton	PA	41°20'N	75°44'W
AYZ	Ft Devins	MA	42°34'N	71°36'W
BAB	Beale AFB	CA	39°08'N	121°26'W
BAD	Barksdale AFB	LA	32°30'N	93°40'W
BCE	Bryce Canyon	UT	37°42'N	112°09'W
BDL	Hartford	CT	41°56'N	72°41'W
BDR	Bridgeport	CT	41°10'N	73°08'W
BFD	Bradford	PA	41°48'N	78°38'W
BFF	Scottsbluff	NE	41°52'N	103°36'W
BFL	Bakersfield	CA	35°25'N	119°03'W
BGM	Binghamton	NY	42°13'N	75°59'W
BGR	Dangor	ME	44°48'N	68°49'W
BHM	Birmingham	AL	33°34'N	86°45'W
BIL	Billings	MT	45°48'N	108°32'W
BIS	Bismark	ND	46°46'N	100°45'W
BIX	Keesler AFB	MS	30°25'N	88°55'W
BKF	Buckley ANG	CO	39°42'N	104°45'W
BKW	Beckley	WV	37°47'N	81°07'W
BLV	Scott AFB	IL	38°33'N	89°51'W
BNA	Nashville	TN	36°07'N	86°41'W

<u>CALL</u>	<u>LOCATION</u>	<u>STATE</u>	<u>LAT</u>	<u>LONG</u>
BNO	Burns	OR	43°36'N	113°57'W
BOI	Boise	ID	43°34'N	116°13'W
BOS	Boston	MA	42°22'N	71°02'W
BRL	Burlington	IA	40°47'N	91°07'W
BRO	Brownsville	TX	25°54'N	97°26'W
BSM	Bergstrom AFB	TX	30°03'N	97°40'W
BTR	Baton Rouge	LA	30°32'N	91°09'W
BTU	Burlington	VT	44°28'N	73°09'W
BUF	Buffalo	NY	42°56'N	78°44'W
BVE	Boothville	LA	29°20'N	89°24'W
BWI	Baltimore	MD	39°11'N	76°40'W
BYH	Blytheville AFB	AR	35°58'N	89°57'W
CAE	Columbia	SC	33°57'N	81°07'W
CAK	Akron-Canton	OH	40°55'N	81°26'W
CAR	Caribou	ME	46°52'N	68°01'W
CBM	Columbus AFB	MS	33°39'N	88°27'W
CDC	Cedar City	UT	37°42'N	113°06'W
CEF	Westover AFB	MA	42°12'N	72°32'W
CHA	Chattanooga	TN	35°02'N	85°12'W
CHD	Williams AFB	AZ	33°18'N	111°40'W
CHS	Charleston	SC	32°54'N	80°02'W
CLE	Cleveland	OH	41°24'N	81°51'W
CLT	Charlotte	NC	35°13'N	80°56'W
CMH	Columbus	OH	40°00'N	82°53'W
CNK	Concordia	KS	39°33'N	97°39'W
COF	Patrick AFB	FL	28°14'N	80°36'W
CON	Concord	NH	43°12'N	71°30'W
COS	Colorado Spgs	CO	38°49'N	104°43'W
COU	Columbia	MO	38°49'N	92°13'W
CPR	Casper	WY	42°55'N	106°28'W
CRP	Corpus Christi	TX	27°46'N	97°30'W
CRW	Charleston	WV	38°22'N	81°36'W
CSM	Clinton-Sherman FAA	OK	35°21'N	99°12'W
CVG	Cincinnati	OH	39°03'N	84°40'W
CVS	Cannon AFB	NM	34°23'N	103°19'W
CYS	Cheyenne	WY	41°09'W	104°49'W
DAA	Davison AAF	VA	38°43'N	77°11'W
DAB	Daytona Beach	FL	29°11'N	81°03'W
DAG	Daggett	CA	34°52'N	116°47'W
DAL	Dallas	TX	32°51'N	96°51'W
DAY	Dayton	OH	39°54'N	84°13'W
DBQ	Dubuque	IA	42°24'N	90°42'W
DCA	Washington	DC	38°51'N	77°02'W
DDC	Dodge City	KS	37°46'N	99°58'W
DEN	Denver	CO	39°45'N	104°52'W
DFW	Dallas-Ft Worth	TX	32°54'N	97°02'W
DLF	Laughlin AFB	TX	29°22'N	100°47'W
DLH	Duluth	MN	46°50'N	92°11'W
DMA	Davis-Monthan AFB	AZ	32°10'N	110°53'W

<u>CALL</u>	<u>LOCATION</u>	<u>STATE</u>	<u>LAT</u>	<u>LONG</u>
DOV	Dover AFB	DE	39°08'N	75°28'W
DPG	Michael AAF	UT	40°12'N	112°56'W
DPI	Eglin 52 AFR	FL	30°30'N	86°18'W
DRT	Del Rio	TX	29°22'N	100°55'W
DSM	Des Moines	IA	41°32'N	93°39'W
DTW	Detroit	MI	42°14'N	83°20'W
DVD	Camp David	MD	39°39'N	77°28'W
DYS	Dyess AFB	TX	32°26'N	99°51'W
EAU	Eau Claire	WI	44°52'N	91°29'W
EDW	Edwards AFB	CA	34°54'N	117°52'W
EFD	Ellington AFB	TX	29°37'N	95°10'W
EKA	Eureka	CA	40°48'N	124°10'W
EKN	Elkins	WV	38°53'N	79°51'W
EKO	Elko	NV	40°50'N	115°47'W
ELP	El Paso	TX	31°48'N	106°24'W
ELY	Ely	NV	39°17'N	114°51'W
END	Vance AFB	OK	36°21'N	97°55'W
ENV	Wendover	UT	40°44'N	114°02'W
ERI	Erie	PA	42°05'N	80°11'W
EUG	Eugene	OR	44°07'N	123°12'W
EVV	Evansville	IN	38°03'N	87°32'W
EWR	Newark	NJ	40°42'N	74°10'W
EYW	Key West	FL	24°33'N	81°45'W
FAF	Felker AAF	VA	37°08'N	76°37'W
FAR	Fargo	ND	46°54'N	96°48'W
FAT	Fresno	CA	36°46'N	119°43'W
FCA	Kalispell	MT	48°18'N	114°16'W
FCS	Butts AAF (Ft Carson)	CO	38°41'N	104°46'W
FEW	F.E. Warren AFB	WY	41°09'N	104°48'W
FFO	Wright-Patterson AFB	OH	39°50'N	84°03'W
FHU	Ft. Huachuca	AZ	31°35'N	110°20'W
FLG	Flagstaff	AZ	35°08'N	111°40'W
FLV	Sherman AAF	KS	39°22'N	94°55'W
FME	Tipton AAF	MD	39°05'N	76°46'W
FMH	Falmouth/Otis AFB	MA	41°39'N	70°31'W
FMN	Farmington	NM	36°45'N	108°14'W
FMY	Fort Myers	FL	26°35'N	81°52'W
FNT	Flint	MI	42°58'N	83°44'W
FOE	Forbes AFB	KS	38°57'N	95°40'W
FRI	Marshall AAF	KS	39°03'N	96°46'W
FSD	Sioux Falls	SD	43°34'N	96°44'W
FSI	Ft. Sill	OK	34°39'N	98°24'W
FSM	Fort Smith	AR	35°20'N	94°22'W
FTK	Godman AAF	KY	37°54'N	85°58'W
FWA	Fort Wayne	IN	41°00'N	85°12'W
FWH	Carswell AFB	TX	32°47'N	97°26'W
GBN	Gila Bend AFR	AZ	32°56'N	112°42'W
GEG	Spokane	WA	47°38'N	117°32'W
GFA	Malmstrom AFB	MT	47°30'N	111°11'W

<u>CALL</u>	<u>LOCATION</u>	<u>STATE</u>	<u>LAT</u>	<u>LONG</u>
GGW	Glasgow	MT	48°13'N	106°37'W
GJT	Grand Junction	CO	39°07'N	108°32'W
GLD	Goodland	KS	39°22'N	101°42'W
GRB	Green Bay	WI	44°29'N	88°08'W
GRF	Gray AAF	WA	47°05'N	122°35'W
GRI	Grand Island	NE	40°58'N	98°19'W
GRK	Robert-Gray AAF	TX	31°04'N	97°50'W
GRR	Grand Rapids	MI	42°53'N	85°31'W
GSB	Seymour-Johnson AB	NC	35°20'N	77°58'W
GSG	Glasgow AFB	MT	48°25'N	106°32'W
GSO	Greensboro	NC	36°05'N	79°57'W
GSP	Greenville	SC	34°54'N	82°13'W
GTB	Ft Drum AFR	NY	44°03'N	75°44'W
GTF	Great Falls	MT	47°29'N	111°22'W
GUS	Grissom AFB	IN	40°39'N	86°09'W
GVW	Richards Gebaur AFB	MO	38°51'N	94°33'W
HAR	Harrisburg	PA	40°14'N	77°01'W
HAT	Cape Hatteras	NC	35°16'N	75°33'W
HIF	Hill AFB	UT	41°07'N	111°58'W
HLN	Helena	MT	46°36'N	112°00'W
HMN	Holloman AFB	NM	32°51'N	106°06'W
HON	Huron	SD	44°23'N	98°13'W
HOP	Campbell AAF	KY	36°40'N	87°30'W
HRT	Hurlburt Fld	FL	30°25'N	86°41'W
HST	Homestead AFB	FL	25°29'N	80°23'W
HSV	Huntsville	AL	34°39'N	86°46'W
HTL	Houghton Lake	MI	44°22'N	84°41'W
HTS	Huntington	WV	38°22'N	82°33'W
HVR	Havre	MT	48°33'N	109°46'W
IAB	McConnell AFB	KS	37°37'N	97°16'W
IAD	Washington-Dulles Intl	VA	38°57'N	77°27'W
IAH	Houston	TX	29°58'N	95°21'W
ICT	Wichita	KS	37°39'N	97°16'W
ILG	Wilmington	DE	39°40'N	75°36'W
ILM	Wilmington	NC	34°16'N	77°55'W
IND	Indianapolis	IN	39°44'N	86°17'W
INL	International Falls	MN	48°34'N	93°23'W
INR	Kincheloe AFB	MI	46°15'N	84°28'W
INS	Nellis 60 AFR	NV	36°35'N	115°41'W
INW	Winslow	AZ	35°01'N	110°44'W
IPT	Williamsport	PA	41°15'N	76°55'W
ISN	Williston	ND	48°11'N	103°38'W
ISP	Islip	NY	40°47'N	73°06'W
JAN	Jackson	MS	32°19'N	90°05'W
JAX	Jacksonville	FL	30°30'N	81°42'W
JFK	New York	NY	40°39'N	73°47'W
LAN	Lansing	MI	42°47'N	84°36'W
LAS	Las Vegas	NV	36°05'N	115°10'W
LAX	Los Angeles	CA	33°56'N	118°24'W

<u>CALL</u>	<u>LOCATION</u>	<u>STATE</u>	<u>LAT</u>	<u>LONG</u>
LBB	Lubbock	TX	33°39'N	101°49'W
LBF	North Platte	NE	41°08'N	100°41'W
LCH	Lake Charles	LA	30°07'N	93°13'W
LCK	Rickenbacker ANGB	OH	39°49'N	82°56'W
LEX	Lexington	KY	38°02'N	84°36'W
LFI	Langley AFB	VA	37°05'N	76°21'W
LFK	Lufkin	TX	31°14'N	94°45'W
LGA	New York	NY	40°46'N	73°54'W
LGB	Long Beach	CA	33°49'N	118°09'W
LHW	Wright AAF	GA	31°53'N	81°34'W
LIT	Little Rock	AR	34°44'N	92°14'W
LIZ	Loring AFB	ME	46°57'N	67°53'W
LND	Lander	WY	42°49'N	108°44'W
LOL	Lovelock	NV	40°04'N	118°33'W
LRF	Little Rock AFB	AR	34°55'N	92°09'W
LSE	La Crosse	WI	43°52'N	91°15'W
LSF	Lawson AAF	GA	32°20'N	85°00'W
LSV	Nellis AFB	NV	36°15'N	115°02'W
LTS	Altus AFB	OK	34°39'N	99°16'W
LUF	Luke AFB	AZ	33°33'N	112°22'W
LYH	Lynchburg	VA	37°20'N	79°12'W
MAF	Midland	TX	31°57'N	102°11'W
MCC	McClellan AFB	CA	38°40'N	121°24'W
MCF	MacDill AFB	FL	27°51'N	82°30'W
MCI	Kansas City	MO	39°18'N	94°43'W
MCN	Macon	GA	32°42'N	83°39'W
MCW	Mason City	IA	43°09'N	93°20'W
MC2	Ft Carson AFR	CO	38°30'N	104°48'W
MDW	Chicago Midway	IL	41°47'N	87°45'W
MEI	Meridian	MS	32°20'N	88°45'W
MEM	Memphis	TN	35°03'N	90°00'W
MER	Castle AFB	CA	37°22'N	120°34'W
MFR	Medford	OR	42°22'N	122°52'W
MGE	Dobbins AFB	GA	33°55'N	84°31'W
MGM	Montgomery	AL	32°18'N	86°24'W
MHR	Mather AFB	CA	38°34'N	121°18'W
MIA	Miami	FL	25°48'N	80°16'W
MIB	Minot AFB	ND	48°25'N	101°21'W
MIL	Saylor Creek AFR	ID	42°32'N	115°42'W
MKE	Milwaukee	WI	42°57'N	87°54'W
MKG	Muskegon	MI	43°10'N	86°14'N
MLI	Moline	IL	41°27'N	90°31'W
MMT	McEntire ANGB	SC	33°55'N	80°48'W
MOB	Mobile	AL	30°41'N	88°15'W
MOT	Minot	ND	48°16'N	101°17'W
MSN	Madison	WI	43°08'N	89°20'W
MSO	Missoula	MT	46°55'N	114°05'W
MSP	Minneapolis	MN	44°53'N	93°13'W
MSS	Massena	NY	44°56'N	74°51'W

<u>CALL</u>	<u>LOCATION</u>	<u>STATE</u>	<u>LAT</u>	<u>LONG</u>
MSY	New Orleans	LA	29°59'N	90°15'W
MTC	Selfridge AFB	MI	42°36'N	82°50'W
MTN	Martin Marietta	MD	39°20'N	76°25'W
MUI	Muir AAF	PA	40°26'N	76°34'W
MUO	Mountain Home AFB	ID	43°03'N	115°52'W
MXF	Maxwell AFB	AL	32°23'N	86°22'W
MYR	Myrtle Beach	SC	33°41'N	78°56'W
NCL	Cuddeback AFB	CA	35°16'N	117°26'W
OAK	Oakland	CA	37°44'N	122°12'W
OAR	Fritzsche AAF	CA	36°41'N	121°46'W
OFF	Offutt AFB	NE	41°07'N	95°54'W
OKC	Oklahoma City	OK	35°24'N	97°36'W
OLM	Olympia	WA	46°58'N	122°54'W
OMA	Omaha	NE	41°18'N	95°54'W
ORD	Chicago	IL	41°59'N	87°54'W
ORF	Norfolk	VA	36°54'N	76°12'W
ORL	Orlando	FL	28°33'N	81°20'W
OSC	Wurtsmith AFB	MI	44°27'N	83°24'W
OTH	North Bend	OR	43°25'N	124°15'W
OZR	Cairns AAF	AL	31°16'N	85°43'W
PAM	Tyndall AFB	FL	30°04'N	85°35'W
PBG	Plattsburg AFB	NY	44°39'N	73°28'W
PBI	West Palm Beach	FL	26°41'N	80°06'W
PDT	Pendleton	OR	45°41'N	118°51'W
PDX	Portland	OR	45°36'N	122°36'W
PHL	Philadelphia	PA	39°53'N	75°15'W
PHX	Phoenix	AZ	33°26'N	112°01'W
PIA	Peoria	IL	40°40'N	89°41'W
PIH	Pocatello	ID	42°55'N	112°36'W
PIR	Pierre	SD	44°23'N	100°17'W
PIT	Pittsburgh	PA	40°30'N	80°13'W
POB	Pope AFB	NC	35°10'N	79°01'W
POE	Ft Polk	LA	31°03'N	93°11'W
PSM	Pease AFB	NH	43°05'N	70°49'W
PUB	Pueblo	CO	38°17'N	104°31'W
PVD	Providence	RI	41°44'N	71°26'W
PWM	Portland	ME	43°39'N	70°19'W
QOS	Oscara AFB	NM	34°00'N	106°18'W
RAP	Rapid City	SD	44°03'N	103°04'W
RBL	Red Bluff	CA	40°09'N	122°15'W
RCA	Ellsworth AFB	SD	44°09'N	103°06'W
RDM	Redmond	OR	44°16'N	121°09'W
RDR	Grand Forks AFB	ND	47°57'N	97°24'W
RDU	Raleigh-Durham	NC	35°52'N	78°47'W
REE	Reese AFB	TX	33°36'N	102°03'W
RFD	Rockford	IL	42°12'N	89°06'W
RIC	Richmond	VA	37°30'N	77°20'W
RIV	March AFB	CA	33°54'N	117°15'W
RKS	Rock Springs	WY	41°36'N	109°04'W

<u>CALL</u>	<u>LOCATION</u>	<u>STATE</u>	<u>LAT</u>	<u>LONG</u>
RME	Griffiss AFB	NY	43°14'N	75°24'W
RND	Randolph AFB	TX	29°32'N	98°17'W
RNO	Reno	NV	39°30'N	119°47'W
ROA	Roanoke	VA	37°19'N	79°58'W
ROC	Rochester	NY	43°07'N	77°40'W
RSL	Russell	KS	38°52'N	98°49'W
RST	Rochester	MN	43°55'N	92°30'W
SAC	Sacramento	CA	38°31'N	121°30'W
SAN	San Diego	CA	32°44'N	117°10'W
SAT	San Antonio	TX	29°32'N	98°28'W
SAV	Savannah	GA	32°08'N	81°12'W
SAW	K.I.Sawyer AFB	MI	46°21'N	87°24'W
SBD	Norton AFB	CA	34°06'N	117°14'W
SBN	South Bend	IN	41°02'N	86°19'W
SCK	Stockton	CA	37°54'N	121°15'W
SDF	Louisville	KY	38°11'N	85°44'W
SEA	Seattle-Tacoma	WA	47°27'N	122°18'W
SEM	Craig AFB	AL	32°20'N	86°59'W
SFO	San Francisco	CA	37°37'N	122°23'W
SGF	Springfield	MO	37°14'N	93°23'W
SHR	Sheridan	WY	44°46'N	106°58'W
SHV	Shreveport	LA	32°28'N	93°49'W
SJT	San Angelo	TX	31°22'N	100°30'W
SKA	Fairchild AFB	WA	47°38'N	117°39'W
SKF	Kelly AFB	TX	29°23'N	98°35'W
SLC	Salt Lake City	UT	40°46'N	111°58'W
SLE	Salem	OR	44°55'N	123°01'W
SMX	Santa Maria	CA	34°54'N	120°27'W
SPI	Springfield	IL	39°50'N	89°40'W
SPS	Wichita Falls	TX	33°58'N	98°29'W
SSC	Shaw AFB	SC	33°58'N	80°28'W
SSM	Sault St Marie	MI	46°28'N	84°22'W
STJ	St Joseph	MO	39°46'N	94°55'W
STL	St Louis	MO	38°45'N	90°23'W
SUU	Travis AFB	CA	38°16'N	121°56'W
SUX	Sioux City	IA	42°24'N	96°23'W
SVN	Hunter AAF	GA	32°01'N	81°09'W
SYR	Syracuse	NY	43°07'N	76°07'W
SZL	Whiteman AFB	MO	38°43'N	93°33'W
TBN	Ft Leonard Wood	MO	37°45'N	92°09'W
TCC	Tucumcari	NM	35°11'N	103°36'W
TCM	McChord AFB	WA	47°09'N	122°29'W
TCS	Truth or Consequences	NM	33°14'N	107°16'W
TIK	Tinker AFB	OK	35°25'N	97°23'W
TLH	Tallahassee	FL	30°23'N	84°22'W
TOL	Toledo	OH	41°36'N	83°48'W
TOP	Topeka	KS	39°04'N	95°38'W
TPA	Tampa	FL	27°58'N	82°32'W
TPH	Tonopah	NV	38°04'N	117°05'W

<u>CALL</u>	<u>LOCATION</u>	<u>STATE</u>	<u>LAT</u>	<u>LONG</u>
TRI	Bristol	TN	36°29'N	82°24'W
TYS	Knoxville	TN	35°49'N	83°59'W
T01	Wallops I TACR	VA	37°30'N	74°00'W
T02	Ft Jackson TACR	SC	34°06'N	80°48'W
T03	Myrtle Beach TACR	SC	33°12'N	78°48'W
T04	Sarasota TACR	FL	26°43'N	83°48'W
T05	Smokey Hill TACR	KS	38°48'N	97°54'W
T06	Camp Shelby TACS	MS	31°06'N	89°00'W
T07	Green River TACR	UT	39°00'N	110°06'W
T08	Hill/Eagle TACR	UT	41°06'N	113°24'W
UCC	Nellis 70 AFR	NV	36°57'N	116°03'W
VAD	Moody AFB	GA	30°58'N	83°12'W
VBG	Vandenberg AFB	CA	34°43'N	120°34'W
VCV	George AFB	CA	34°35'N	117°23'W
VPS	Eglin AFB	FL	30°29'N	86°31'W
WRB	Robins AFB	GA	32°38'N	83°36'W
WRI	McGuire AFB	NJ	40°01'N	74°36'W
YKM	Yakima	WA	46°34'N	120°32'W
YNG	Youngstown	OH	41°16'N	80°40'W
YUM	Yuma	AZ	32°40'N	114°36'W
ZUN	Zuni	NM	35°06'N	108°48'W
01R	Claiborne AFR	LA	31°11'N	92°38'W
2DP	Dare County AFR	NC	35°41'N	75°54'W
2PJ	Poinsett AFR	SC	33°50'N	80°29'W
3RN	Grayling AFR	MI	44°50'N	84°33'W
4MR	Melrose AFR	NM	34°18'N	103°43'W

ALASKAN SOFTRIX STATIONS

<u>Identifier</u>	<u>Name</u>	<u>Lat</u>	<u>Lon</u>
ADQ	Kodiak	57°45'N	152°31'W
AKN	King Salmon	58°41'N	156°39'W
ANC	Anchorage Intl	61°10'N	150°01'W
ANN	Annette Island	55°02'N	131°34'W
BET	Bethel/Muni	60°47'N	161°48'W
BIG	Big Delta/Allen AAF	64°00'N	145°44'W
BRW	Barrow	71°18'N	156°47'W
BTI	Barter Island AFS	70°08'N	143°38'W
BTT	Bettles	66°55'N	151°31'W
CDB	Cold Bay	55°12'N	162°43'W
CDV	Cordova/Mile 13	60°30'N	145°30'W
DLG	Dillingham Muni	59°03'N	158°31'W
ENA	Kenai	60°34'N	151°15'W
FAI	Fairbanks Intl	64°49'N	147°52'W
GKN	Gulkana	62°09'N	145°27'W
HOM	Homer Muni	59°38'N	151°30'W
JNU	Juneau	58°22'N	134°35'W
MCG	McGrath	62°58'N	155°37'W
OME	Nome Muni	64°30'N	165°26'W
ORT	Northway	62°57'N	141°56'W
OTZ	Kotzebue/Ralph Wien	66°52'N	162°38'W
PACZ	Cape Romanzoff AFS	61°47'N	166°02'W
PAED	Elmendorf AFB	61°15'N	149°48'W
PAEH	Cape Newenham AFS	58°39'N	162°04'W
PAEI	Eielson AFB	64°39'N	147°04'W
PAGA	Galena	64°44'N	156°56'W
PAIM	Indian Mountain AFS	66°00'N	153°42'W
PALU	Cape Lisburne AFS	68°53'N	166°08'W
PASV	Sparrevohn AFS	61°06'N	155°34'W
PATC	Tin City AFS	65°34'N	167°55'W
PATL	Tatalina AFS	62°54'N	155°58'W
PSG	Petersburg	56°49'N	132°57'W
SIT	Sitka	57°04'N	135°21'W
SGY	Skagway	59°27'N	135°19'W
SNP	St Paul Island	57°09'N	170°13'W
TAL	Tanana	65°10'N	152°06'W
TKA	Talkeetna	62°18'N	150°06'W
VDZ	Valdez	61°08'N	146°15'W
YAK	Yakutat	59°31'N	139°40'W

GLOSSARY OF TERMS

Bias. Refers to either mean forecast minus mean observed values (a mathematical mean error) or to the ratio of the frequency of categorical forecasts to the frequency of that same category's occurrences (a contingency table bias).

Brier Probability Score. A statistic that measures the mean square error of probability forecast values against the resultant zero/one verification. The Brier Score embodies both sharpness and reliability into a single value. This score ranges from 0 (perfect) to 2 (perfectly opposite).

Category. A partitioning of an event. Ceilings below 200 feet AGL is an example.

Conditional Climatology. Same as climatology, but a subset conditioned on a selected stratification such as month, wind direction, persistence, etc. For example, the relative frequency of fog occurrence may be 0.12, but when the wind is from the SE the relative frequency is 0.35.

Climatology. A term referring to the long-term record of a meteorological event. Climatology values may be scalar or in terms of relative frequency. For example, the daily expected maximum temperature for a particular location is in scalar form, whereas the frequency of below-minimums flying weather is in decimal form.

Critical Probability. Another term for threshold probability.

Probability. The chance that a predefined event will occur. Values of probability range between zero and one and are expressed either in decimal or percent format (e.g., 0.37 or 37% chance of rain).

Reliable Probability Values. The degree to which forecast probability values resemble the ultimate outcome frequency. For example, if over a long period of time an event occurs 30% of the time for those cases where a 30% forecast was given, perfect reliability is shown.

Sharp Probability Values. The degree to which forecast probability values attempt to quantify the certainty of an events occurrence. To say an event has a 50% chance of occurring illustrates a weak certainty; hence, not sharp. Sharpness is more noticed when probabilities cluster toward 0% and 100%. Perfectly sharp forecast values would be those that only forecast 0% and 100%.

Threshold Probability Value. A predetermined value between zero and one that is used to convert probability forecasts into 2-case categorical forecasts such as yes/no. For example, if the forecast probability is 40% a categorical forecast of NO-rain will be made. Here, the POP values must exceed the 40% threshold before a YES-rain forecast is made.

ACRONYMS

AFGWC	Air Force Global Weather Central
AWDS	Automated Weather Distribution System
AWS	Air Weather Service (MAC/USAF)
AWSPE	6-level Primitive Equation model at AFGWC
C	Relative frequency of a categorical event (also referred to as climatology of the event).
CONUS	The 48 conterminous United States of America
CRC	Contingency Response Capability
DOD	Department of Defense
IFR	Instrument Flight Rules
LFM	Limited Fine Mesh--NWS's 7LPE model at finer grid spacing.
MOS	Model Output Statistics
MOSVER	MOS Verification
MVFR	Marginal Visual Flight Rules
NH	Northern Hemisphere
NMC	National Meteorological Center
NWS	National Weather Service (NOAA)
PIREP	Pilot report
POP	Probability of precipitation
R	Correlation coefficient
SH	Southern Hemisphere
SOFTRIX	Station-oriented forecast matrix
SWANEA	Southwest Asia - Northeast Africa
TDL	Techniques Development Laboratory (NWS/NOAA)
TSMS	The Statistical Systems Section at AFGWC.

USAFETAC	USAF Environmental Technical Applications Center
USAFETAC/DN	Aerospace Sciences Branch at USAFETAC
USAFETAC/OL-A	Operating location A of USAFETAC located in Ashville, NC
USAF	United States Air Force
VFR	Visual Flight Rules
WMCCS	Worldwide Military Command and Control System
5LYR	Five-layer cloud forecast model at AFGWC
3DNEPH	Three-dimensional cloud analysis model at AFGWC

DISTRIBUTION:

1WW (1)
2WW (1)
3WW (1)
4WW (1)
5WW (1)
7WW (1)
AWS/DNT (1)
2WS (1)
AFGWC (4)
USAFETAC/DN (1)
USAFETAC/OL-A (1)
USAFETAC/LDK (5)

END

FILMED

4-84

DTIC

BIS Bismark
BIX Keesler AFB
BKF Buckley ANG
BKW Beckley
BLV Scott AFB
BNA Nashville

MT 45°48'N 108°32'W
ND 46°46'N 100°45'W
MS 30°25'N 88°55'W
CO 39°42'N 104°45'W
WV 37°47'N 81°07'W
IL 38°33'N 89°51'W
TN 36°07'N 86°41'W

DAY	Dayton	OH	39°54'N	84°13'W
DBQ	Dubuque	IA	42°24'N	90°42'W
DCA	Washington	DC	38°51'N	77°02'W
DDC	Dodge City	KS	37°46'N	99°53'W
DEN	Denver	CO	39°45'N	104°52'W
DFW	Dallas-Ft Worth	TX	32°54'N	97°02'W
DLF	Laughlin AFB	TX	29°22'N	100°47'W
DLH	Duluth	MN	46°50'N	92°11'W
DMA	Davis-Monthan AFB	AZ	32°10'N	110°53'W